BEAMFORMING DESIGN FOR NETWORK MULTIPLE-INPUT MULTIPLE-OUTPUT (MIMO) SYSTEMS WITH MULTIPLE COOPERATING BASE STATIONS

A THESIS SUBMITTED TO
THE GRADUATE SCHOOL OF NATURAL AND APPLIED SCIENCES
OF
MIDDLE EAST TECHNICAL UNIVERSITY

BY

FEHMI EMRE KADAN

IN PARTIAL FULFILLMENT OF THE REQUIREMENTS
FOR
THE DEGREE OF DOCTOR OF PHILOSOPHY
IN
ELECTRICAL AND ELECTRONICS ENGINEERING

SEPTEMBER 2021

Approval of the thesis:

BEAMFORMING DESIGN FOR NETWORK MULTIPLE-INPUT MULTIPLE-OUTPUT (MIMO) SYSTEMS WITH MULTIPLE COOPERATING BASE STATIONS

submitted by **FEHMI EMRE KADAN** in partial fulfillment of the requirements for the degree of **Doctor of Philosophy in Electrical and Electronics Engineering Department, Middle East Technical University** by,

Prof. Dr. Halil Kalıpçılar
Dean, Graduate School of **Natural and Applied Sciences** ________________

Prof. Dr. İlkay Ulusoy
Head of Department, **Electrical and Electronics Engineering** ________________

Prof. Dr. Ali Özgür Yılmaz
Supervisor, **Electrical and Electronics Eng. Dept., METU** ________________

Examining Committee Members:

Prof. Dr. Elif Uysal
Electrical and Electronics Eng. Dept., METU ________________

Prof. Dr. Ali Özgür Yılmaz
Electrical and Electronics Eng. Dept., METU ________________

Prof. Dr. Tolga Mete Duman
Electrical and Electronics Eng. Dept., Bilkent Univ. ________________

Assoc. Prof. Dr. Tolga Girici
Electrical and Electronics Eng. Dept., TOBB ETU ________________

Assist. Prof. Dr. Gökhan Muzaffer Güvensen
Electrical and Electronics Eng. Dept., METU ________________

Date:

I hereby declare that all information in this document has been obtained and presented in accordance with academic rules and ethical conduct. I also declare that, as required by these rules and conduct, I have fully cited and referenced all material and results that are not original to this work.

Name, Surname: Fehmi Emre Kadan

Signature :

ABSTRACT

BEAMFORMING DESIGN FOR NETWORK MULTIPLE-INPUT MULTIPLE-OUTPUT (MIMO) SYSTEMS WITH MULTIPLE COOPERATING BASE STATIONS

Kadan, Fehmi Emre

Ph.D., Department of Electrical and Electronics Engineering

Supervisor: Prof. Dr. Ali Özgür Yılmaz

September 2021, 149 pages

New generation cellular systems are required to support high data rates. The performance of conventional systems with a single central base station is limited by inter-cell interference. Furthermore, the network densities grow exponentially and it is not cost-effective for operators to use a large number of fully equipped base stations in small areas. Using multiple cooperating base stations, each equipped with multiple antennas, inter-cell interference can be eliminated by a proper beamforming design. In this thesis, beamforming strategies for cloud radio access networks and integrated access and backhaul systems are studied. In these systems, the baseband processing is centralized, and hence by an optimized resource allocation, the coverage can be significantly increased. Furthermore, the usage of simpler base stations decreases the cost of deployment, resulting in efficient and cost-effective system designs. Wireless fronthaul/backhaul solutions further decrease the capital and operational expenditures of operators. The beamforming design problem has a combinatorial nature due to fronthaul/backhaul transmissions. Applying some relaxations and transformations, the beamforming vectors are designed and cooperation schemes of base stations are optimized to minimize total power consumption and maximize the total users served under fronthaul capacity and transmit power constraints. Heuristic search, smooth approximation, bound-based link selection, and convex optimization-based algorithms are proposed to find suitable beamformers under realistic channel conditions. Some novel theoretical performance bounds are also derived to observe the limits of the algorithms and make the optimality analysis. The detailed simulations show the performance benefits of the proposed techniques compared to the existing baseline methods.

Keywords: Cloud Radio Access Network, Beamforming, Integrated Access and Backhaul, Fronthaul, Convex Optimization

ÖZ

BİRDEN ÇOK ORTAK ÇALIŞAN BAZ İSTASYONU İÇEREN ÇOK GİRDİLİ ÇOK ÇIKTILI VERİ AĞLARI İÇİN HÜZME BİÇİMLENDİRME TASARIMI

Kadan, Fehmi Emre
Doktora, Elektrik ve Elektronik Mühendisliği Bölümü
Tez Yöneticisi: Prof. Dr. Ali Özgür Yılmaz

Eylül 2021 , 149 sayfa

Yeni nesil hücresel haberleşme sistemlerinin yüksek veri hızlarını desteklemesi istenmektedir. Standart tek merkezi baz istasyonu içeren sistemlerin performansı farklı hücreler arası girişim yüzünden sınırlıdır. Ayrıca ağ yoğunlukları büyük bir hızla artmakta ve küçük bir alanda çok sayıda tam donanımlı baz istasyonu kullanımı mali açıdan verimli olmamaktadır. Birden çok, her biri çok sayıda anten içeren, birbiriyle koordinasyon halinde çalışan baz istasyonu kullanımı ve uygun bir hüzme biçimlendirme tasarımı ile hücreler arası girişim yok edilebilir. Bu çalışmada bulut tabanlı radio ağları ve entegre erişim ve arka ağ sistemleri için hüzme biçimlendirme tasarımı incelenmiştir. Bu sistemlerde taban bant işlemler merkezi biçimde yapılmakta ve kaynak kullanımının optimizasyonu ile kapsama alanları genişletilebilmektedir. Ayrıca basit baz istasyonlarının kullanımı ile dağıtım maliyetleri düşürülerek etkin ve verimli sistemler elde edilmektedir. Kablosuz ön ve arka bağlantı kullanımı ile operatörlerin kısa ve uzun vadeli harcamaları daha da düşürülebilmektedir. Hüzme biçimlendirme problemi doğası gereği ön ve arka ağ iletimleri yüzünden birleşimseldir. Bazı gevşetme ve dönüşümler kullanılarak toplam güç tüketimini en aza indirip toplam hizmet verilen kullanıcı sayısı en çok olacak şekilde arka ağ kapasite ve güç iletim koşulları altında hüzme biçimlendirme vektörleri tasarlanmakta ve baz istasyonları arasındaki koordinasyon optimize edilmektedir. Gerçekçi kanal koşulları altında uygun hüzme biçimlendirme vektörlerinin tasarımı için sezgisel tarama, sonsuz türevli yaklaşım, sınır tabanlı link seçimi ve konveks optimizasyon tabanlı yöntemler önerilmiştir. Algoritmaların performans sınırlarını görmek ve eniyilik analizi yapmak için bazı özgün teorik performans sınırları bulunmuştur. Önerilen yöntemlerin mevcut metotlara kıyasla performans açısından faydaları detaylı benzetimlerle gösterilmiştir.

Anahtar Kelimeler: Bulut Tabanlı Radyo Ağları, Hüzme Biçimlendirme, Entegre Erişim ve Arka Bağlantı, Ön Bağlantı, Konveks Optimizasyon

To my family and Ezgi...

ACKNOWLEDGMENTS

I would like to present my gratitude to my supervisor Prof. Dr. Ali Özgür Yılmaz for his precious suggestions in this study. He showed me how to approach the problem and make efficient solutions. He also provided this thesis work to be more realistic by his valuable guidance.

I would also like to thank other thesis monitoring committee members Prof. Dr. Tolga Mete Duman and Assist. Prof. Dr. Gökhan Muzaffer Güvensen for their detail-oriented review of this study. Throughout all thesis work, they provided significant suggestions and corrections when necessary.

I want to thank TÜBİTAK for their scholarship that helped me to finish this research.

Finally, I would like to thank my family and Ezgi for their constant support during my thesis study.

TABLE OF CONTENTS

LIST OF TABLES

TABLES

LIST OF FIGURES

FIGURES

LIST OF ABBREVIATIONS

3GPP	Third Generation Partnership Project
5GPPP	Fifth Generation Infrastructure Public Private Partnership
AF	Amplify-and-Forward
AO	Alternating Optimization
AWGN	Additive White Gaussian Noise
BB	Barzilai and Borwein
BBLS	Bound Based Link Selection
BBU	Base Band Unit
BS	Base Station
CAPEX	Capital Expenditure
CoMP	Coordinated Multi-Point
CP	Central Processor
C-RAN	Cloud Radio Access Network
CSI	Channel State Information
DCF	Decompress-and-Forward
DF	Decode-and-Forward
ES	Exhaustive Search
GSB	Group Sparse Beamforming
IAB	Integrated Access and Backhaul
ILA	Iterative Link Addition
ILR	Iterative Link Removal
IUA	Iterative User Addition
i.i.d.	independent identically distributed
LTE	Long Term Evolution

MBS	Macro Base Station
MILR	Modified Iterative Link Removal
MIMO	Multiple Input Multiple Output
MISO	Multiple Input Single Output
MM	Majorization-Minimization
MRC	Maximal Ratio Combining
NCO	Number of Convex Optimizations
NFV	Network Function Virtualization
NP	Non-Polynomial
OPEX	Operational Expenditure
PD	Positive Definite
PSD	Positive Semi-Definite
QCQP	Quadratically Constrained Quadratic Programming
QoS	Quality-of-Service
RF	Radio Frequency
RRH	Remote Radio Head
SBS	Small Base Station
SCA	Successive Convex Approximation
SCFA	Smooth Constraint-Free Approximation
SDN	Software Defined Network
SDP	Semi-Definite Programming
SDR	Semi-Definite Relaxation
SeDuMi	Self Dual Minimization
SI	Self Interference
SIC	Successive Interference Cancellation
SINR	Signal-to-Interference-and-Noise-Ratio
SNR	Signal-to-Noise Ratio

SOCP	Second Order Cone Programming
SVD	Singular Value Decomposition
TSM	Total SNR Max
UE	User Equipment
ZF	Zero Forcing

CHAPTER 1

INTRODUCTION

In new generation communication systems, the number of devices participating in the network grows exponentially. Cisco has predicted that the number of devices connected to IP networks will be more than three times the global population, and mobile speeds will more than triple by 2023 [1]. Fifth Generation Infrastructure Public Private Partnership (5GPPP) states that 1 Gbps data rate should be supported to nearly 10^4 devices per square kilometer with a very low transmission delay (1-10 ms) [2]. As a result of the densification of the communication networks, data rate requirements become challenging. The communication systems should be well-optimized in terms of spectral efficiency, resource allocation, energy efficiency, latency to satisfy the end-user requirements of a huge number of communication devices.

The older cellular communication systems (2G, 3G, 4G) fail to satisfy the demands of dense networks. In 4G LTE-A, for heterogeneous networks with a large number of devices, small cells have been used together with existing macrocells. This approach has increased the inter-cell interference, and Capital Expenditure (CAPEX) and Operational Expenditure (OPEX) of the operators [3]. Furthermore, energy-spectral efficiency, and data rate requirements cannot be satisfied with existing network structures. Therefore, in new generation 5G cellular communication systems, a dramatic change in radio access networks is required.

Cloud Radio Access Network (C-RAN) technology has the potential of meeting all demands and it is a strong candidate for 5G and beyond. This technology was first outlined by IBM in 2010 as a completely new network structure compared to current systems [4]. In C-RAN, some complex functions of standard base stations (BSs) are moved to baseband unit (BBU) pools including central processors (CPs). Centralization allows to optimize the network more efficiently and decreases the CAPEX/OPEX of operators. Cloud-assisted base stations cooperatively serve mobile devices in an optimized way. The cooperative transmission/reception is also used in 4G LTE-A systems and named as Coordinated Multi-Point (CoMP) [5]. In this approach, base stations jointly serve user equipment (UE) to increase spectral and energy efficiency. In C-RAN, a centralized CoMP can be performed to increase the benefits of coordination. As in network MIMO [6], where different base stations jointly perform beamforming to increase the signal-to-interference-and-noise-ratios (SINRs) and data rates, CP can design proper beamformers for each simple BS using the channel vectors. Furthermore, software-defined networking (SDN) and network function virtualization (NFV) provides relaxed and efficient network designs [7]. With all promising properties, C-RAN technology allows relaxed radio resource allocation, interference management, adaptation to non-uniform traffic, and reconfigurable BBU pools. [8].

In the C-RAN hierarchy, base stations are simple radio units called remote radio heads (RRHs) which only implement radio functionality such as RF conversions, filtering, and amplifying. All baseband processing is done over a pool of CPs, which are connected to RRHs with finite capacity fronthaul links [9]. This approach decreases the cost of deployment as compared to the traditional systems where each BS has its own on-site baseband processor. Fronthaul links can be implemented using fiber optical cables, standard wireless channels, or millimeter wave communications [10]. Wired fronthaul can carry high-speed data at the expense of high cost and inflexible deployment. On the other hand, wireless fronthaul is more flexible and can significantly decrease the cost of deployment at the expense of a lower capacity. The main architecture of a typical C-RAN system is described in [11].

Integrated Access and Backhaul (IAB) is a similar technology to C-RAN with wireless fronthaul, which is planned to be used in 5G and beyond. It was first standardized in 3GPP Rel. 16, and some enhancements will be done in 3GPP Rel. 17. The motivation behind making the backhaul transmissions wireless is to decrease the cost of deployment of fiber optical cables. [12] states that one-meter optical fiber deployment is estimated to cost approximately 100-200 USD in the downtown area. Therefore, using wireless backhaul can significantly decrease the costs of operators. In IAB, base stations share the backhaul data of users among each other and hence the coverage can be significantly increased. IAB involves macro base stations (MBSs) (or IAB donors) that are connected to the core network, and small base stations (SBSs) (or IAB nodes) that are used as relays for backhaul data forwarding [13]. In downlink transmission, MBSs can directly send user data to UEs as well as they can send necessary backhaul data to some SBSs. SBSs have not access to the core network and they are used as relays. An SBS decodes the user backhaul data received from an MBS, and then forward the related user data to UEs. Alternatively, an SBS can also broadcast the user backhaul data to other SBSs to further increase the coverage.

There are different IAB transmission strategies used in the literature. As a one way, the backhaul and access link transmissions can be performed in orthogonal resources (different time slots or different frequency bands) to avoid interference. To increase the spectral efficiency, full-duplex transmission can be adopted where backhaul and access link transmissions are performed in the same time/frequency resources [14]. In such a case, SBS should perform a self-interference cancellation operation to increase SINRs in backhaul data decoding.

In C-RAN with wired fronthaul, all RRHs are connected to a CP by fiber cables. In this type of network, there is a natural combinatorial user selection problem. CP should optimize the cooperation of RRHs by determining which user data is sent to which RRHs. Because of the limited capacity of fronthaul links, full cooperation where each user is served by all RRHs may not be performed. In such a case, the cooperation of RRHs should be optimized under fronthaul capacity constraints. In general, the optimal strategy is to try all possible combinations but this approach becomes impractical due to high computational complexity as the network size increases. One needs to apply efficient algorithms to determine the RRH sets serving each UE. In [15], we optimize cooperation of RRHs and beamforming vectors under per-RRH data transfer and power transmit constraints for downlink transmissions. We propose some heuristic methods using semi-definite programming (SDP).

Power consumption is one of the major costs of an operator. In C-RAN, CP can optimize power allocation to minimize total power consumption in the network, resulting in less inter-cell interference and lower cooling costs. Both fronthaul and access link (link between RRHs and UEs) transmissions are needed to be considered to minimize the total power. Even for wired fronthaul networks, the fronthaul power consumption may not be negligible. In [16], we propose a novel beamformer design method to minimize total power consumption in downlink C-RAN with wired fronthaul. Our method is based on a smooth approximation of discontinuous functions.

In dense networks, one of the major problems is to serve all users with finite resources. As the bandwidth is limited, some UEs should be served in the same time/frequency slots. To support high data rates, multi-user interference should be eliminated. This requires well-optimized beamforming. In a cluster consisting of CP, RRHs, and UEs, it may not be possible to serve all UEs when RRH-to-UE channel conditions are not good enough. In such a case, we aim to serve as many UEs as possible. On the other hand, to decrease the latency and not exceed the capacity of the fronthaul links, the total fronthaul data rate should be minimized. To obtain an energy-efficient network, all tasks should be performed with minimum possible power consumption. In [17], we propose a novel method to jointly maximize the number of users served, and minimize the fronthaul data rate and total power consumption. The proposed method finds a proper link configuration of RRHs and UEs based on a theoretical upper bound.

To decrease the cost of deployment, one can use a large base station located close to CP to send the user data from CP to RRHs through wireless links. By this method, the rate of data transmission in fronthaul links can be adaptively adjusted using proper power allocations and beamforming schemes. In wireless fronthaul networks, RRHs are used as relays. In such networks, both fronthaul and access link beamformer designs are needed, making the problem highly complex. As another study, we consider a beamforming design problem for downlink C-RAN with wireless fronthaul [18]. We find a tight theoretical performance bound, and propose some novel beamformer design methods.

As in the C-RAN systems, beamformer and SBS cooperation optimization can significantly enhance the performance of IAB systems. As the user backhaul data is shared by SBSs, amplify-and-forward (AF) type relaying cannot be performed as the backhaul data cannot be decoded by UEs. SBSs should perform decoding and backhaul data should be transformed into user access link data before being transmitted to

UEs. Hence, a user selection problem should also be addressed in IAB systems. In the thesis work, we propose a beamformer design method for a downlink full-duplex IAB system.

The organization of the thesis is as follows:

In **Chapter 2**, the design parameters, system models for C-RAN and IAB systems, and contributions of the thesis are explained.

Chapter 3 presents a study on C-RAN with capacity-limited wired fronthaul. We optimize the cooperation scheme of RRHs using some heuristic search and SDP methods. We have published a conference paper in International Conference on Communications (ICC) 2017 related to this study.

In **Chapter 4**, we describe a power minimization problem for C-RAN with wireless fronthaul. We propose a smooth constraint-free approximation method where discontinuous functions in objective and constraints are approximated as the limits of some smooth function sequences. The related study was published in IEEE Access in March 2021.

Chapter 5 addresses a user admission problem where the number of users served, total fronthaul data rate, and total normalized power consumption is jointly optimized. We again focus on downlink C-RAN with wired fronthaul. We have published a paper on this work in IEEE Communications Letters in August 2021.

In **Chapter 6**, we consider a beamformer design problem for C-RAN with wireless fronthaul. We derive a novel theoretical performance bound that shows a performance limit for any design method. We also propose some algorithms based on convex optimization as well as hybrid beamformer design methods to show the tightness of the bound. In August 2021, a paper related to this study was accepted by IEEE Transactions on Wireless Communications.

Chapter 7 describes a beamformer design study on downlink full-duplex IAB system. We propose a solution technique based on a link removal and SDP method.

Chapter 8 is the conclusion chapter.

CHAPTER 2

DESIGN PARAMETERS, SYSTEM MODELS, AND CONTRIBUTIONS

In this chapter, we describe the design parameters, system models, and contributions of the thesis. We focus on the beamforming design problem where we optimize some network parameters under available resources. Throughout the thesis, we consider a downlink transmission for C-RAN with wired and wireless fronthaul and IAB. For both three cases, we define channel and beamformer parameters and then derive the received signal equations. We propose novel beamformer design methods for the cooperative multi-point transmission problem. We also derive some state-of-art theoretical performance bounds showing the limit of optimization.

2.1 Design Parameters

In the beamforming design, we use some channel models and optimization criteria. The resource allocation in the network can be performed according to the available sources and target optimization parameters.

2.1.1 Channel Error Models

To optimize a C-RAN network by designing beamformers, channel coefficients should be known with some accuracy. In general, perfect channel state information (CSI) is not available as the channel estimation is done via pilot signals with finite power. There are different models for channel estimation error. It can be shown that linear channel estimation methods with orthogonal pilot signals yield an additive channel estimation error. The error is a random vector whose statistics may be known or not known. Some works assume that first or second-order statistics are known [19]-[23], and some other works use the model where the error is norm-bounded [24]-[26]. The first approach is used when quantization error in channel estimation is negligible and the second one is used when quantization error is dominant [27]. Using the knowledge about the channel error vectors, the beamforming design problem can be well optimized and robustness against errors can be achieved.

To design beamformers, channel coefficients should be known with some accuracy. In the beamformer design problems, three types of channel error models are mostly used.

2.1.1.1 Perfect CSI Model

In this model, channel coefficients are assumed to be perfectly known. Although it is unrealistic, the methods proposed for this case may provide some insights. Furthermore, in most cases, it is possible to modify the corresponding algorithms accordingly when the channel is partially known. The papers [28]-[42] all assume perfect CSI.

2.1.1.2 Norm Bounded Error Model

In this assumption, it is assumed that the error vectors are in some sphere with a known radius. This approach is used when the quantization error is dominant in channel estimation [27]. The works with this assumption perform beamforming design using worst-case SINRs which can be defined as the minimum value of SINRs for given error norm bounds. [24]-[27] are some of the reference papers using this model.

2.1.1.3 Statistical Error Model

This model assumes that second-order statistics of the channel estimation error vectors are known. This approach is used when the quantization error in the channel estimation is negligible and the main source of error is the thermal noise in the receivers performing the channel estimation [27]. In this model, the mean powers of signal, interference, and noise terms are used in the design process. [19]-[23] use this model.

2.1.2 Optimization Criteria

In the literature, there are different approaches to optimize the beamformers in a network. User data rates, user SINRs, power consumption, and the number of users served are widely used optimization parameters.

2.1.2.1 User Data Rate Maximization

In this method, the user data rates are maximized under transmit power and backhaul/fronthaul capacity constraints [32]-[34]. In general, minimum or a weighted sum of user data rates is maximized. In this approach, we optimize the beamformers to provide high data rates to users by using all available resources in the system.

2.1.2.2 SINR Maximization

By the Shannon capacity theorem, it can be shown that the achievable rate is an increasing function of the SINR [43]. Hence, to maximize the user data rates, a straightforward approach is to maximize user SINRs. A widely used approach includes the maximization of the minimum SINR of users under transmit power constraints [44]-[45]. This method is also called max-min fairness in the literature and can be viewed as a similar version of the problem of maximization of the minimum data rate of users.

2.1.2.3 Power Minimization

The transmit power is one of the major costs of an operator. By minimizing the power consumption, we also decrease the cost of cooling the equipment. Furthermore, the inter-cell interference will also be minimized when the transmit power is optimized. The power consumption should be considered in both backhaul/fronthaul links and access links. In general, access link power consumption has a higher portion in total consumption as the access link is wireless. On the other hand, the backhaul/fronthaul power consumption may not be negligible especially when a wireless transmission in backhaul/fronthaul links is performed.

The power minimization problem is also called Quality-of-Service (QoS) problem in the literature. In this approach, the total power spent in the system is minimized under user SINR constraints [24], [45]. In this method, it is guaranteed to satisfy a certain quality of service to each user by minimizing the total power consumption in both backhaul/fronthaul and access links.

2.1.2.4 User Admission

The number of devices participating in the network grows exponentially in new-generation communication systems. When the channel conditions are not good enough, it may not be possible to serve all UEs in a cluster. In such cases, a useful approach is to maximize the number of users served. This problem is studied under the user admission problem in the literature [38]. In the related method, a predefined SINR threshold value is used to determine whether a user is served. It is assumed to have as many users as possible with SINRs larger than the threshold value.

2.1.2.5 Hybrid Criteria

An operator may prefer to jointly optimize some set of data rate, SINR, power, and user admission criteria. In such a case, an objective function including the selected optimization parameters is defined. A widely used objective function consists of a weighted sum of the target parameters. In [37], the cost function consists of a weighted sum of the total transmit power and the total fronthaul data in a downlink C-RAN system. In [17], we use a linear combination of the number of users served, total fronthaul data, and the normalized power consumption as the objective function.

2.2 Notations

Throughout the thesis, the vectors are denoted by bold lowercase letters and matrices are denoted by bold uppercase letters. $(\cdot)^T, (\cdot)^H, \mathrm{tr}(\cdot), \mathbb{E}(\cdot), \|\cdot\|, \mathrm{sgn}(\cdot)$, and $\otimes$ indicate the transpose, conjugate transpose, trace, expectation, ℓ_2 norm, sign, and kronecker product operators, respectively. $\mathbf{0}$ describes the all-zero matrix, $\mathbf{0}_{m\times n}$ and $\mathbf{1}_{m\times n}$ are all-zero and all-one matrices with dimensions $m \times n$, respectively. $\mathbf{I}_n$ is $n \times n$ identity matrix, and $\mathbf{A} \succeq 0$ implies that the matrix $\mathbf{A}$ is Hermitian and positive semi-definite. $\mathrm{diag}(x_1, x_2, \ldots, x_n)$ denotes the diagonal matrix with diagonal elements $x_1, x_2, \ldots, x_n$ and $\mathrm{diag}(\mathbf{A})$ is the diagonal matrix with diagonal entries of the matrix $\mathbf{A}$. $\mathrm{vec}(\mathbf{A})$ denotes the column vector formed by the columns of the matrix $\mathbf{A}$ in their natural order. $\mathbb{C}$ is the set of complex numbers. $\delta[\cdot]$ corresponds to the function satisfying $\delta[0] = 1,\ \delta[x] = 0$ for all $x \neq 0$. $\lambda_{\text{min}}(\cdot), \lambda_{\text{max}}(\cdot), \lambda_i(\cdot), e_i(\cdot)$ denote the minimum eigenvalue, maximum eigenvalue, i-th largest eigenvalue and the corresponding unit-norm eigenvector of the corresponding Hermitian positive semi-definite (PSD) matrix, respectively. $\mathbf{x} \sim \mathcal{CN}(\mathbf{m}, \mathbf{C})$ means that $\mathbf{x}$ is a circularly symmetric complex Gaussian random vector with mean vector $\mathbf{m}$ and covariance matrix $\mathbf{C}$.

2.3 General System Models

2.3.1 MIMO Communications

Using multiple antennas at transmitter and receiver sides in a communication system can increase the signal SINRs and provides higher data rates. For AWGN channels, the SINR can be increased by a factor of the number of transmit/receive antennas by maximal ratio combining. When there is some fading in the channel, MIMO communications can further increase the performance using spatial diversity. In this case, beamforming can decrease the fluctuation of the received signal strength. When the fading in different transmit-receive antenna pairs are independent, the gain provided by beamforming becomes much better.

When there are multiple users to be served, one can use the spatial domain to multiplex different user signals. For a flat fading channel between a transmitter and receiver, the augmented user signal vector $\mathbf{x} = [x_1 x_2 \ldots x_K]^T$ is sent by the transmitter. The received noise-free signal $\mathbf{r}$ can be written as

$$\mathbf{r} = \mathbf{HWx} \tag{2.1}$$

where $\mathbf{W}$ is the beamforming matrix and $\mathbf{H}$ is the channel matrix. The matrix $\mathbf{HW}$ is referred to as the effective channel matrix of the receiver. The number of columns of the effective channel matrix is equal to the number of users.

Theoretically, the number of users to be served in the same time/frequency resource can be as high as the rank of the corresponding channel matrix. The dimension of the range space of $\mathbf{HW}$ is at most the rank of $\mathbf{H}$. For a receiver to obtain $x_1, x_2, \ldots, x_K$ separately, the equation (2.1) should have a unique solution. This is true when the dimension of the range space of the matrix $\mathbf{HW}$ is equal to the number of users. As the rank of a matrix is limited by the number of columns, we conclude that in a multi-user MIMO system, the number of users simultaneously served in the same time/frequency resource can be at most the number of transmit antennas.

Throughout the thesis, we assume that multiple-antenna base stations serve multiple users each with a single antenna. This system can be considered as a distributed multi-user multiple-input-single-output (MISO) system.

2.3.2 Propagation Models

To design beamformers for MIMO systems, the corresponding channel coefficients should be estimated. In this study, we assume that all channels are flat fading, constant over a transmission period, and known by CP by some additive error. The channel estimation can be performed using pilot signals in the uplink transmission stage for time-division-duplex systems.

We assume that beamforming coefficients are designed for narrowband signals where the channel is assumed to be flat fading. For OFDMA systems, this corresponds to design beamformers for each resource block. We model channel coefficients considering large and small-scale fading effects. The large-scale effects are composed of distance-dependent path-loss and log-normal shadowing. We adopt some path-loss models according to the network type, base station type, and distance between transmitter and receiver. The shadowing variance also depends on the network and base station type. The small-scale fading is formed by Rayleigh distribution. We assume that the small-scale fading component is a complex random variable with independent Gaussian real and imaginary parts. The channel coefficient between a transmitter and receiver antenna pair is given by

$$h = h_{\text{large}} h_{\text{small}} \tag{2.2}$$

where $h_{\text{large}} = 10^{(a+b\log(d))/20}$ and $h_{\text{small}} \sim \mathcal{CN}(0,1)$. Here a and b are parameters of the path-loss model, and d denotes the distance between the transmitter and the receiver. In general, the parameters a and b depend on the frequency, and the network and base station types.

2.3.3 User and Base Station Locations

In all thesis work, we consider a cluster of UEs and BSs. All users and BSs in this cluster are distributed in a circular area. We focus on a specific time/frequency resource block to serve multiple users in a cluster. We ignore inter-cluster interference due to other nearby clusters. This can be achieved by using different frequency resource blocks for adjacent clusters.

The base station antennas cover some interval of elevation angles and hence the signal levels are low when the receiver is very close to the base station. Due to this fact, we need different path-loss models for small distances. Furthermore, because of security reasons, it will not be possible to be present very close to a base station. Therefore, we define forbidden regions around base stations and distribute all users randomly in the permitted region following a uniform distribution.

2.3.4 Coordinated Transmission

When BSs are managed by a central unit, it becomes possible to serve a user by jointly coordinated transmissions. We assume that the time synchronization of coordinated

BSs is perfect. Multiple BSs transmit the same information from different locations simultaneously to the same UE. In this scenario, the received noise-free signal r_k of the k-th UE can be written as

$$r_k = \sum_{n=1}^{N} \mathbf{h}_{k,n}^H \mathbf{w}_{k,n} s_k \tag{2.3}$$

where $\mathbf{h}_{k,n}$'s are channel vectors between BSs and the k-th UE, and $\mathbf{w}_{k,n}$'s are beamformer vectors for the k-th user signal. (We define $\mathbf{h}_{k,n}$ as a column vector and hence we use the term $\mathbf{h}_{k,n}^H$ in the received signal equation.) s_k denotes the k-th user information signal. According to this model, as we assume perfect time synchronization, the received signals coming from all BSs are coherently added at the user receiver. When the beamformer vectors are jointly optimized by the central unit, the received signal power can be increased and the performance of the system can be enhanced.

2.4 Radio Access Network Types and Signal Models

In multi-base-station networks, base stations share the user data among each other to increase the coverage. In C-RAN, the user fronthaul data is transmitted from CP to RRHs. In IAB, the user backhaul data is sent from MBSs to SBSs. In this thesis, we consider C-RAN with wired and wireless fronthaul, and IAB networks having wireless backhaul. For each network type, we derive the system model and define the necessary parameters. The received signals by the RRHs, SBSs, and UEs will be written in terms of channel and beamformer vectors. These models will be used in SINR derivations and beamformer design methods that we propose.

2.4.1 C-RAN with Wired Fronthaul

The standard C-RAN includes a wired fronthaul where user data is sent by CP to RRHs over fiber optical cables. Throughout this thesis, in these types of networks, we consider a downlink C-RAN scenario where there are N RRHs, which are all connected to a CP via wired fronthaul links, and K users. Each RRH has L antennas and each UE has a single antenna. All RRH-to-UE channels include both small and large scale fading and they are assumed to be constant over a transmission period.

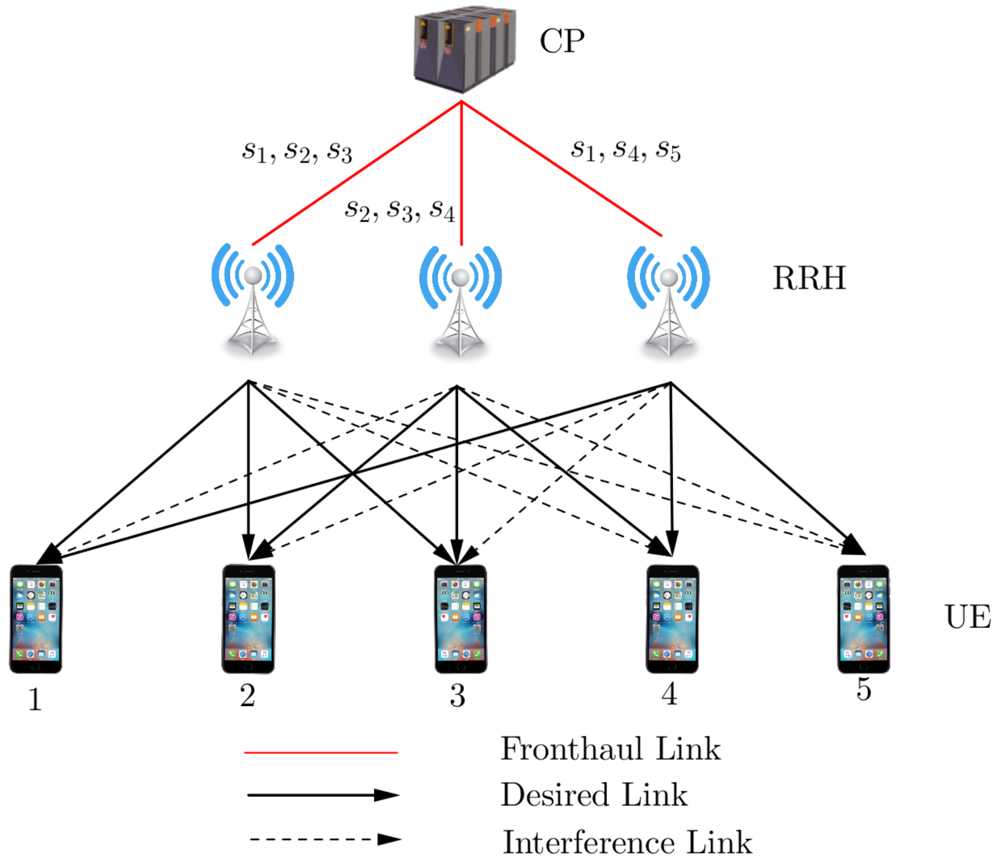

Figure 2.1: A block diagram of a downlink C-RAN with wired fronthaul.

In Fig. 2.1, we see a typical block diagram of a downlink C-RAN with wired fronthaul. In this example, there are 3 RRHs and 5 UEs. Each RRH serves 3 UEs. There are 9 data streams in total transmitted through fronthaul links.

In Table 2.1, we list all variables used in the equations derived for C-RAN with wired fronthaul. We use the complex baseband model. We denote the channel and the corresponding beamformer vectors between the n-th RRH and the k-th UE as $\mathbf{h}_{k,n} \in \mathbb{C}^L$ and $\mathbf{w}_{k,n} \in \mathbb{C}^L$, respectively.

Table 2.1: Description of Variables for C-RAN with Wired Fronthaul

Variable	Description
K	the number of UEs
N	the number of RRHs
L	the number of RRH antennas
s_k : scalar	user data of the k-th UE
$\mathbf{h}_{k,n}$: $L \times 1$	true channel vector between the n-th RRH and the k-th UE
$\widehat{\mathbf{h}}_{k,n}$: $L \times 1$	estimated channel vector between the n-th RRH and the k-th UE
$\Delta\mathbf{h}_{k,n}$: $L \times 1$	channel error vector between the n-th RRH and the k-th UE
$\mathbf{h}_k = [\mathbf{h}_{k,1}^T\ \mathbf{h}_{k,2}^T\ \cdots\ \mathbf{h}_{k,N}^T]^T$	augmented true channel vector between the RRHs and the k-th UE
$\widehat{\mathbf{h}}_k = [\widehat{\mathbf{h}}_{k,1}^T\ \widehat{\mathbf{h}}_{k,2}^T\ \cdots\ \widehat{\mathbf{h}}_{k,N}^T]^T$	augmented estimated channel vector between the RRHs and the k-th UE
$\Delta\mathbf{h}_k = [\Delta\mathbf{h}_{k,1}^T\ \Delta\mathbf{h}_{k,2}^T\ \cdots\ \Delta\mathbf{h}_{k,N}^T]^T$	augmented channel error vector between the RRHs and the k-th UE
$\mathbf{w}_{k,n}$: $L \times 1$	beamforming vector of the n-th RRH for the k-th UE
$\mathbf{w}_k = [\mathbf{w}_{k,1}^T\ \mathbf{w}_{k,2}^T\ \cdots\ \mathbf{w}_{k,N}^T]^T$	augmented beamforming vector of the k-th UE
$z_{\text{UE},k}$: scalar	receiver noise term of the k-th UE
$\sigma_{\text{UE},k}^2$	average receiver noise power of the k-th UE
$\sigma_{k,n}^2$	average channel estimation error power of $\Delta\mathbf{h}_{k,n}$

We use the statistical channel error model where the second order statistics of the additive channel error vectors are known. We use the channel model

$$\mathbf{h}_{k,n} = \widehat{\mathbf{h}}_{k,n} + \Delta\mathbf{h}_{k,n} \tag{2.4}$$

where $\widehat{\mathbf{h}}_{k,n}$ is the estimated channel vector for the channel between the n-th RRH and k-th UE, and $\Delta\mathbf{h}_{k,n}$ is the corresponding error with $\Delta\mathbf{h}_{k,n} \sim \mathcal{CN}(0, \sigma_{k,n}^2\mathbf{I}_L)$. $\Delta\mathbf{h}_{k,n}$'s are assumed to be independent for all k, n. We assume that $\sigma_{k,n}$ for all k, n is known by CP. In this study, we assume that CP uses instantaneous channel estimates $\widehat{\mathbf{h}}_{k,n}$ and error standard deviations $\sigma_{k,n}$ to design transmit beamformers.

If the n-th RRH does not send the data of the k-th UE, then we assume that $\mathbf{w}_{k,n} = \mathbf{0}$. We define augmented channel and beamformer vectors as $\mathbf{h}_k = \widehat{\mathbf{h}}_k + \Delta\mathbf{h}_k = [\mathbf{h}_{k,1}^T\ \ \mathbf{h}_{k,2}^T\ \ \cdots\ \ \mathbf{h}_{k,N}^T]^T$ and $\mathbf{w}_k = [\mathbf{w}_{k,1}^T\ \ \mathbf{w}_{k,2}^T\ \ \cdots\ \ \mathbf{w}_{k,N}^T]^T$. We denote the information data of the k-th user by s_k whose power is assumed to be unity. We assume that

$z_{\text{UE},k} \sim \mathcal{CN}(0, \sigma^2_{\text{UE},k})$ where $z_{\text{UE},k}$ is the noise term in the k-th UE receiver. In this case, the signal received by the k-th UE can be expressed by

$$\begin{aligned} r_{\text{wired},k} &= \sum_{n=1}^{N} \mathbf{h}_{k,n}^H \sum_{\ell=1}^{K} \mathbf{w}_{n\ell} s_\ell + z_{\text{UE},k} = \mathbf{h}_k^H \sum_{\ell=1}^{K} \mathbf{w}_\ell s_\ell + z_{\text{UE},k} \\ &= \underbrace{\widehat{\mathbf{h}}_k^H \mathbf{w}_k s_k}_{\text{desired}} + \underbrace{\Delta \mathbf{h}_k^H \mathbf{w}_k s_k}_{\text{mismatch}} + \underbrace{\mathbf{h}_k^H \sum_{\ell \neq k} \mathbf{w}_\ell s_\ell}_{\text{interference}} + \underbrace{z_{\text{UE},k}}_{\text{noise}}, \quad \forall k. \end{aligned} \tag{2.5}$$

In (2.5), the desired part includes the desired signal for the k-th UE. Notice that it contains only the channel estimate for the k-th user which is the only useful part for the receiver of the corresponding UE. We assume that the effective channel coefficient $\widehat{\mathbf{h}}_k^H \mathbf{w}_k$ is known by the k-th user. The mismatch part is stemming from the channel error for the k-th user signal. Although it includes s_k term, the corresponding signal is not useful as its coefficient is not known by the receiver due to uncertainty in the channel estimates. The interference part contains the interference signal including the signals for other users. The noise term is related to UE receiver noise.

Notice that when we have a perfect channel knowledge, we can obtain the related equations by setting $\sigma_{k,n} = 0$ for all k, n. In this case, the mismatch part becomes zero as there is no channel estimation error.

2.4.1.1 Literature Overview

There are a lot of studies related to C-RAN with wired fronthaul. The beamforming design and user selection methods involve different techniques. ℓ_0/ℓ_1 norm approximation [46]-[51], group sparse beamforming with ℓ_0/ℓ_2 norm approximation [39], [52], [53], successive convex approximation [54]-[55], uplink-downlink duality [56], smooth approximation with subspace projection [37], [57], zero-forcing beamforming [58], heuristic search with convex optimization [41], [42] are some of the techniques used in the C-RAN system optimization. As another approach, it can be aimed to find the largest set of users which can be served by the RRHs where each user data is sent only by a single RRH [38]. The power consumption of RRHs under active and sleeping modes can also be included in the power minimization problem as done in [39], [57]. In [37], the cost function consists of a weighted sum of the total transmit power and the total fronthaul data. Cluster formation [59], effect of user traffic delay [60], and codebook-based designs [55] are also analyzed in the literature.

2.4.2 C-RAN with Wireless Fronthaul

The C-RAN with wireless fronthaul concept is similar to two-hop multi-destination multi-antenna relaying networks. Usage of wireless fronthaul decreases the cost of deployment of fiber cables at the expense of higher interference and worse channel conditions in fronthaul transmissions.

In C-RAN with wireless fronthaul, RRHs forward user data, and they are used as relays. In relay systems, there are different types of multi-hop mechanisms such as AF, decode-and-forward (DF), and decompress-and-forward (DCF), etc. The corresponding method is determined by the operation applied by RRHs to the signal received from fronthaul links before transmitting to users. AF-type systems are the simplest ones where RRHs only apply some scaling to the received data [24]-[25]. In DF-based systems, RRHs apply decoding to the UE data requiring baseband processing ability for RRHs [28]-[29]. In DCF-based systems, both decoding and decompressing capabilities are necessary [30]-[31]. In DF and DCF based systems, some cooperation should be performed between CP and RRHs to decide which RRHs to decode which user data. In general, this requires a combinatorial search that makes the design complex. On the other hand, as the user data is decoded, assuming perfect decoding for sufficiently high SINR, the interference between user signals can be eliminated at RRHs allowing to satisfy a higher performance for users. In general, AF systems are simpler but when we use AF relaying, the interference cannot be perfectly eliminated at RRHs. In C-RAN systems, it is intended to make RRHs as simple as possible to decrease the deployment cost, and hence AF systems are more attractive.

In the wireless fronthaul case, frequency bands of the fronthaul and the access links (links between RRHs and UEs) may be the same or different. In the in-band scenario where the two frequency bands are the same, the RRHs should be capable of performing self-interference cancellation which increases the equipment complexity. To make the RRHs simpler, either the two frequency bands may be separated or a time-division-based transmission can be used.

We consider the downlink of a C-RAN cluster including a CP with M antennas, N RRHs each with L transmit/receive antennas, and K UEs each with a single antenna. All CP-to-RRH and RRH-to-UE channels are assumed to be flat, constant over a transmission period. We assume a two-stage transmission scheme where fronthaul and access link transmissions are performed in different time slots. In the first stage, the user data is sent from CP to RRHs over wireless channels. RRHs apply some linear transformation to the received data as in AF relaying using beamforming matrices and forward the transformed signal to the UEs in the second stage. We assume that RRHs are simple radio units without the capability of baseband processing and hence they cannot decode the user data. Therefore, AF relaying mechanism is considered in this model. In Fig. 2.2, we see the general block diagram of the model used.

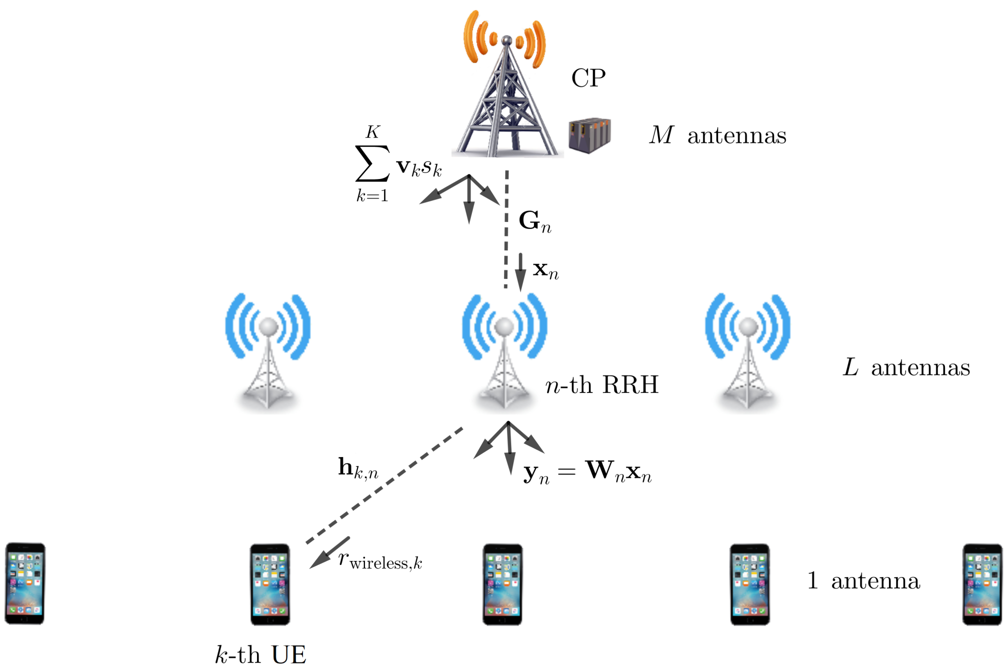

Figure 2.2: Block Diagram of Downlink C-RAN with Wireless Fronthaul.

Table 2.2 shows all variables used in the equations derived for wireless fronthaul case. We consider the complex baseband model and denote the channel between CP and n-th RRH as $\mathbf{G}_n \in \mathbb{C}^{M\times L}$, the channel between n-th RRH and k-th UE as $\mathbf{h}_{k,n} \in \mathbb{C}^{L}$, the beamformer vector of CP for k-th UE as $\mathbf{v}_k \in \mathbb{C}^{M}$, and beamforming matrix for n-th RRH as $\mathbf{W}_n \in \mathbb{C}^{L\times L}$. The received signal of the n-th RRH in the first transmission

Table 2.2: Description of Variables for C-RAN with Wireless Fronthaul

Variable	Description
K	the number of UEs
N	the number of RRHs
L	the number of RRH antennas
M	the number of CP antennas
s_k : scalar	user data of the k-th UE
$\mathbf{h}_{k,n}$: $L \times 1$	true channel vector between the n-th RRH and the k-th UE
$\widehat{\mathbf{h}}_{k,n}$: $L \times 1$	estimated channel vector between the n-th RRH and the k-th UE
$\Delta\mathbf{h}_{k,n}$: $L \times 1$	channel error vector between the n-th RRH and the k-th UE
$\mathbf{h}_k = [\mathbf{h}_{k,1}^T\ \mathbf{h}_{k,2}^T\ \cdots\ \mathbf{h}_{k,N}^T]^T$	augmented true channel vector between the RRHs and the k-th UE
$\widehat{\mathbf{h}}_k = [\widehat{\mathbf{h}}_{k,1}^T\ \widehat{\mathbf{h}}_{k,2}^T\ \cdots\ \widehat{\mathbf{h}}_{k,N}^T]^T$	augmented estimated channel vector between the RRHs and the k-th UE
$\Delta\mathbf{h}_k = [\Delta\mathbf{h}_{k,1}^T\ \Delta\mathbf{h}_{k,2}^T\ \cdots\ \Delta\mathbf{h}_{k,N}^T]^T$	augmented channel error vector between the RRHs and the k-th UE
$\mathbf{G}_n$: $M \times L$	true channel matrix between the CP and the n-th RRH
$\widehat{\mathbf{G}}_n$: $M \times L$	estimated channel matrix between the CP and the n-th RRH
$\Delta\mathbf{G}_n$: $M \times L$	channel error matrix between the CP and the n-th RRH
$\mathbf{G} = [\mathbf{G}_1\ \mathbf{G}_2\ \cdots\ \mathbf{G}_N]$	augmented channel matrix between CP and RRHs
$\mathbf{W}_n$: $L \times L$	beamforming matrix of the n-th RRH
$\mathbf{W} = \text{diag}\left(\mathbf{W}_1,\ \mathbf{W}_2,\ \ldots,\ \mathbf{W}_N\right)$	augmented beamforming matrix of the n-th RRH
$\mathbf{v}_k$: $M \times L$	beamforming vector of the CP for the k-th UE
$z_{\text{UE},k}$: scalar	receiver noise term of the k-th UE
$\mathbf{z}_{\text{RRH},n}$: $L \times 1$	receiver noise term of the n-th RRH
$\mathbf{z}_{\text{RRH}} = [\mathbf{z}_{\text{RRH},1}^T\ \mathbf{z}_{\text{RRH},2}^T\ \cdots\ \mathbf{z}_{\text{RRH},N}^T]^T$	augmented noise vector of RRHs
$\sigma_{\text{UE},k}^2$	average receiver noise power of the k-th UE
$\sigma_{\text{RRH},n}^2$	average receiver noise power of each receive channel of the n-th RRH
$\sigma_{1,n}^2$	variance of each entry of $\Delta\mathbf{G}_n$
$\sigma_{2,k,n}^2$	variance of each entry of $\Delta\mathbf{h}_{k,n}$

stage can be written as

$$\mathbf{x}_n = \mathbf{G}_n^H \sum_{k=1}^{K} \mathbf{v}_k s_k + \mathbf{z}_{\text{RRH},n}, \quad n = 1, 2, \ldots, N \tag{2.6}$$

where s_k denotes the k-th UE data which satisfies $\mathbb{E}[|s_k|^2] = 1, \quad \forall k = 1, 2, \ldots, K$ and $\mathbf{z}_{\text{RRH},n} \sim \mathcal{CN}(\mathbf{0}, \sigma^2_{\text{RRH},n}\mathbf{I}_L)$ is the noise term in the corresponding RRH. After the first stage, the transformed signal by n-th RRH is given by

$$\mathbf{y}_n = \mathbf{W}_n \mathbf{x}_n, \quad n = 1, 2, \ldots, N. \tag{2.7}$$

In this case, the received signal by the k-th UE can be expressed by

$$\begin{aligned} r_{\text{wireless},k} &= \sum_{n=1}^{N} \mathbf{h}_{k,n}^H \mathbf{y}_n + z_{\text{UE},k} = \sum_{n=1}^{N} \mathbf{h}_{k,n}^H \mathbf{W}_n \left(\mathbf{G}_n^H \sum_{\ell=1}^{K} \mathbf{v}_\ell s_\ell + \mathbf{z}_{\text{RRH},n} \right) + z_{\text{UE},k} \\ &= \sum_{n=1}^{N} \mathbf{h}_{k,n}^H \mathbf{W}_n \mathbf{G}_n^H \mathbf{v}_k s_k + \sum_{n=1}^{N} \sum_{\ell \neq k}^{K} \mathbf{h}_{k,n}^H \mathbf{W}_n \mathbf{G}_n^H \mathbf{v}_\ell s_\ell + \sum_{n=1}^{N} \mathbf{h}_{k,n}^H \mathbf{W}_n \mathbf{z}_{\text{RRH},n} \\ &+ z_{\text{UE},k}. \end{aligned} \tag{2.8}$$

Here $z_{\text{UE},k} \sim \mathcal{CN}(0, \sigma^2_{\text{UE},k})$ denotes the noise term in the k-th UE. In order to simplify expressions, we define augmented channel, beamformer and noise vectors/matrices as given below:

$$\begin{aligned} &\mathbf{h}_k = [\mathbf{h}_{k,1}^T \; \mathbf{h}_{k,2}^T \; \cdots \; \mathbf{h}_{k,N}^T]^T, \quad \mathbf{W} = \text{diag}\left(\mathbf{W}_1, \; \mathbf{W}_2, \; \ldots, \; \mathbf{W}_N\right), \\ &\mathbf{G} = [\mathbf{G}_1 \; \mathbf{G}_2 \; \cdots \; \mathbf{G}_N], \quad \mathbf{z}_{\text{RRH}} = [\mathbf{z}_{\text{RRH},1}^T \; \mathbf{z}_{\text{RRH},2}^T \; \cdots \; \mathbf{z}_{\text{RRH},N}^T]^T. \end{aligned} \tag{2.9}$$

Using the augmented variables, we can write $r_{\text{wireless},k}$ as

$$r_{\text{wireless},k} = \mathbf{h}_k^H \mathbf{W} \mathbf{G}^H \mathbf{v}_k s_k + \sum_{\ell \neq k} \mathbf{h}_k^H \mathbf{W} \mathbf{G}^H \mathbf{v}_\ell s_\ell + \mathbf{h}_k^H \mathbf{W} \mathbf{z}_{\text{RRH}} + z_{\text{UE},k}. \tag{2.10}$$

We model the channel estimates as $\mathbf{G}_n = \widehat{\mathbf{G}}_n + \Delta\mathbf{G}_n, \; \mathbf{h}_{k,n} = \widehat{\mathbf{h}}_{k,n} + \Delta\mathbf{h}_{k,n}$ where $\widehat{\mathbf{G}}_n$ and $\widehat{\mathbf{h}}_{k,n}$ are channel estimates, $\Delta\mathbf{G}_n$ is a zero-mean complex Gaussian matrix with independent entries each with variance $\sigma^2_{1,n}$ and $\Delta\mathbf{h}_{k,n} \sim \mathcal{CN}\left(\mathbf{0}, \sigma^2_{2,k,n}\mathbf{I}_L\right)$ is a circularly symmetric Gaussian vector. We also assume that $\Delta\mathbf{G}_n$ and $\Delta\mathbf{h}_{k,n}$ are independent for all k and n. Using the error vectors and matrices, we can form the corresponding augmented variables as shown in (2.11).

$$\begin{aligned} &\widehat{\mathbf{h}}_k = [\widehat{\mathbf{h}}_{k,1}^T \; \widehat{\mathbf{h}}_{k,2}^T \; \cdots \; \widehat{\mathbf{h}}_{k,N}^T]^T, \quad \widehat{\mathbf{G}} = \left[\widehat{\mathbf{G}}_1 \; \widehat{\mathbf{G}}_2 \; \cdots \; \widehat{\mathbf{G}}_N\right], \\ &\Delta\mathbf{h}_k = [\Delta\mathbf{h}_{k1}^T \; \Delta\mathbf{h}_{k2}^T \; \cdots \; \Delta\mathbf{h}_{kN}^T]^T, \quad \Delta\mathbf{G} = [\Delta\mathbf{G}_1 \; \Delta\mathbf{G}_2 \; \cdots \; \Delta\mathbf{G}_N]. \end{aligned} \tag{2.11}$$

Using the new variables and (2.10), we can write $r_{\text{wireless},k}$ as

$$r_{\text{wireless},k} = \underbrace{\widehat{\mathbf{h}}_k^H \mathbf{W} \widehat{\mathbf{G}}^H \mathbf{v}_k s_k}_{\text{desired}} + \underbrace{\left(\mathbf{h}_k^H \mathbf{W} \mathbf{G}^H \mathbf{v}_k - \widehat{\mathbf{h}}_k^H \mathbf{W} \widehat{\mathbf{G}}^H \mathbf{v}_k \right) s_k}_{\text{interference part 1}} + \underbrace{\sum_{\ell \neq k} \mathbf{h}_k^H \mathbf{W} \mathbf{G}^H \mathbf{v}_\ell s_\ell}_{\text{interference part 2}}$$
$$+ \underbrace{\mathbf{h}_k^H \mathbf{W} \mathbf{z}_{\text{RRH}} + z_{\text{UE},k}}_{\text{noise}} . \tag{2.12}$$

In (2.12), the desired part includes the desired signal for the k-th UE. Notice that it contains only the channel estimates for the k-th UE which is the only useful part for the receiver of the corresponding UE. Interference part 1 is related to the channel mismatch for the k-th UE signal. Although it includes the s_k term, the corresponding signal is not useful as its coefficient is not known by the receiver due to uncertainty in the channel estimates. Interference part 2 is the actual interference signal including the signals for other users. The noise term is the combination of the amplified and forwarded RRH receiver noise and UE receiver noise.

2.4.2.1 Literature Overview

Works related to wireless fronthaul cases are limited in number compared to the standard wired case. The problem for wireless fronthaul case is similar to two-hop relaying. Most studied relaying mechanisms for C-RAN with wireless fronthaul concept are AF, DF, and DCF. In [28] DF relaying is assumed where each RRH can decode only a single user's data at once. If more than one user's data is to be decoded, decoding is done by time division. The combinatorial problem of choosing the set of user data to be decoded by each RRH is solved in [28] while an semi-definite relaxation (SDR) based beamformer optimization is done under the perfect CSI assumption. [29] also analyzes DF relaying where a weighted sum of user data rates is maximized under power transmit limit. There is a constraint that each RRH can serve a single user. Beamformer optimization is performed using SDR and perfect CSI is assumed. In [30] both DF and DCF approaches are considered where the set of user data to be decoded by each RRH is assumed to be known and beamforming optimization is done using the difference of convex method. Data rate maximization under power limit is analyzed for the perfect CSI case. [31] is the generalized version of [30] where there is more than one RRH cluster each controlled by a different CP. [24] uses AF type relaying with a norm-bounded channel estimation error model. Using worst-case SINR formulas total power is minimized under SINR constraints. In that work, fronthaul beamformers are assumed to be known and access link beamformers are designed using SDR methods along with a zero-forcing based approach implemented for comparison. In [25], a two-hop AF relaying problem is studied under the norm-bounded channel error model. As all independent sources have a single antenna, fronthaul beamforming is not applicable, only access link beamforming design is studied. SDR method is used to minimize the total transmit power under SINR constraints.

2.4.3 Integrated Access and Backhaul (IAB)

In IAB, there are macro and small base stations denoted by MBS and SBS, respectively. They are also referred to as IAB donors and IAB nodes [12]. The main properties of MBS and SBS are listed below [13]:

MBS:
1) MBS is connected to the core network by cables.
2) MBS can directly serve a user.
3) MBS can send the backhaul data of some users to SBSs to increase the coverage.

SBS:
1) Core network access is not available.
2) They can be used as decode-and-forward type relays. They can decode the user backhaul data coming from MBSs.
3) They can serve a set of users.
4) They can broadcast the user backhaul data to other SBSs. (Multi-hop relaying)
5) SBSs can use the same antennas for backhaul transmissions between MBSs and access link transmissions between UEs. (Virtual IAB mobile termination antenna)
6) SBSs can use full-duplex radio where backhaul and access link transmissions are performed in the same time/frequency resources.

In Fig. 2.3, we see a typical IAB system diagram.

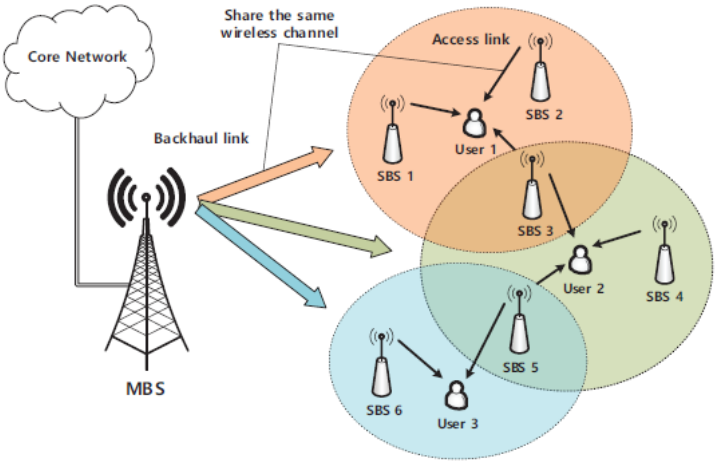

Figure 2.3: A typical full-duplex IAB system diagram [14].

C-RAN has a lot of similarities to IAB. C-RAN with wireless fronthaul can be viewed as a special case of IAB. We list the similarities and differences of IAB and C-RAN in Table 2.3:

Table 2.3: IAB vs C-RAN

IAB	C-RAN
MBS sends the backhaul data to SBSs	CP sends the fronthaul data to RRHs
SBSs are used as relays	RRHs are used as relays
Half/Full-duplex radio in SBS is possible	Half/Full-duplex radio in RRH is possible
SBSs decodes the backhaul data	RRHs can use AF, DF, or DCF type relaying
MBS can directly serve users	In standard C-RAN, only RRHs send access link data to users

We design beamformers for a downlink full-duplex IAB system. To obtain the system model, we follow the assumptions given below:

1) There is a single MBS sharing user backhaul data with N SBSs. There are K UEs.
2) Single hop relaying is used. SBSs do not share the backhaul data.
3) MBS-to-SBS and SBS-to-UE transmissions are performed in the same time slot and frequency band. MBS-to-UE transmissions (direct access) are performed in the orthogonal resource blocks and do not interfere with MBS-to-SBS and SBS-to-UE

transmissions.
4) MBS has M antennas, UEs have a single antenna. SBSs have $L+1$ antennas. They use 1 antenna to receive the backhaul signals from MBS and L antennas to transmit user data in access links.
5) A user k is served by a set $\mathcal{N}_k$ of SBSs. Different $\mathcal{N}_k$ sets may overlap. An SBS n serves a set $\mathcal{K}_n$ of users. Different $\mathcal{K}_n$ sets may overlap.
6) SBSs can perform self-interference cancellation to eliminate the interference signal due to access links.

In this study, we do not consider direct access by MBS to UEs as it is a well-known multi-user beamforming problem. We focus on relaying scheme consisting of MBS-to-SBS and SBS-to-UE transmissions. We consider backhaul and access links separately. In Table 2.4, we list the description of variables used in the equations.

Table 2.4: Description of Variables for IAB

Variable	Description
$\mathcal{K}_n$	index set of users served by the n-th SBS
$\mathcal{N}_k$	index set of SBSs serving the k-th UE
s_k^A : scalar	access link data of k-th UE
s_k^B : scalar	backhaul link data of k-th UE
$\mathbf{h}_{k,n}$: $L \times 1$	channel vector between the n-th SBS and the k-th UE
$\mathbf{h}_{k,0}$: $M \times 1$	channel vector between the MBS and the k-th UE
$\mathbf{g}_{m,n}$: $L \times 1$	channel vector between the n-th SBS and the m-th SBS
$\mathbf{g}_{n,0}$: $M \times 1$	channel vector between the MBS and the n-th SBS
$\mathbf{v}_k$: $M \times 1$	backhaul link beamforming vector of the MBS for the k-th UE
$\mathbf{w}_{k,n}$: $L \times 1$	access link beamforming vector of the n-th SBS for the k-th UE
β_{SI}	reduction factor of self-interference in SBSs
$z_{\text{SBS},n}$: scalar	receiver noise term of n-th SBS
$z_{\text{UE},k}$: scalar	receiver noise term of k-th UE
$\sigma^2_{\text{SBS},n}$	average receiver noise power of n-th SBS
$\sigma^2_{\text{UE},k}$	average receiver noise power of k-th UE

To interpret the sets $\mathcal{K}_n$ and $\mathcal{N}_k$, we define a network link matrix $\mathbf{C}$ with dimensions

$K \times N$ and entries $c_{k,n}$ such that $c_{k,n} = 0$ if and only if $k \in \mathcal{K}_n$ and $n \in \mathcal{N}_k$, and $c_{k,n} = 1$ otherwise. We assume that if $c_{k,n} = 1$ then $\mathbf{w}_{k,n} = 0$. In other words, if a user is not served by an SBS, then the corresponding access link beamformer is set to zero. We also assume that the signal terms s_k^A and s_k^B have unity power for all k.

2.4.3.1 Backhaul Link

To serve all users in a cluster of MBS, SBSs, and UEs, all user backhaul data is sent from MBS to SBSs. The received signal of n-th SBS can be written as

$$x_{\text{backhaul},n} = \sum_{k=1}^{K} \mathbf{g}_{n,0}^H \mathbf{v}_k s_k^B + \sum_{k=1}^{K} \sum_{m=1}^{N} \mathbf{g}_{m,n}^H \mathbf{w}_{k,m} s_k^A + z_{\text{SBS},n}. \tag{2.13}$$

The second term in the equation (2.13) includes both self-interference of n-th SBS and interference due to access link transmissions of other SBSs. We assume that the self-interference term can be reduced by a factor β_{SI}.

2.4.3.2 Access Link

In the access link, user access link data is sent from SBSs to UEs. It is assumed that each SBS can decode the related user data perfectly in the backhaul transmission stage and form the user access link data without any error. The received signal by the k-th user can be written as

$$x_{\text{access},k} = \sum_{n=1}^{N} \mathbf{h}_{k,n}^H \mathbf{w}_{k,n} s_k^A + \sum_{\ell \neq k}^{K} \sum_{n=1}^{N} \mathbf{h}_{k,n}^H \mathbf{w}_{\ell,n} s_\ell^A + \sum_{\ell=1}^{K} \mathbf{h}_{k,0}^H \mathbf{v}_\ell s_\ell^B + z_{\text{UE},k}. \tag{2.14}$$

In (2.14), the first term is the desired signal term, the second term corresponds to the multi-user interference in the access link and the third term is related to the interference due to backhaul transmissions.

2.4.3.3 Literature Overview

For IAB systems, the related literature work is generally studied under self-backhauling. Interference mitigation [61]-[63], power minimization [64]-[66], throughput maximization [67]-[69], utility optimization [70]-[72], energy [73] and spectral efficiency maximization [74]-[75] are investigated in the literature.

2.5 Contributions of the Thesis

The thesis studies focus on beamformer design in downlink transmissions of C-RAN with wired and wireless fronthaul and IAB. We propose novel beamforming algorithms and state-of-the-art theoretical performance bounds. We list all contributions in the following subsections.

2.5.1 Cooperation Optimization in C-RAN with Capacity Limited Wired Fronthaul

In this study, we aim to find a cooperation scheme under per-RRH data transfer constraint where each RRH can send a limited number of user data streams, which can be used to ensure not to exceed the capacity of any of the fronthaul links [15]. The original problem is NP-hard and requires an extensive number of combinatorial searches. We solve the design problem using novel heuristic search methods. We propose two sub-optimal approaches to find a low complexity solution. In the first method, we start with an initial user set and iteratively increase the number of users served by the BSs. In the second method, we start with a case where each user data is sent to a single BS, and iteratively adds a user to a BS while satisfying the SINR constraints of all users. Finally, we consider several scenarios to present the performance results of the proposed algorithms by detailed simulations.

2.5.2 Power Optimization for C-RAN with Wired Fronthaul

In this study, we minimize total fronthaul and access link power consumption by optimizing beamformers under per-RRH power transmit constraints and imperfect channel knowledge [16]. We first define an equivalent combinatorial search problem that can be optimally solved by a finite number of convex optimizations. The original problem includes discontinuous terms in both cost and constraints. We transform the original problem into a smooth constraint-free function optimization problem and propose a novel method to find a solution using gradient descent. To make a comparison, we consider a heuristic search method and three sparse techniques with ℓ_0/ℓ_1, ℓ_0/ℓ_2 norm approximations, and convex approximation, respectively. We find a theoretical lower bound for the power spent in terms of channel vectors. The resulting bound can be used for optimality analysis of an algorithm as no algorithm can perform better than the bound. We perform detailed simulations with realistic channel conditions and compare the performances of all algorithms analyzed. We also make an optimality analysis by comparing the power values of the algorithms with the theoretical lower bound.

2.5.3 User Admission for C-RAN with Wired Fronthaul

In this work, we optimize a mixed expression including the number of UEs served, total fronthaul data, and total transmit power [17]. All these target parameters are separately optimized in the literature with different techniques. The main contribution of the related paper is to find a new beamformer design method that jointly optimizes all the target parameters under imperfect channel state information and power constraints. We show that the original problem is equivalent to solving a finite number of convex problems, each corresponding to a different cooperation topology. The number of such trials grows exponentially with the number of RRHs and UEs. To find a practical solution we find a theoretical upper bound to the expression defined and propose a novel method that uses a link selection algorithm based on the bound derivation. To make a comparison, we consider four different methods, all of which are modified versions of existing techniques. We compare the performances of all methods by various simulations.

2.5.4 A Theoretical Performance Bound for C-RAN with Wireless Fronthaul

This work finds a novel theoretical lower bound for total power spent in the C-RAN system with wireless fronthaul [18]. The bound expression includes network and channel parameters. By detailed simulations, we show the tightness of the bound. In general, the papers related to C-RAN propose different design methods whose optimality is not known due to the lack of a theoretical bound or a globally optimum solution. To the best of our knowledge, there is no other work deriving a bound. We also propose four novel design methods. Two of them are based on convex optimization with the SDR approach and the other two are based on a combination of well-known methods. Because of the mixed structure of CP and RRH beamformers in SINR expressions, convex optimization cannot be directly applied. We organize the related expressions for which the SDR approach is applicable. For similar reasons, the direct application of well-known methods is also not possible. We solve a system of equations to apply these algorithms. We perform detailed simulations to observe the performances of the proposed methods. We make a comparison to the theoretical bound for different network parameters.

2.5.5 Power Optimization for Integrated Access and Backhaul

We perform a beamformer design study on a downlink full-duplex IAB system. Using semi-definite programming and iterative link removal methods, we propose a novel solution technique minimizing total power consumption under user SINR and power transmit constraints. The simulations show the effectiveness of the proposed technique.

CHAPTER 3

COOPERATION OPTIMIZATION FOR C-RAN WITH CAPACITY LIMITED WIRED FRONTHAUL

3.1 Problem Definition

In this chapter, we describe a beamformer design problem for downlink C-RAN with capacity-limited wired fronthaul [15]. In this study, we assume that fronthaul capacities are limited, and hence full cooperation may not be possible. We optimize the cooperation strategy of the RRHs to minimize total power consumption under per-RRH data transfer constraints, which is related to fronthaul capacities.

We use the system model described in Section 2.4.1. Throughout this work, we assume that all channel vectors are perfectly known by the CP.

To eliminate the interference between the users, a cooperative transmission idea is used by sharing the UE signals among the RRHs via the CP. To reduce the interference, all the UE data may be sent to each RRH, which is referred to as full cooperation. However, this may result in exceeding the capacity of the fronthaul links. To mitigate this problem, we put a cooperation constraint on each RRH. We assume that an RRH can serve at most K_{max} users. Since each UE data should be sent by at least one RRH, we have the constraint $K/N \leq K_{\text{max}} \leq K$.

Using the received signal equation given in (2.5), the received SINR for the k-th UE is given by

$$\text{SINR}_k = \frac{|\mathbf{h}_k^H \mathbf{w}_k|^2}{\sum\limits_{\ell \neq k} |\mathbf{h}_k^H \mathbf{w}_\ell|^2 + \sigma_{\text{UE},k}^2}, \quad \forall k. \tag{3.1}$$

Notice that we assume perfect channel knowledge and hence we can write the SINR expressions as given in (3.1). In order the ensure high quality reception for UEs, an SINR constraint is used for each user, i.e.

$$\mathrm{SINR}_k \geq \gamma_k, \quad \forall k \tag{3.2}$$

where γ_k's are predefined SINR thresholds. In order to express per-RRH data transfer constraints, we define a network link matrix $\mathbf{C}$ with dimensions $K \times N$, where each entry $c_{k,n}$ is either 0 or 1. If the n-th RRH sends the information signal of the k-th UE, then $c_{k,n} = 0$, otherwise $c_{k,n} = 1$. There is a link between the n-th RRH and the k-th UE if and only if $c_{k,n} = 0$. Then we have

$$\sum_{n=1}^{N} c_{k,n} \mathbf{B}_n \mathbf{w}_k = \mathbf{0}, \quad \forall k \tag{3.3}$$

where $\mathbf{B}_n$ is an $NL \times NL$ diagonal matrix defined as

$$\mathbf{B}_n = \mathrm{diag}(\overbrace{0, 0, \ldots, 0}^{(n-1)L}, \overbrace{1, 1, \ldots, 1}^{L}, \overbrace{0, 0, \ldots, 0}^{(N-n)L}), \quad n = 1, 2, \ldots, N. \tag{3.4}$$

Hence, per-RRH data transfer constraints can be written as

$$\sum_{k=1}^{K} c_{k,n} \geq K - K_{\max}, \quad \forall n = 1, 2, \ldots, N. \tag{3.5}$$

(Notice that $c_{k,n} = 1$ when the corresponding link is not used.)

Let $\mathbf{W}_k = \mathbf{w}_k \mathbf{w}_k^H$, $\mathbf{H}_k = \mathbf{h}_k \mathbf{h}_k^H$. Then the SINR expressions can also be written as

$$\mathrm{SINR}_k = \frac{\mathrm{tr}\left(\mathbf{H}_k \mathbf{W}_k\right)}{\sum_{\ell \neq k} \mathrm{tr}\left(\mathbf{H}_k \mathbf{W}_\ell\right) + \sigma^2_{\mathrm{UE},k}}, \quad k = 1, 2, \ldots, K. \tag{3.6}$$

The matrices of the form $\sum_{n=1}^{N} c_{k,n} \mathbf{B}_n$ are diagonal with diagonal entries 0 and 1, and hence they are all positive semi-definite. Therefore, we obtain that

$$\sum_{n=1}^{N} c_{k,n} \mathbf{B}_n \mathbf{w}_k = \mathbf{0} \quad \Longleftrightarrow \quad \sum_{n=1}^{N} c_{k,n} \, \mathrm{tr}\left(\mathbf{B}_n \mathbf{W}_k\right) = 0, \quad \forall k. \tag{3.7}$$

In the asymmetric cooperation problem, our aim is to minimize the total transmitted power by the RRHs under the SINR and per-RRH data transfer constraints. Using

(3.5), (3.6) and (3.7), the problem can be formulated as

$$
\begin{aligned}
\text{(P1)} \quad & \min_{\{\mathbf{W}_k\}_{k=1}^K, \mathbf{C}} \sum_{k=1}^{K} \operatorname{tr}(\mathbf{W}_k) \\
& \text{s.t.} \quad \frac{\operatorname{tr}\left(\mathbf{H}_k \mathbf{W}_k\right)}{\sum_{\ell \neq k} \operatorname{tr}\left(\mathbf{H}_k \mathbf{W}_\ell\right) + \sigma_{\mathrm{UE},k}^2} \geq \gamma_k \quad \forall k, \\
& \qquad \sum_{n=1}^{N} c_{k,n} \operatorname{tr}\left(\mathbf{B}_n \mathbf{W}_k\right) = 0 \quad \forall k, \\
& \qquad \sum_{k=1}^{K} c_{k,n} \geq K - K_{\max} \quad \forall n, \\
& \qquad \operatorname{rank}(\mathbf{W}_k) = 1, \mathbf{W}_k \succeq 0 \quad \forall k.
\end{aligned}
\tag{3.8}
$$

(P1) is a separable homogeneous quadratically constrained quadratic programming (QCQP) type problem which is known to be NP-hard [76]. Given the network link matrix $\mathbf{C}$, the problem (P1) can be optimally solved using the SDR approach by omitting the rank 1 constraints. Consider the relaxed problem (P1-r) for a given $\mathbf{C}$ defined in (3.9).

$$
\begin{aligned}
\text{(P1-r)} \quad & \min_{\{\mathbf{W}_k\}_{k=1}^K} \sum_{k=1}^{K} \operatorname{tr}(\mathbf{W}_k) \\
& \text{s.t.} \quad \frac{\operatorname{tr}\left(\mathbf{H}_k \mathbf{W}_k\right)}{\sum_{\ell \neq k} \operatorname{tr}\left(\mathbf{H}_k \mathbf{W}_\ell\right) + \sigma_{\mathrm{UE},k}^2} \geq \gamma_k \quad \forall k, \\
& \qquad \sum_{n=1}^{N} c_{k,n} \operatorname{tr}\left(\mathbf{B}_n \mathbf{W}_k\right) = 0 \quad \forall k, \\
& \qquad \mathbf{W}_k \succeq 0 \quad \forall k.
\end{aligned}
\tag{3.9}
$$

For full-cooperation case where $\mathbf{C} = \mathbf{0}$, (P1) can be solved using generalized uplink-downlink duality [41], [77], however, this solution cannot be directly generalized to all $\mathbf{C}$ matrices. Since the cost and all constraints are convex, standard interior point algorithms using convex optimization can be applied to find the solution of (P1). Using the ideas in [54], [78], in Appendix A, it is proved that the relaxed problem (P1-r) yields an optimal solution satisfying $\operatorname{rank}(\mathbf{W}_k) = 1, \ \forall k$. Hence, to find the optimal solution of (P1), we need to solve (P1-r) for all possible $\mathbf{C}$ matrices with an exhaustive search (ES) and determine the one with the minimum total power. This is a combinatorial search problem that requires a lot of convex optimizations. Sub-optimal approaches will be discussed in the following section.

3.2 Sub-Optimal Techniques for Asymmetric Cooperation under per-RRH Data Transfer Constraint

Combinatorial search can be effectively reduced by the iterative selection of **C** matrices based on the full cooperation scenario where **C** is all-zero. In this study, we discuss 4 algorithms originating from the full cooperation case. Each algorithm iteratively finds a proper **C** matrix which satisfies the constraints in (P1), i.e.,

$$\begin{aligned} &\sum_{k=1}^{K} c_{k,n} \geq K - K_{\text{max}}, \quad \forall n = 1, 2, \ldots, N \\ &\sum_{n=1}^{N} c_{k,n} < N, \quad \forall k = 1, 2, \ldots, K. \end{aligned} \tag{3.10}$$

In (3.10), the first constraint is the per-RRH data transfer constraint, and the second one is to ensure that each UE data is sent by at least one RRH, which is needed for the corresponding SINRs to be non-zero. Adding an extra link to the system does not increase the optimal transmitted power, hence in the optimal case, each RRH has exactly K_{max} links. Using this fact, the number of convex optimizations required for ES can be calculated as given in Theorem 3.1.

Theorem 3.1: The number NCO_{ES} of convex optimizations required for ES is given by

$$\text{NCO}_{\text{ES}} = \sum_{i=0}^{K} (-1)^i \binom{K}{i} \binom{K-i}{K_{\text{max}}}^N. \tag{3.11}$$

Proof. The main idea is to count the number of bipartite graphs with one set having N elements where each element has degree K_{max} and the other set having K elements where each element has degree at least 1. The counting is based on the inclusion-exclusion principle [79].

3.2.1 Iterative Link Removal (ILR)

This algorithm is discussed in [41], where the total power is limited and the main concern is to minimize the total cooperation among the RRHs. According to the beamformers found in the full cooperation case, corresponding entries of **C** are prioritized. Then the entries with less priority are iteratively equalized to 1 until the problem becomes infeasible.

In our problem, the cooperation is limited by per-RRH data transfer constraints and hence the solution can be found using only 2 convex optimizations. The algorithm steps are summarized in Algorithm 3.1.

Algorithm 3.1: (Iterative Link Removal, ILR)

Initialization

Solve (P1-r) for full cooperation case. Let $\mathbf{w}_{k,n}$ be the corresponding beamformer vectors. Sort $\mathbf{w}_{k,n}$'s with respect to their ℓ_2 norms in ascending order and the corresponding pairs of indices (k, n), $\quad k = 1, 2, \ldots, K,\ n = 1, 2, \ldots, N.$

Repeat

Take the next pair of indices (k, n) in the list and make $c_{k,n} = 1$. If (3.10) is violated, then make $c_{k,n} = 0$ again and skip this pair.

Until

All RRHs serve exactly K_{max} users, i.e.,

$$\sum_{k=1}^{K} c_{k,n} = K - K_{\text{max}}, \quad \forall n.$$

Final Step

Solve (P1-r) with the obtained final **C** matrix.

Notice that this algorithm requires only 2 convex optimizations and hence its complexity is very low. On the other hand, as we will see, its performance is not satisfactory.

3.2.2 Modified Iterative Link Removal (MILR)

The ILR algorithm can be modified by revising the priority list at each step. The algorithm steps are explained in Algorithm 3.2.

Algorithm 3.2: (Modified Iterative Link Removal, MILR)

Initialization

Solve (P1-r) for full cooperation case. Let $\mathbf{w}_{k,n}$ be the corresponding beamformer vectors.

Repeat

- Sort $\mathbf{w}_{k,n}$'s with respect to their ℓ_2 norms in ascending order and the corresponding pairs of indices (k, n),
  $k = 1, 2, \ldots, K,\ n = 1, 2, \ldots, N.$
- Find the first pair (k, n) in the list which satisfies (3.10) when $c_{k,n} = 1$. Update $\mathbf{C}$ by making $c_{k,n} = 1$ for the pair (k, n) found.
- Solve (P1-r) and find the new beamformer vectors $\mathbf{w}_{k,n}$.

Until

$$\sum_{k=1}^{K} c_{k,n} = K - K_{\text{max}}, \quad \forall n.$$

This algorithm applies a convex optimization for each link removal and there are at most $NK - NK_{\text{max}} + 1$ steps. Because of the per-RRH data transfer constraints, in some cases, the number of steps may be less than this value.

3.2.3 Iterative User Addition (IUA)

The IUA algorithm is based on iteratively selecting UEs served by RRHs. Starting from an initial UE set with K_{max} elements, we consecutively add a new UE to the previous user set by exchanging some links. The initial UE set and the addition order of UEs are determined according to the full cooperation scenario. The steps of the algorithm are given in Algorithm 3.3.

Algorithm 3.3: (Iterative User Addition, IUA)

Initialization

- Solve (P1-r) for full cooperation case. Let $\mathbf{w}_{k,n}$ be the corresponding beamformer vectors. Sort $\mathbf{w}_{k,n}$'s with respect to their ℓ_2 norms in descending order and the corresponding pairs of indices (k, n), $\quad k = 1, 2, \ldots, K,\ n = 1, 2, \ldots, N$.

- Form a list $\mathcal{L}$ of UE indices k corresponding to the list of pairs (k, n). (If the i-th element of the list of pairs is (k_i, n_i) then the i-th element of $\mathcal{L}$ is k_i.) We will form a priority list for users by considering $\mathcal{L}$. For each UE with index k find the first place j_k that it occurs in $\mathcal{L}$. Sort j_k's in ascending order and sort the UE indices correspondingly. The last sequence is the priority list of the users.

- Choose the first K_{max} users in the priority list as the initial set U. Solve (P1-r) for full cooperation case with the chosen set with K_{max} users. Find the corresponding beamformer vectors $\mathbf{w}_{k,n}$.

Repeat

- Sort the corresponding beamformer vectors $\mathbf{w}_{k,n}$ with respect to their ℓ_2 norms in ascending order and the corresponding pairs of indices (k, n). Let $\mathcal{L}_\ell$ be the list of pairs (links) (k, n).

- Let k_0 be the next UE index in the priority list of users that is not included in the current set U. Initially set $c_{k_0,n} = 1, \quad \forall n$.

- Iteratively remove a link from the current set and add it to the UE k_0 by following $\mathcal{L}_\ell$. (Here when a link (k, n) is removed and added to user k_0, we mean letting $c_{k,n} = 1$ and $c_{k_0,n} = 0$.) If all links of a UE in U are removed, or if more than one link is removed from an RRH[1], then skip this pair. Solve (P1-r) at each step and find the optimal total power. Continue in this manner until there is no possible removals, and choose the one with the minimum total power.

[1] Since we can add at most one link from an RRH to the UE k_0, we do not allow removal of more than one links from an RRH.

- Update $\mathbf{C}$ according to the optimal exchange of links, and the UE set U by adding the UE k_0 to the set. Find the new beamformer vectors $\mathbf{w}_{k,n}$ by solving (P1-r) for the new UE set.

Until

All UEs are added to the set U.

In the IUA algorithm, at each step, a new UE is added to the set U initially consisting of K_{max} elements. Since we remove at most 1 link from an RRH at each UE addition step, this algorithm requires at most $N(K - K_{\text{max}}) + 1$ convex optimizations.

3.2.4 Iterative Link Addition (ILA)

The ILA algorithm is based on iteratively adding links to the system until all RRHs have K_{max} links. Initially, we determine a priority list for all possible links between RRHs and UEs and choose K links (one for each UE) based on the full cooperation scheme. At each step, we solve a series of (P1-r) to determine which link to add. If none of the trials results in a feasible solution, then we select a link based on the priority list. The detailed steps are explained in Algorithm 3.4.

Algorithm 4 (Iterative Link Addition, ILA)

Initialization

- Solve (P1-r) for full cooperation case. Let $\mathbf{w}_{k,n}$ be the corresponding beamformer vectors. Sort $\mathbf{w}_{k,n}$ with respect to their ℓ_2 norms in descending order and the corresponding pairs of indices $(k, n), \quad k = 1, 2, \ldots, K,\ n = 1, 2, \ldots, N$. Let the list of pairs be $\mathcal{L}_\ell$.

- Following the elements of $\mathcal{L}_\ell$, select a link for each UE. If the total number of links of an RRH exceeds the limit K_{max}, then skip the corresponding element. Continue until each UE has one link.

Repeat

- Try all possible links one by one by adding the corresponding link to the system. If the per-RRH data transfer constraint is violated once a link is added, then skip this trial. Solve (P1-r) at each trial and find the one yielding the minimum total power. If none of the trials results in a feasible solution[2], then choose the link with the highest priority considering the elements of $\mathcal{L}_\ell$.

- Update the matrix $\mathbf{C}$ according to the optimal link found.

Until

Each RRH has exactly K_{max} links, i.e.,

$$\sum_{k=1}^{K} c_{k,n} = K - K_{\text{max}}, \quad \forall n.$$

The ILA algorithm iteratively adds a link to the system. Initially, there are K links and finally, there will be $K_{\text{max}}N$ links. After each step, the number of possible links decreases by 1 and if the total number of links of an RRH reaches K_{max}, then this corresponds to an extra $K - K_{\text{max}}$ reduction. The upper bound for the number of convex optimizations for ILA is stated in Theorem 3.2.

Theorem 3.2: For the ILA algorithm, the number of convex optimizations NCO_{ILA} satisfies

$$\begin{aligned}\text{NCO}_{\text{ILA}} \leq \; & \frac{1}{2}(2KN - K_{\text{max}}N - K + 1)(K_{\text{max}}N - K) \\ & - \left[\binom{N-\ell}{2} + (K_{\text{max}}N - K)\ell\right](K - K_{\text{max}})\end{aligned} \tag{3.12}$$

where $\ell = \max\{0,\ N + K - K_{\text{max}}N\}$.

Proof. The main idea is to consider the case where each RRH reaches the total number K_{max} in one of the last N steps. The variable ℓ given in the bound expression is the minimum number of RRHs initially having K_{max} links.

[2] At the beginning of the algorithm, there is a possibility to have infeasible solutions for all trials since there are a small number of links.

3.3 Simulation Results

In this section, we compare the performances of the four algorithms under various cases. Throughout the simulations, we assume that $\gamma_k = \gamma$, $\sigma_{\text{UE},k} = \sigma$, $\quad \forall k$. Each entry of the channel vectors h_k are assumed to be i.i.d. complex Gaussian with independent real and imaginary parts, zero-mean, and unity variance. As the performance criterion, we define a normalized power P which is given by

$$P = \frac{1}{\sigma^2} \sum_{k=1}^{K} \text{tr}(\mathbf{W}_k). \tag{3.13}$$

We run 100 Monte-Carlo trials in each case.

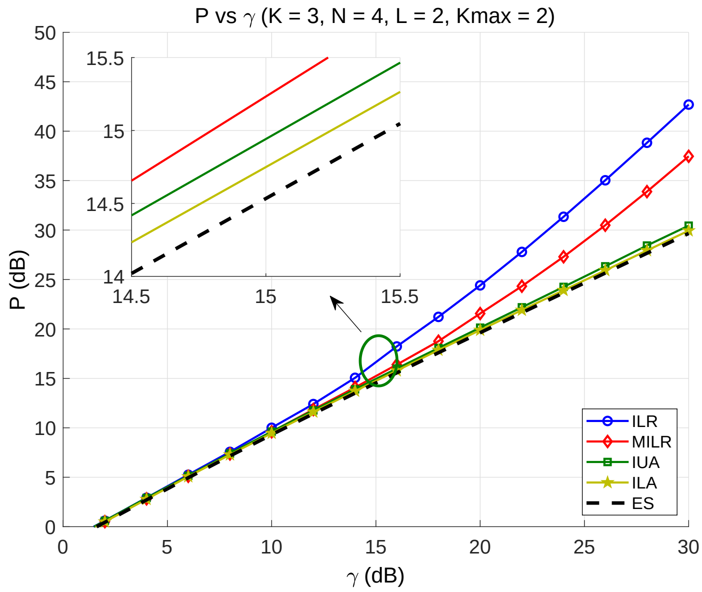

Figure 3.1: P vs γ. $K = 3, N = 4, L = 2, K_{\text{max}} = 2$.

In Fig. 3.1, we set $K = 3, N = 4, L = 2, K_{\text{max}} = 2$ and consider the various values of γ. We observe that at the high SINR region, ILA outperforms other methods and at $\gamma = 15$ dB, it is only 0.25 dB worse than ES. The performance of IUA is again satisfactory for all γ values, and it is about 0.5 dB worse than ES at $\gamma = 15$ dB. The mean values of the number of convex optimizations required for each algorithm are listed in Table 3.1. Notice that the number of convex optimizations required for ILA is roughly 5 times more than that of IUA.

In Fig. 3.2, we set $K = 4, N = 4, L = 2, K_{\text{max}} = 2$ and repeat the same analysis. In this case, we do not run ES since it requires a large number of convex optimiza-

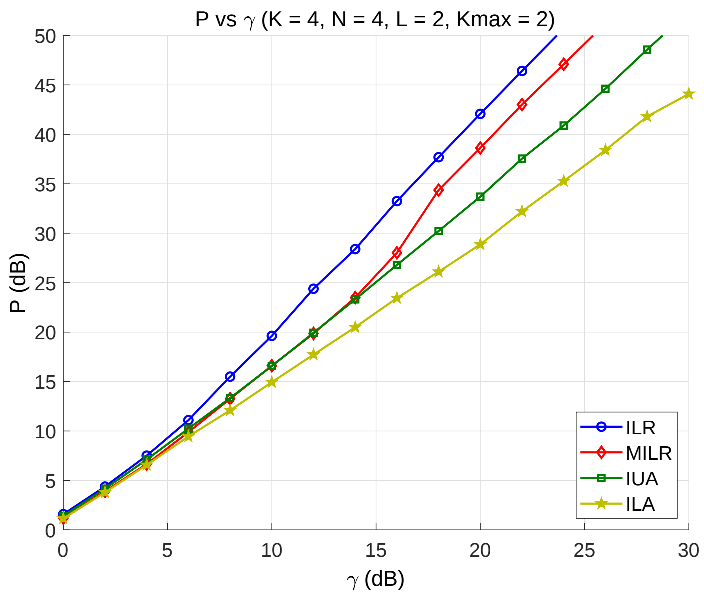

Figure 3.2: P vs γ. $K = 4, N = 4, L = 2, K_{\max} = 2$.

tions. The results show that ILA again outperforms the other three methods and the difference is more significant in this case. We also see that the addition of a single UE may significantly increase the power required to serve all UEs. The mean values of the number of convex optimizations required for each algorithm are listed in Table 3.1. In this case, ILA requires roughly 3 times more convex optimizations than IUA.

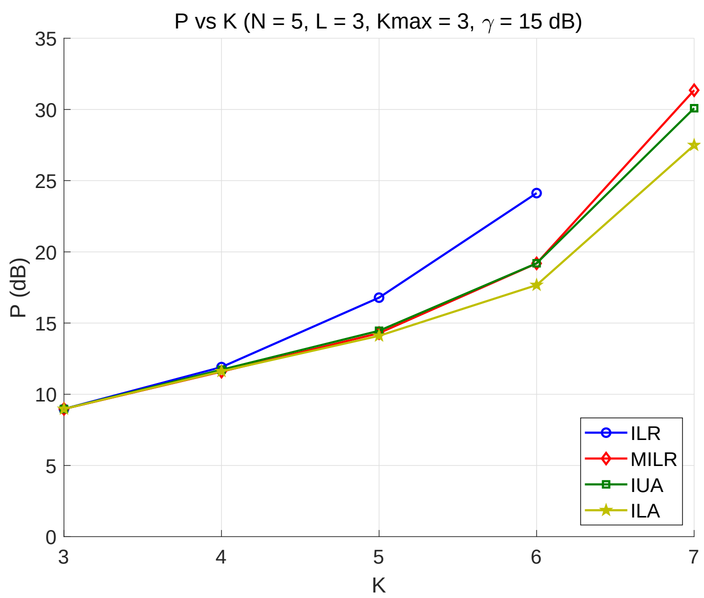

Figure 3.3: P vs K. $N = 5, L = 3, K_{\max} = 3, \gamma = 15$ dB.

In Fig. 3.3, we set $N = 5, L = 3, K_{\max} = 3$ and observe the effect of number of

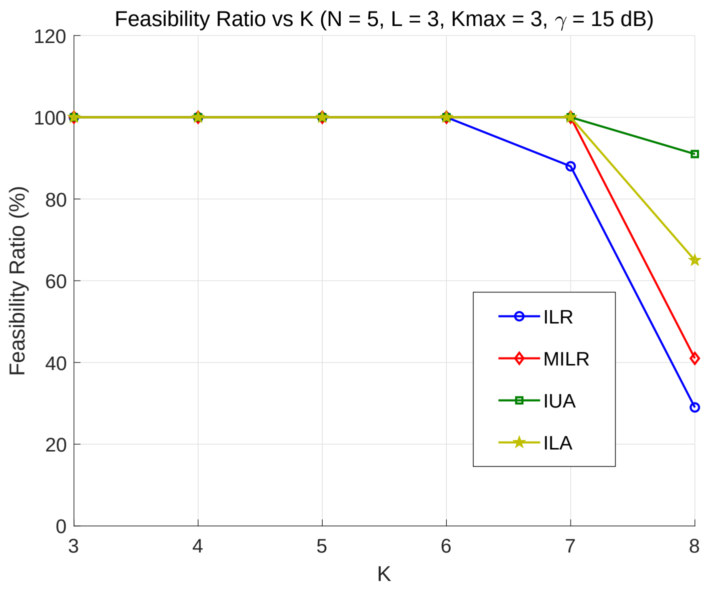

Figure 3.4: Feasibility Ratio vs K. $N = 5, L = 3, K_{\max} = 3, \gamma = 15$ dB.

UEs K. It is seen that as K increases, the required power also increases for both methods. We know that none of these algorithms guarantees to obtain a feasible solution even if the original problem (P1) is feasible. In Fig. 4, we present the ratio of reaching a feasible solution for each algorithm with various K values. We observe that when the number of UEs increases, finding a feasible solution becomes less likely for all algorithms. This is expected since it becomes harder to satisfy all user's SINR constraints as the number of UEs increases. As seen in Fig. 3.4, the ILR method produces some infeasible results for $K > 6$. (Since some of the trials result in an infeasible solution for $K > 6$, we do not plot the performance of ILR after $K = 6$ in Fig 3.3.) Other methods result in infeasible solutions after $K = 7$. Although the feasibility is not guaranteed by any algorithm that we discuss, simulation results show that each one can be safely used for a certain range of K values. The corresponding number of convex optimizations required for each algorithm are again listed in Table 3.1.

We observe that ILR is a very simple technique that can be used if the computational capability of the CP is limited. More complex algorithms such as MILR, IUA, and ILA can be used to enhance the performance. IUA seems a better fit for optimizations in loaded networks where K is large. In less loaded scenarios, ILA can minimize the transmit power better at the expense of higher computational complexity.

Table 3.1: Mean number of convex optimizations required for each algorithm

K	N	L	$K_{\max}$	γ (dB)	$\mathrm{NCO}_{\mathrm{ILR}}$	$\mathrm{NCO}_{\mathrm{MILR}}$	$\mathrm{NCO}_{\mathrm{IUA}}$	$\mathrm{NCO}_{\mathrm{ILA}}$	$\mathrm{NCO}_{\mathrm{ES}}$
3	4	2	2	15	2	5	5	26.4	78
4	4	2	2	15	2	9	9	26.8	978
3	5	3	3	15	2	1	1	79	1
4	5	3	3	15	2	6	6	104.5	1020
5	5	3	3	15	2	11	11	119.6	94890
6	5	3	3	15	2	16	16	127.3	2615340
7	5	3	3	15	2	21	21	128.1	32186070
8	5	3	3	15	2	24.9	26	118.1	214628400

3.4 Conclusions

In this study, we analyze the asymmetric cooperation problem for downlink C-RAN under per-RRH data transfer constraint. We propose two methods IUA and ILA and compare them with the ILR and its modified version MILR. We observe that by the use of IUA, the performance increases compared to MILR in most cases. ILA can be used to further increase the performance, however, its complexity is generally higher than those of the others. We also note that none of the algorithms guarantees a feasible solution, however, simulation results show that all algorithms can be safely used when the number of UEs is less than a certain value.

CHAPTER 4

POWER OPTIMIZATION FOR C-RAN WITH WIRED FRONTHAUL

4.1 Problem Definition

In this chapter, we propose a beamformer design method to minimize total power consumption in downlink C-RAN with wired fronthaul [16]. We optimize cooperation and beamforming coefficients for QoS problems under imperfect channel knowledge. We assume that channel estimation is already performed and channel estimates are available. The corresponding channel vectors can be estimated from uplink transmissions in time division duplex systems, however, there is always some estimation error. Hence, in general, CSI in CP is imperfect, and the beamforming design algorithms should be robust to channel errors. We assume that channel estimation includes additive errors with known second-order statistics. We aim to serve all users in the cluster of interest by minimizing the total power spent in the system. In this study, it is assumed that power has two main components. Firstly, each user data should be first sent by CP to related RRHs. This operation requires some power which can be considered as fronthaul power. Each user data is also sent from RRHs to target users which is the second component of the power in the system. Because both fronthaul and RRH power consumptions are significant [57], we aim to minimize total power spent under per-RRH power transmit constraints by designing beamforming vectors.

We use the system model described in Section 2.4.1. Using the received signal equation given in (2.5), the received SINR for the k-th UE is given by

$$\text{SINR}_k = \frac{P_d}{P_m + P_{\text{int}} + P_{\text{noise}}} \tag{4.1}$$

where

$$P_d = \mathbb{E}[|\,\widehat{\mathbf{h}}_k^H\,\mathbf{w}_k s_k|^2],\;\; P_m = \mathbb{E}[|\Delta\mathbf{h}_k^H\mathbf{w}_k s_k|^2]$$
$$P_{\text{int}} = \mathbb{E}[|\mathbf{h}_k^H \sum_{\ell\neq k}\mathbf{w}_\ell s_\ell|^2],\;\; P_{\text{noise}} = \mathbb{E}[|z_{\text{UE},k}|^2]. \tag{4.2}$$

Using the fact that $\mathbb{E}\left[s_k^* s_\ell\right] = \delta[k-\ell]$ and statistics of the channel error and noise terms, we find that[1]

$$P_d = \operatorname{tr}(\widehat{\mathbf{H}}_k\,\mathbf{W}_k),\; P_m = \operatorname{tr}(\mathbf{D}_k\mathbf{W}_k)$$
$$P_{\text{int}} = \sum_{\ell\neq k}\operatorname{tr}(\widetilde{\mathbf{H}}_k\,\mathbf{W}_\ell),\; P_{\text{noise}} = \sigma^2_{\text{UE},k}. \tag{4.3}$$

where

$$\begin{aligned}
\widehat{\mathbf{H}}_k &= \widehat{\mathbf{h}}_k\,\widehat{\mathbf{h}}_k^H\,,\\
\mathbf{D}_k &= \mathbb{E}[\Delta\mathbf{h}_k\Delta\mathbf{h}_k^H] = \text{diag}\left(\sigma^2_{k,1}\mathbf{I}_L, \sigma^2_{k,2}\mathbf{I}_L, \ldots, \sigma^2_{k,N}\mathbf{I}_L\right),\\
\widetilde{\mathbf{H}}_k &= \mathbb{E}[\mathbf{h}_k\mathbf{h}_k^H] = \widehat{\mathbf{H}}_k + \mathbf{D}_k,\\
\mathbf{W}_k &= \mathbf{w}_k\mathbf{w}_k^H, \quad \forall k.
\end{aligned} \tag{4.4}$$

Using (4.1) and (4.3), we can write

$$\text{SINR}_k = \frac{\operatorname{tr}(\widehat{\mathbf{H}}_k\,\mathbf{W}_k)}{\sum_{\ell\neq k}\operatorname{tr}(\widetilde{\mathbf{H}}_k\,\mathbf{W}_\ell) + \operatorname{tr}(\mathbf{D}_k\mathbf{W}_k) + \sigma^2_{\text{UE},k}}, \quad \forall k. \tag{4.5}$$

In Appendix B, we show that the rate $\log_2(1+\text{SINR}_k)$ is achievable for the k-th user. Hence, the SINR that we defined can be used as a design criterion.

A certain SINR is needed to decode the received signals in the UEs. Hence, we compare the SINRs with a pre-determined threshold γ_k to decide whether the corresponding user is served. In other words, we assume that k-th user is served if and only if $\text{SINR}_k \geq \gamma_k$. If the SINR condition is satisfied, the rate $r_k = \log_2(1+\gamma_k)$ is achievable for k-th user. Notice that due to channel estimation errors, the denominator of the SINR expression includes extra positive terms related to $\mathbf{D}_k$'s making the SINR smaller compared to the perfect CSI case. Therefore, it is harder to satisfy SINR constraints under imperfect CSI.

[1] To calculate the expectations, all channel estimates are assumed to be given and known at the CP which also reveals beamforming vectors to RRHs.

Another design term that can be optimized is the total power spent in the system. The total power P has two components P_{CP} and P_{RRH} which correspond to the power consumed by CP and RRHs, respectively. We know that P_{CP} is an increasing function of the total fronthaul data rate. This is because the user data should be first sent by CP to RRHs over fronthaul links before being transmitted by RRHs to users. Furthermore, if the cooperation of the RRHs increases, i.e. if the number of RRHs serving a certain user increases, the total fronthaul rate increases resulting in a larger P_{CP}. We use the linear power model as also used in [57], where P_{CP} linearly increases with the total fronthaul rate. In this model P_{CP} can be written as

$$P_{\text{CP}} = \epsilon_1 r_{\text{tot}} = \epsilon_1 \sum_{k=1}^{K} \sum_{n \in S_k} r_k \tag{4.6}$$

where ϵ_1 is a constant multiplier whose unit is W $\cdot$ Hz/bps, the total fronthaul rate is denoted by r_{tot} and S_k is the index set of RRHs serving the UE k. Using the fact that

$$n \in S_k \quad \Longleftrightarrow \quad \mathbf{w}_{k,n} \neq \mathbf{0} \quad \Longleftrightarrow \quad \delta\left[\|\mathbf{w}_{k,n}\|\right] = 0 \tag{4.7}$$

we get

$$P_{\text{CP}} = \epsilon_1 \sum_{k=1}^{K} \sum_{n=1}^{N} r_k \left(1 - \delta\left[\|\mathbf{w}_{k,n}\|\right]\right). \tag{4.8}$$

The term P_{RRH} is related to total power transmitted by RRHs which can be written as

$$P_{\text{tot}} = \sum_{k=1}^{K} \sum_{n=1}^{N} \|\mathbf{w}_{k,n}\|^2 . \tag{4.9}$$

In general, the power spent by RRHs is larger than that of its transmit power due to the inefficiency of power amplifiers. We assume that power spent by RRHs is equal to $P_{\text{RRH}} = \epsilon_2 P_{\text{tot}}$ where ϵ_2 is a unitless constant multiplier.

We know that there is a natural power transmit constraint for each RRH, which can be formulated as

$$P_n = \sum_{k=1}^{K} \|\mathbf{w}_{k,n}\|^2 \leq P_t, \quad \forall n \tag{4.10}$$

where P_n is the transmit power of n-th RRH and P_t is the power transmit threshold value which is assumed to be the same for all RRHs.

In this study, we aim to serve all K UEs by minimizing $P = P_{\text{CP}} + P_{\text{RRH}}$ under per-RRH power transmit constraints. Considering all constraints, the design problem can be given by

$$
\begin{aligned}
\text{(P2)} \quad & \min_{\mathbf{w}_{k,n}} \sum_{k=1}^{K}\sum_{n=1}^{N} \epsilon_1 r_k \left(1-\delta\left[\|\mathbf{w}_{k,n}\|\right]\right) + \epsilon_2 \left\|\mathbf{w}_{k,n}\right\|^2 \\
\text{s.t.} \; & \sum_{k=1}^{K} \|\mathbf{w}_{k,n}\|^2 \le P_t, \quad \forall n = 1,2,\ldots,N, \\
& \text{SINR}_k \ge \gamma_k, \quad \forall k = 1,2,\ldots,K.
\end{aligned} \tag{4.11}
$$

4.2 Algorithms

In this section, we present the algorithms that we use while solving (P2). Firstly, we define an equivalent combinatorial search problem. We propose a novel method that transforms the problem into a smooth constraint-free form and solves it using gradient descent. The initial point of this method is found from the equivalent problem. As a comparison, we also consider a heuristic search method that solves the equivalent problem using successive convex optimizations, and three sparse algorithms using ℓ_0/ℓ_1 norm approximation, ℓ_0/ℓ_2 norm approximation, and convex approximation, respectively.

4.2.1 Equivalent Combinatorial Search Problem

(P2) can be transformed into a combinatorial search problem which can be optimally solved with a finite number of convex optimizations. Firstly, to analyze the cooperation between the RRHs, as in Chapter 3, we define a network link matrix $\mathbf{C}$ with dimensions $K \times N$, where each entry $c_{k,n}$ is either 0 or 1. If the n-th RRH sends the k-th user data, then we say that there is a link between the n-th RRH and the k-th user and set $c_{k,n} = 0$. Otherwise $c_{k,n} = 1$. Similarly, we can relate the entries of $\mathbf{C}$ with the index sets S_k as

$$
n \in S_k \quad \Longleftrightarrow \quad c_{k,n} = 0. \tag{4.12}
$$

Using this definition, we can write a relation between beamformers and entries of $\mathbf{C}$ as

$$
\sum_{n=1}^{N} c_{k,n} \mathbf{B}_n \mathbf{w}_k = \mathbf{0}, \quad \forall k \tag{4.13}
$$

where $\mathbf{B}_n$ is an $NL \times NL$ diagonal matrix defined as

$$\mathbf{B}_n = \text{diag}\left(\mathbf{0}_{(n-1)L},\ \mathbf{1}_L,\ \mathbf{0}_{(N-n)L}\right),\ n = 1, 2, \ldots, N. \tag{4.14}$$

The matrices $\sum_{n=1}^{N} c_{k,n}\mathbf{B}_n$ are diagonal with diagonal entries 0 and 1, and hence they are all positive semi-definite. Therefore, it follows that

$$\sum_{n=1}^{N} c_{k,n}\mathbf{B}_n\mathbf{w}_k = \mathbf{0} \iff \sum_{n=1}^{N} c_{k,n}\,\text{tr}\left(\mathbf{B}_n\mathbf{W}_k\right) = 0, \quad \forall k. \tag{4.15}$$

Using the $\mathbf{B}_n$ matrices defined, the total transmit power of the n-th RRH can be written as

$$P_n = \sum_{k=1}^{K} \|\mathbf{w}_{k,n}\|^2 = \sum_{k=1}^{K} \text{tr}(\mathbf{B}_n\mathbf{W}_k). \tag{4.16}$$

(P2) is a problem involving terms related to the number of zero beamformers which are discontinuous functions of $\mathbf{w}_{k,n}$'s. To find a solution, we can consider the problem for a fixed $\mathbf{C}$ which is denoted by (P2-r). If we solve (P2-r) for all possible $\mathbf{C}$ matrices, then we can find the optimal solution of (P2) by finding the optimal $\mathbf{C}$ that minimizes P. When we fix $\mathbf{C}$, the term P_{CP} becomes also fixed, and the problem reduces to finding optimal beamformers minimizing the total transmit power from RRHs-to-UEs. Using (4.13)-(4.16), (P2-r) can be expressed by

$$\text{(P2-r)} \quad \min_{\{\mathbf{W}_k\}_{k=1}^{K}} \sum_{k=1}^{K} \text{tr}(\mathbf{W}_k) \tag{4.17}$$

$$\text{s.t.} \quad \frac{\text{tr}(\widehat{\mathbf{H}}_k\,\mathbf{W}_k)}{\sum_{\ell \neq k} \text{tr}(\widetilde{\mathbf{H}}_k\,\mathbf{W}_\ell) + \text{tr}(\mathbf{D}_k\mathbf{W}_k) + \sigma_k^2} \geq \gamma_k \ \forall k, \tag{4.18}$$

$$\sum_{n=1}^{N} c_{k,n}\,\text{tr}\left(\mathbf{B}_n\mathbf{W}_k\right) = 0 \quad \forall k, \tag{4.19}$$

$$\sum_{k=1}^{K} \text{tr}(\mathbf{B}_n\mathbf{W}_k) \leq P_t \quad \forall n, \tag{4.20}$$

$$\text{rank}(\mathbf{W}_k) = 1, \mathbf{W}_k \succeq 0 \quad \forall k. \tag{4.21}$$

In (4.18) the SINR constraints are given. (4.19) is the relation between $\mathbf{C}$ matrix and beamformers. (4.20) is the per-RRH power constraint. Finally, (4.21) includes a rank constraint which makes the problem non-convex. Using a similar method as discussed in [37], it can be shown that (P2) is NP-hard. As done in [37], [39], we can make a semi-definite relaxation by omitting the rank constraint. In the relaxed problem, cost and constraints are convex, and hence standard convex optimization methods can be applied to find a solution. As a result, to find a solution of (P2), we need to solve (P2-r) for all possible **C** matrices and determine the one with the minimum P value. This is a combinatorial search problem that requires a lot of convex optimizations. To find a practical solution, one way is to apply a heuristic search over **C** matrices. In general, the performance of this approach enhances as the number of trials increases. Another way is to apply a direct approximation on the variables in cost and constraints of the problem which is discussed in subsection 4.1.3.

4.2.2 Rank-1 Approximation

In (P2-r), we find a solution by omitting the rank constraint. If the result is rank-1, the solution becomes optimal. In Appendix C, using the idea in [54], we prove that the optimal solution of the relaxed problem is always rank-1. Hence by applying eigenvalue decomposition and taking the principal eigenvalue and eigenvector, we find the optimal solution of (P2-r). If (P2-r) is solved for all possible **C** matrices, then we can find the optimal solution of (P2).

4.2.3 Smooth Constraint-Free Approximation (SCFA)

The combinatorial method involving a series of convex optimizations for (P2-r) can be used to find the optimal solution of (P2); however, the computational complexity is very high when the numbers K, N, L are large. To find a practical solution, we propose a new method that is based on approximating discontinuous functions with a sequence of smooth function sequences. [37], [57] also use a similar idea, but there is an additional constraint that requires a subspace projection at each iteration step. In the related papers, authors only approximate the cost function to be optimized while the constraints are kept the same. Their solution requires an extra subspace projection step. They first optimize an approximated cost function where constraints are not considered. After this step, the solution is projected onto the space defined by the constraints. In our method, we shift all constraints to the main cost function to be optimized using a similar approximation idea. Hence, standard gradient search methods can be applied to the final constraint-free smooth function of beamformer vectors. In this way, we can directly optimize the approximated cost function without any extra subspace projection operations.

Firstly, we prove a theorem about the SINR terms for the optimal solution:

Theorem 4.1: For the optimal solution of (P2), we have

$$\text{SINR}_k = \gamma_k, \;\; \forall k.$$

Proof: The proof is given in Appendix D.

Using Theorem 4.1, we prefer to express SINR constraints as $\text{SINR}_k = \gamma_k$, i.e., $\rho_k = 0, \; \forall k$ where ρ_k is defined as

$$\rho_k = \text{tr}\left((\widehat{\mathbf{H}}_k - \gamma_k \mathbf{D}_k)\mathbf{W}_k\right) - \gamma_k \sum_{\ell \neq k} \text{tr}(\widetilde{\mathbf{H}}_k \mathbf{W}_\ell) - \gamma_k \sigma^2_{\text{UE},k}. \tag{4.22}$$

As we see in (4.8), the term related to P_{CP} is discontinuous with respect to $\mathbf{w}_{k,n}$'s, but can be expressed as the limit of some smooth function sequences. For this purpose, we use the fact

$$\text{Fact 1:} \quad e^{-\frac{x^2}{a}} \to \delta[x] \quad \text{as} \quad a \to 0^+. \tag{4.23}$$

Using Fact 1, we can approximate P_{CP} as

$$P_{\text{CP}} \approx \epsilon_1 \sum_{k=1}^{K} \sum_{n=1}^{N} r_k \left(1 - \exp\left(-\frac{\|\mathbf{w}_{kn}\|^2}{a}\right)\right) \tag{4.24}$$

where a is a small positive number. Using (4.24), the approximate expression for P becomes smooth with respect to beamforming vectors. We use a similar way to shift the constraints to the main expression. Notice that

$$\text{Fact 2:} \quad e^{\frac{x}{a}} \to \begin{cases} 0, & \text{if} \quad x < 0 \\ \infty, & \text{if} \quad x > 0 \end{cases} \quad \text{as} \quad a \to 0^+. \tag{4.25}$$

$$\text{Fact 3:} \quad e^{\frac{x^2}{a}} - 1 \to \begin{cases} 0, & \text{if} \quad x = 0 \\ \infty, & \text{if} \quad x \neq 0 \end{cases} \quad \text{as} \quad a \to 0^+. \tag{4.26}$$

Consider the expressions

$$\begin{aligned} c_1 &= \sum_{n=1}^{N} \exp\left(\frac{1}{a}\left(\sum_{k=1}^{K} \|\mathbf{w}_{k,n}\|^2 - P_t\right)\right), \\ c_2 &= \sum_{k=1}^{K} \left[\exp\left(\frac{\rho_k^2}{a}\right) - 1\right]. \end{aligned} \tag{4.27}$$

Using Fact 2, c_1 tends to 0 if the per-RRH power transmit constraints are satisfied and tends to infinity otherwise. Similarly, by Fact 3, c_3 tends to 0 if SINR constraints are satisfied, and tends to infinity otherwise. Therefore, we can delete the constraints and express the problem as

$$\begin{aligned} P &= \epsilon_1 r_{\text{tot}} + \epsilon_2 P_{\text{tot}} \approx Q \\ &= \sum_{k=1}^{K}\sum_{n=1}^{N} \epsilon_1 r_k \left(1 - \exp\left(-\frac{\|\mathbf{w}_{k,n}\|^2}{a}\right)\right) + \epsilon_2 \|\mathbf{w}_{k,n}\|^2 \\ &+ \eta_1 \sum_{n=1}^{N} \exp\left(\frac{1}{a}\left(\sum_{k=1}^{K} \|\mathbf{w}_{k,n}\|^2 - P_t\right)\right) \\ &+ \eta_2 \sum_{k=1}^{K} \left[\exp\left(\frac{\rho_k^2}{a}\right) - 1\right] \end{aligned} \tag{4.28}$$

where $a > 0$ is a small number[2], and η_1, η_2 are two positive weights. Notice that using (4.28), we shift the constraints to the main expression. When the constraints in (4.11) is satisfied, corresponding terms in (4.28) becomes 0 and does not affect the value of Q. If they are not satisfied, we get $Q \to \infty$. So, once Q is minimized, the constraints should be automatically satisfied. Note that using this approach, Q becomes a smooth function in terms of $\mathbf{w}_{k,n}$'s and hence standard gradient search algorithms can be applied. We can directly minimize Q without any constraint using the SCFA algorithm.

In SCFA, we start from an initial point and update the beamformers iteratively by evaluating the gradient. In the update equation, we use the augmented beamformer $\mathbf{w} = [\mathbf{w}_1^T \mathbf{w}_2^T \cdots \mathbf{w}_K^T]^T$. The equation in (4.28) can be written in terms of $\mathbf{w}$ as given in

[2] In fact, we can use different a's for approximating P_{CP} and for constraint shifting. However, to make the expression simpler, we use the same a for all three approximations.

(4.29).

$$\begin{aligned} Q = \epsilon_1 \sum_{k=1}^{K} \sum_{n=1}^{N} r_k \left[1 - \exp\left(-\frac{\mathbf{w}^H \mathbf{B}_{k,n} \mathbf{w}}{a} \right) \right] + \epsilon_2 \mathbf{w}^H \mathbf{w} \\ + \eta_1 \sum_{n=1}^{N} \exp\left(\frac{\mathbf{w}^H \mathbf{C}_n \mathbf{w} - P_t}{a} \right) \\ + \eta_2 \sum_{k=1}^{K} \left[\exp\left(\frac{\left(\mathbf{w}^H \mathbf{A}_k \mathbf{w} - d_k \right)^2}{a} \right) - 1 \right] \end{aligned} \tag{4.29}$$

where

$$\begin{aligned} \mathbf{A}_k &= \text{diag}\big(-\gamma_k \widetilde{\mathbf{H}}_k,\ \ldots,\ -\gamma_k \widetilde{\mathbf{H}}_k,\ \overbrace{\widehat{\mathbf{H}}_k - \gamma_k \mathbf{D}_k}^{k\text{-th}},\ -\gamma_k \widetilde{\mathbf{H}}_k, \\ &\quad \ldots, -\gamma_k \widetilde{\mathbf{H}}_k \big) \\ \mathbf{B}_{k,n} &= \text{diag}\left(\mathbf{0}_{((k-1)N+n-1)L},\ \mathbf{1}_L,\ \mathbf{0}_{((K-k+1)N-n)L} \right) \\ \mathbf{C}_n &= \sum_{k=1}^{K} \mathbf{B}_{kn} = \text{diag}(\overbrace{\mathbf{B}_n, \mathbf{B}_n, \ldots, \mathbf{B}_n}^{K}), \quad d_k = \sigma_k^2 \gamma_k \end{aligned} \tag{4.30}$$

for all $n = 1, 2, \ldots, N$ and $k = 1, 2, \ldots, K$. In this case, the update equation can be given as

$$\mathbf{w}^{(t+1)} = \mathbf{w}^{(t)} - \mu^{(t)} \boldsymbol{\nabla}(\mathbf{w}^{(t)}). \tag{4.31}$$

Here t denotes the iteration index, $\mu^{(t)}$ is the step-size, $\boldsymbol{\nabla}(\mathbf{w}^{(t)})$ is the gradient vector which can be calculated through (4.29).

We know that a small step-size causes slow convergence and large step-size implies divergence. To obtain a suitable step-size, we use a well-known variable step-size Barzilai-Borwein (BB) method [80], which calculates the step-size as

$$\mu^{(t)} = \frac{\left(\delta \boldsymbol{\nabla}^{(t)} \right)^H \delta \mathbf{w}^{(t)}}{\left(\delta \boldsymbol{\nabla}^{(t)} \right)^H \delta \boldsymbol{\nabla}^{(t)}} \tag{4.32}$$

where

$$\begin{aligned} \delta \boldsymbol{\nabla}^{(t)} &= \boldsymbol{\nabla}(\mathbf{w}^{(t)}) - \boldsymbol{\nabla}(\mathbf{w}^{(t-1)}), \\ \delta \mathbf{w}^{(t)} &= \mathbf{w}^{(t)} - \mathbf{w}^{(t-1)}. \end{aligned} \tag{4.33}$$

In SCFA, the choice of initial point $\mathbf{w}^{(0)}$ is crucial to obtain a good convergence. We know that for a given link configuration, the problem can be optimally solved using convex optimization. Using this idea, we choose the initial point as the solution of the full cooperation case. We operate the algorithm until the rate of change of Q is small enough. To obtain a faster convergence, we change the value of a throughout the iterations. If the rate of change of Q is small enough, we decrease a by some factor.

After convergence, we obtain a solution that satisfies a local minimum for Q. On the other hand, because of the approximation done, the value of Q may not be exactly equal to P. Therefore, we first find the link configuration and the corresponding $\mathbf{C}$ matrix according to the ℓ_2 norms of the beamformers obtained at the last step of the iteration, then solve the problem using convex optimization for the matrix $\mathbf{C}$ found. After the convergence, some beamformers become very close to zero which means that the corresponding links should not be used. The steps are listed in Algorithm 4.1.

Algorithm 4.1: (Smooth Constraint-Free Approximation, SCFA)

Step 1, Initialization:

Solve (P2-r) for full cooperation case. Set the initial value $\mathbf{w}^{(0)}$. Define $\mu^{(1)} = 10^{-4}, t_{\text{max}} = 10^5, \tau = 10^{-6}, \xi = 0.1, Q_t = 10^{-6}, \kappa = 10^{-2}, \Delta = 5, \eta_1 = \eta_2 = (\epsilon_1 + \epsilon_2)/2$.

Step 2, Gradient Descent:

For $t = 1, 2, \ldots, t_{\text{max}}$ repeat the following steps:

1) Find the gradient $\boldsymbol{\nabla}(\mathbf{w}^{(t)})$ and step-size $\mu^{(t)}$.

2) Update the beamformers:

$$\mathbf{w}^{(t+1)} = \mathbf{w}^{(t)} - \mu^{(t)} \boldsymbol{\nabla}(\mathbf{w}^{(t)}).$$

3) Check the condition for a:

$$a^{(t+1)} = \begin{cases} \xi a^{(t)}, & \text{if } |Q^{(t+1)} - Q^{(t)}| < \tau a^{(t)} \\ a^{(t)}, & \text{otherwise} \end{cases}$$

4) Check the condition for termination:

$$\text{If } \max_{t-\Delta \leq t_s \leq t} |Q^{(t+1)} - Q^{(t_s)}| < Q_t, \text{ then terminate.}$$

After the termination, evaluate the ℓ_2 norms of the final beamformer vectors. Make a priority list of pairs (k, n) so that (k_1, n_1) is more prior than (k_2, n_2) if and only if $\|\mathbf{w}_{k_1,n_1}\| > \|\mathbf{w}_{k_2,n_2}\|$.

Step 3, Find the link configuration:

Form a network link matrix $\mathbf{C}$ such that

$$c_{k,n} = \begin{cases} 1, \text{ if } \|\mathbf{w}_{k,n}\| < \kappa P_t \\ 0, \text{ otherwise} \end{cases}$$

Repeat the following steps until the problem becomes feasible:

1) Solve (P2-r) using $\mathbf{C}$ with convex optimization. If the problem is feasible, then stop.

2) If it is not feasible, find the most prior pair (k, n) with $c_{kn} = 1$. Update $\mathbf{C}$ by making $c_{kn} = 0$. [3]

In Step 1, we find the initial point to start the algorithm. In Step 2, the iterative gradient descent process is operated. In the final step, the network link matrix is determined and the final solution is found by a small number of convex optimizations.

4.2.4 Heuristic Search Algorithms

We know that the optimal solution of (P2) can be found by solving (P2-r) for all possible $\mathbf{C}$ matrices. In Theorem 4.2, we give the total number of such $\mathbf{C}$ matrices.

Theorem 4.2: The number of all possible $\mathbf{C}$ matrices is given by

$$N_{\mathbf{C}} = (2^N - 1)^K. \tag{4.34}$$

Proof: Notice that there are 2^{NK} possible $\mathbf{C}$ matrices, however, in order to serve all users, each column of $\mathbf{C}$ should include at least one 0, making the total number smaller. For each column of $\mathbf{C}$, there are $2^N - 1$ possible arrangements (all possible

[3] There may be some cases where direct removal of links with small norm results in an infeasible problem. Hence, we iteratively add a new link until the problem becomes feasible.

arrangements except all 1 case) and hence there are $(2^N - 1)^K$ many possible **C** matrices.

As we see in Theorem 4.2, the number of convex optimizations required grows exponentially with N and K. Therefore, we can apply a heuristic search over **C** matrices to find a practical solution. In this study, we consider a heuristic search method based on successive link removal. To make a comparison, we can also apply the exhaustive search method which tries all possible **C** matrices. In all these methods, we try some subset of all possible **C** matrices and find the solution among them corresponding to the minimum P value.

Method 4.1: Iterative Link Removal (ILR)
This algorithm is discussed in [41] for a problem where the total power is limited and the main concern is to minimize the cooperation among the RRHs. According to the beamformers found in the full cooperation case, corresponding entries of **C** are prioritized. The entries with less priority are iteratively equalized to 1 until the problem becomes infeasible. Since there are NK links in total and each user should have at least one link, this algorithm requires at most $NK - K$ convex optimizations.

Method 4.2: Exhaustive Search (ES)
This method optimally solves (P2) by trying all $(2^N - 1)^K$ possible **C** matrices. As there are a lot of convex optimizations required, this method is not practical and we use it as a comparison only for some small values of K and N.

4.2.5 Sparse Algorithms

The objective function of (P2) includes terms related to the number of zero beamformers. The corresponding terms can be written as ℓ_0 norms of some vectors. ℓ_0 norm can be approximated by ℓ_1 norm [46]-[51], ℓ_2 norm [39], [52], [53] or some convex function [54]-[55].

Method 4.3: Majorization-Minimization (MM)
This method uses the idea of ℓ_0/ℓ_1 norm approximation. In [46]-[51], this approxi-

mation is applied for similar problems. For a non-negative real number x, we have

$$\lim_{\theta \to 0} \frac{\ln(1+\theta^{-1}x)}{\ln(1+\theta^{-1})} = \begin{cases} 1, & \text{if } x > 0 \\ 0, & \text{if } x = 0. \end{cases} \tag{4.35}$$

Using the observation given in (4.35), we can approximate ℓ_0 norm by

$$||x||_0 \approx c_\theta \cdot \ln(1+\theta^{-1}x) \tag{4.36}$$

where $\theta > 0$ is a small number and $c_\theta = \dfrac{1}{\ln(1+\theta^{-1})}$ is a constant. The function $\ln(1+\theta^{-1}x)$ is concave with respect to x and hence it is upper bounded by its first order Taylor series expansion, i. e.,

$$\ln(1+\theta^{-1}x) \leq \frac{x}{x+\theta}. \tag{4.37}$$

Therefore, $||x||_0$ can be approximated by $c_\theta \cdot \dfrac{x}{x+\theta}$ for any non-negative real number x. For a vector $[x_1\ x_2\ \cdots\ x_n]$ with non-negative real elements, we obtain that

$$\|[x_1\ x_2\ \cdots\ x_n]\|_0 \approx c_\theta \cdot \sum_{m=1}^{n} \frac{x_m}{x_m+\theta}. \tag{4.38}$$

This method is called majorization-minimization (MM) method as the upper bound of the ℓ_0 norm will be minimized. To use this method in our problem, we first write the discontinuous term in the objective function in terms ℓ_0 norms.

$$\sum_{n=1}^{N} (1-\delta[||\mathbf{w}_{k,n}||]) = \|[\|\mathbf{w}_{k,1}\|^2\ \|\mathbf{w}_{k,2}\|^2 \cdots\ \|\mathbf{w}_{k,N}\|^2]\|_0. \tag{4.39}$$

We approximate the ℓ_0 norm as

$$\sum_{n=1}^{N} (1-\delta[||\mathbf{w}_{k,n}||]) \approx c_\theta \sum_{n=1}^{N} \frac{\mathbf{w}_{k,n}^H \mathbf{w}_{k,n}}{\mathbf{w}_{k,n}^H \mathbf{w}_{k,n} + \theta} = c_\theta \sum_{n=1}^{N} \frac{\mathrm{tr}(\mathbf{B}_n \mathbf{W}_k)}{\mathrm{tr}(\mathbf{B}_n \mathbf{W}_k) + \theta}. \tag{4.40}$$

In this case, the total power can be written as

$$P \approx \epsilon_1 c_\theta \sum_{k=1}^{K} r_k \sum_{n=1}^{N} \frac{\mathrm{tr}(\mathbf{B}_n \mathbf{W}_k)}{\mathrm{tr}(\mathbf{B}_n \mathbf{W}_k) + \theta} + \epsilon_2 \sum_{k=1}^{K} \mathrm{tr}(\mathbf{W}_k). \tag{4.41}$$

To obtain a convex objective function, as done in [46]-[51], we optimize P iteratively. We approximate the term $\dfrac{\mathrm{tr}(\mathbf{B}_n \mathbf{W}_k)}{\mathrm{tr}(\mathbf{B}_n \mathbf{W}_k) + \theta}$ as $\dfrac{\mathrm{tr}(\mathbf{B}_n \mathbf{W}_k)}{\mathrm{tr}(\mathbf{B}_n \mathbf{W}_k^{(t)}) + \theta}$ where $\mathbf{W}_k^{(t)}$ is the solution found at the previous iteration. After the final approach, the expression of P becomes linear (and hence convex) with respect to $\mathbf{W}_k$'s and the optimization can be performed by omitting the rank-1 constraint of $\mathbf{W}_k$'s. In the first part of Appendix E, we show that the optimal solution of the relaxed problem is always rank-1. The corresponding problem can be expressed as

$$
\begin{aligned}
\text{(P3)} \quad & \min_{\mathbf{W}_k} \sum_{k=1}^{K} \left(r_k \sum_{n=1}^{N} \frac{\epsilon_1 c_\theta \operatorname{tr}(\mathbf{B}_n \mathbf{W}_k)}{\operatorname{tr}(\mathbf{B}_n \mathbf{W}_k^{(t)}) + \theta} + \epsilon_2 \operatorname{tr}(\mathbf{W}_k) \right), \\
\text{s.t.} \quad & \sum_{k=1}^{K} \operatorname{tr}(\mathbf{B}_n \mathbf{W}_k) \leq P_t, \quad \forall n = 1, 2, \ldots, N, \\
& \text{SINR}_k \geq \gamma_k, \quad \mathbf{W}_k \succeq 0 \quad \forall k = 1, 2, \ldots, K.
\end{aligned}
\tag{4.42}
$$

In (4.42), the terms $\mathbf{W}_k^{(t)}$'s are the solutions found at the previous iteration. The steps of the MM algorithm are given in Algorithm 4.2.

Algorithm 4.2: (Majorization-Minimization, MM)

Step 1, Initialization:

Solve (P2-r) for full cooperation case. Set the initial values of $\mathbf{W}_k^{(0)}$ for $k = 1, 2, \ldots, K$. Define $\theta = 10^{-5}$, $t_{\text{max, 1}} = 10^3$, $\Delta_1 = 10^{-5}$, $\kappa_1 = 10^{-3}$.

Step 2, Successive Convex Optimizations:

For $t = 1, 2, \ldots, t_{\text{max, 1}}$ repeat the following steps:

1) Solve (P3) using $\mathbf{W}_k^{(t-1)}$'s found in the previous iteration.

2) Check the condition for termination:

$$\text{If } |P^{(t)} - P^{(t-1)}|/P^{(t)} < \Delta_1, \text{ then terminate.}$$

After the termination, evaluate the ℓ_2 norms of the final beamformer vectors.

Step 3, Find the link configuration:

1) Form a network link matrix $\mathbf{C}$ by removing the links with small norms, i.e., $\|\mathbf{w}_{kn}\| < \kappa_1 P_t$.

2) Solve (P2-r) using $\mathbf{C}$ with convex optimization.

Method 4.4: Group Sparse Beamforming (GSB)

In this algorithm, we use ℓ_0/ℓ_2 norm approximation which corresponds to a homogeneous convex lower bound [39], [52], [53]. Firstly, we define

$$f_{\text{GSB}}(k,n) = \epsilon_1 r_k (1 - \delta[\|\mathbf{w}_{k,n}\|]) + \epsilon_2 \|\mathbf{w}_{k,n}\|^2, \quad \forall k, n. \tag{4.43}$$

We can write the total power spent P as

$$P = \sum_{k=1}^{K} \sum_{n=1}^{N} f_{\text{GSB}}(k,n). \tag{4.44}$$

Using the fact that

$$f_{\text{GSB}}(k,n) = \begin{cases} 0, & \text{if } \mathbf{w}_{k,n} = \mathbf{0} \\ \epsilon_1 r_k + \epsilon_2 \|\mathbf{w}_{k,n}\|^2, & \text{if } \mathbf{w}_{k,n} \neq \mathbf{0}, \end{cases} \tag{4.45}$$

and by the well-known Arithmetic-Geometric Mean Inequality, we obtain that

$$f_{\text{GSB}}(k,n) \geq 2\sqrt{\epsilon_1 \epsilon_2 r_k} \|\mathbf{w}_{k,n}\|, \quad \forall k, n. \tag{4.46}$$

It follows that

$$P \geq \sum_{k=1}^{K} \sum_{n=1}^{N} 2\sqrt{\epsilon_1 \epsilon_2 r_k} \|\mathbf{B}_n \mathbf{w}_k\|. \tag{4.47}$$

The right-hand side of (4.47) is homogeneous and convex with respect to beamformer vectors. In this method, we optimize the convex lower bound for total power spent given in (4.47) under the SINR and per-RRH transmit power constraints. We can write both two constraints as second-order cone constraints. Firstly, we can express SINR constraints as

$$(1+\gamma_k)\mathbf{w}_k^H \widehat{\mathbf{H}}_k \mathbf{w}_k \geq \gamma_k \sum_{\ell=1}^{K} \mathbf{w}_\ell^H \widetilde{\mathbf{H}}_k \mathbf{w}_\ell + \gamma_k \sigma_{\text{UE},k}^2, \quad \forall k. \tag{4.48}$$

As the matrices $\widetilde{\mathbf{H}}_k$'s are positive semi-definite for all k, using the Cholesky factorization, we can find matrices $\mathbf{T}_k$ such that $\widetilde{\mathbf{H}}_k = \mathbf{T}_k^H \mathbf{T}_k$ for all k. Using this fact, we can rewrite (4.48) as

$$(1+\gamma_k)|\widehat{\mathbf{h}}_k^H \mathbf{w}_k|^2 \geq \gamma_k \sum_{\ell=1}^{K} \|\mathbf{T}_k \mathbf{w}_\ell\|^2 + \gamma_k \sigma_k^2, \quad \forall k. \tag{4.49}$$

It is clear that the phases of beamformer vectors $\mathbf{w}_k$ do not affect the objective and constraints expressions. Hence, we can express the SINR constraints as

$$\sqrt{1+\gamma_k^{-1}} \text{Re}\{\widehat{\mathbf{h}}_k^H \mathbf{w}_k\} \geq \sqrt{\sum_{\ell=1}^{K} \|\mathbf{T}_k \mathbf{w}_\ell\|^2 + \sigma_{\text{UE},k}^2}, \quad \forall k. \tag{4.50}$$

Per-RRH transmit power constraints can be written as

$$\sqrt{\sum_{k=1}^{K} \|\mathbf{B}_n \mathbf{w}_k\|^2} \leq \sqrt{P_t} \quad \forall n. \tag{4.51}$$

Both (4.50) and (4.51) are second order cone constraints. Therefore, we can optimize the beamformers using a second order cone problem (P4).

$$\text{(P4)} \quad \min_{\mathbf{w}_k} \sum_{k=1}^{K} \sum_{n=1}^{N} 2\sqrt{\epsilon_1 \epsilon_2 r_k} \|\mathbf{B}_n \mathbf{w}_k\|, \tag{4.52}$$

$$\text{s.t.} \quad \sqrt{1+\gamma_k^{-1}} \text{Re}\{\widehat{\mathbf{h}}_k^H \mathbf{w}_k\} \geq \sqrt{\sum_{\ell=1}^{K} \|\mathbf{T}_k \mathbf{w}_\ell\|^2 + \sigma_k^2}, \quad \forall k,$$

$$\sqrt{\sum_{k=1}^{K} \|\mathbf{B}_n \mathbf{w}_k\|^2} \leq \sqrt{P_t}, \quad \forall n.$$

We can use CVX [81] software to solve the second-order cone programming (SOCP) problem (P4). In [39], [52], [53], this method is referred as group sparse beamforming (GSB). In the related reference papers, it is stated that this problem produces sparse solutions.

To enhance the performance of the GSB method, the links are prioritized according to the solution of (P4). After this step, as in the ILR method, links are removed according to the priority of the links until obtaining a feasible solution. As in [39], [52], [53], we use a priority function considering both beamformer and channel ℓ_2 norms.

$$p_{\text{GSB}}(k,n) = \|\widehat{\mathbf{h}}_{k,n}\| \cdot \|\mathbf{w}_{k,n}\|, \quad \forall k, n \tag{4.53}$$

where $p_{\text{GSB}}(k,n)$ is the priority of link (k,n). The steps of the algorithm are given below.

Algorithm 4.3: (Group Sparse Beamforming, GSB)

---

1) Solve (P4) and evaluate the priority of each link.

2) Starting from the full cooperation case, remove links according to the priorities and solve (P2-r) at each step until obtaining a feasible solution.

Method 4.5: Successive Convex Approximation (SCA)

In this method, we approximate the ℓ_0 norm using an upper bound found from the first order Taylor series [54]-[55]. To apply the approximation, we use the fact that

$$\|x\|_0 \approx f(x) = \frac{x}{x+\theta} \leq f(x_0) + f^{'}(x_0)(x - x_0) \tag{4.54}$$

where $\theta > 0$ is a small number, $x \geq 0$ is a real number, x_0 is a real number close to x, $f(x) = \dfrac{x}{x+\theta}$ is a concave function and $f^{'}$ denotes its first order derivative. Using the idea in (4.54), we can approximate the term in P related to ℓ_0 norm as

$$\sum_{n=1}^{N}(1 - \delta[\|\mathbf{w}_{k,n}\|] \approx \sum_{n=1}^{N} \frac{\theta\|\mathbf{w}_{k,n}\|^2 + \|\mathbf{w}_{k,n}^{(t)}\|^4}{(\|\mathbf{w}_{k,n}^{(t)}\|^2 + \theta)^2} \tag{4.55}$$

where the beamformers $\mathbf{w}_{k,n}^{(t)}$ are found from the previous iteration. The right-hand side of (4.55) is convex with respect to beamformers and hence the optimization can be performed with successive convex approximations by omitting the rank-1 constraints. In the second part of Appendix E, we show that the optimal solution of the relaxed problem is always rank-1. The corresponding problem can be expressed as

$$\begin{aligned}
\text{(P5)} \quad \min_{\mathbf{W}_k} \sum_{k=1}^{K}\sum_{n=1}^{N} \Big(& \frac{\epsilon_1 r_k \theta \operatorname{tr}(\mathbf{B}_n \mathbf{W}_k) + [\operatorname{tr}(\mathbf{B}_n \mathbf{W}_k^{(t)})]^2}{(\operatorname{tr}(\mathbf{B}_n \mathbf{W}_k^{(t)}) + \theta)^2} \\
& + \epsilon_2 \operatorname{tr}(\mathbf{B}_n \mathbf{W}_k) \Big), \qquad (4.56) \\
& \sum_{k=1}^{K} \operatorname{tr}(\mathbf{B}_n \mathbf{W}_k) \leq P_t \quad \forall n = 1, 2, \dots, N, \\
& \text{SINR}_k \geq \gamma_k, \quad \mathbf{W}_k \succeq 0 \quad \forall k = 1, 2, \dots, K,
\end{aligned}$$

where $\mathbf{W}_k^{(t)}$'s are found from the previous iteration. The steps of the algorithm are given below.

Algorithm 4.4: (Successive Convex Approximation, SCA)

Step 1, Initialization:

Solve (P2-r) for full cooperation case. Set the initial values of $\mathbf{W}_k^{(0)}$ for $k = 1, 2, \dots, K$. Define $\theta = 10^{-5},\ t_{\text{max, 2}} = 10^3,\ \Delta_2 = 10^{-5},\ \kappa_2 = 10^{-3}$.

Step 2, Successive Convex Optimizations:

For $t = 1, 2, \dots, t_{\text{max, 2}}$ repeat the following steps:

1) Solve (P5) using $\mathbf{W}_k^{(t-1)}$'s found in the previous iteration.

2) Check the condition for termination:

$$\text{If } |P^{(t)} - P^{(t-1)}|/P^{(t)} < \Delta_2, \text{ then terminate.}$$

After the termination, evaluate the ℓ_2 norms of the final beamformer vectors.

Step 3, Find the link configuration:

1) Form a network link matrix $\mathbf{C}$ by removing the links with small norms, i.e., $\|\mathbf{w}_{k,n}\| < \kappa_2 P_t$.

2) Solve (P2-r) using $\mathbf{C}$ with convex optimization.

4.3 Complexity Comparison

In general, we can measure the computational complexity of an iterative method as the product of number of iterations and the complexity at each iteration. At each iteration of ILR, ES, MM, GSB, SCA, the main component of complexity is related to the convex optimization and all other operations can be neglected. For GSB method, the complexity of initial SOCP solution should also be evaluated. We use Self Dual Minimization (SeDuMi) [82] software (included in CVX [81] package) as the convex optimization and SOCP solver. For the convex optimization based problems (P2-r), (P3), (P5), at each iteration, we minimize $c^H x$ subject to $Ax = b$ where $x \in \mathbb{C}^n$ is the vector of all unknowns and $A \in \mathbb{C}^{m \times n}$, $b \in \mathbb{C}^m$, $c \in \mathbb{C}^n$ are known vectors/matrices. We know by [82] that the corresponding computational complexity is $\mathcal{O}(n^2 m^{2.5} + m^{3.5})$ for SeDuMi. The corresponding m and n values are calculated as

$$\begin{aligned} \text{(P2-r)}:\ & m = 2K + N,\ n = KN^2L^2 + K + N, \\ \text{(P3)}, \text{(P5)}:\ & m = K + N,\ n = KN^2L^2 + K + N. \end{aligned} \tag{4.57}$$

Considering the number of convex optimizations required for ILR and ES, we obtain that

$$\begin{aligned} \mathrm{C}_{\mathrm{ILR}} &= \mathcal{O}\left((NK - K)C_0\right), \\ \mathrm{C}_{\mathrm{ES}} &= \mathcal{O}\left((2^N - 1)^K C_0\right). \end{aligned} \tag{4.58}$$

where $\mathrm{C_{ILR}}$, $\mathrm{C_{ES}}$ are complexities of ILR and ES, respectively, and

$$C_0 = (2K+N)^{2.5}([KN^2L^2+K+N]^2+2K+N). \tag{4.59}$$

The complexities of MM and SCA can be expressed as

$$\begin{aligned} \mathrm{C_{MM}} &= \mathcal{O}\left(N_{\mathrm{MM}}C_1\right), \\ \mathrm{C_{SCA}} &= \mathcal{O}\left(N_{\mathrm{SCA}}C_1\right), \end{aligned} \tag{4.60}$$

where $\mathrm{C_{MM}}$, $\mathrm{C_{SCA}}$, N_{MM}, N_{SCA} are complexities and number of iterations of MM and SCA, respectively, and

$$C_1 = (K+N)^{2.5}([KN^2L^2+K+N]^2+K+N). \tag{4.61}$$

According to [83], the worst-case complexity of a SOCP problem can be calculated as $\mathcal{O}(\sqrt{n_1}n_2^2n_3)$ where n_1 is the total number of constraints, n_2 is the total number of real optimization variables, and n_3 is the total dimension of constraints. In (P4), the number of constraints is equal to $K+N$, the number of real optimization variables is equal to $2KNL$. Each SINR constraint has dimension $KNL+1$ and each per-RRH transmit power constraint has dimension KL. Hence, the total dimension of constraints is equal to $K(KNL+1)+KNL$. As a result, we obtain the complexity of (P4) as $\mathcal{O}(C_2)$ where

$$C_2 = \sqrt{K+N}4(KNL)^2[K(KNL+1)+KNL]. \tag{4.62}$$

After the prioritization of links by solving (P4), GSB method also solves (P2) iteratively by link removals. Therefore, the complexity of GSB can be calculated as

$$\mathrm{C_{GSB}} = \mathcal{O}(C_2+(NK-K)C_0). \tag{4.63}$$

For SCFA, we can show that the main component of the complexity is related to calculation of gradient. The gradient calculation consists of four parts related to P_{CP}, P_{RRH}, per-RRH power transmit constraints and SINR constraints. It can be shown that the complexities for the first three parts are $\mathcal{O}(KNL)$ and the complexity of the part related to SINR constraints is $\mathcal{O}(K^2N^2L^2)$. Hence, we have

$$\mathrm{C_{SCFA}} = \mathcal{O}\left(N_{\mathrm{SCFA,1}}K^2N^2L^2+N_{\mathrm{SCFA,2}}C_0\right) \tag{4.64}$$

where $\mathrm{C_{SCFA}}$ is the complexity of SCFA, $N_{\mathrm{SCFA,1}}$ is the number of iterations for gradient descent, and $N_{\mathrm{SCFA,2}}$ is the number of convex optimizations in the Step 3 of the algorithm. Using (4.59), (4.64) and the fact that $(x+y)^{2.5} \geq 2^{2.5}(xy)^{1.25}$ for any $x, y > 0$, [4] it can be shown that

$$
\begin{aligned}
\mathrm{C}_{\mathrm{SCFA}} &\approx \mathcal{O}(N_{\mathrm{SCFA,1}} K^2 N^2 L^2 + N_{\mathrm{SCFA,2}} K^{3.25} N^{5.25} L^4), \\
\mathrm{C}_{\mathrm{ILR}} &\approx \mathcal{O}(K^{4.25} N^{6.25} L^4), \\
\mathrm{C}_{\mathrm{ES}} &\approx \mathcal{O}(2^{KN} K^{3.25} N^{5.25} L^4).
\end{aligned} \tag{4.65}
$$

Similarly, the complexities of MM, SCA and GSB can be approximately written as

$$
\begin{aligned}
\mathrm{C}_{\mathrm{MM}} &\approx \mathcal{O}(N_{\mathrm{MM}} K^{3.25} N^{5.25} L^4), \\
\mathrm{C}_{\mathrm{SCA}} &\approx \mathcal{O}(N_{\mathrm{SCA}} K^{3.25} N^{5.25} L^4), \\
\mathrm{C}_{\mathrm{GSB}} &\approx \mathcal{O}(K^{4.25} N^{3.25} L^3 + K^{4.25} N^{6.25} L^4).
\end{aligned} \tag{4.66}
$$

In Table 4.1, we see the problems solved by each algorithm and the approximate complexities.

Table 4.1: Problems solved and average complexity for each algorithm

Method	Problems Solved	Approximate Complexity
SCFA	Gradient Descent, (P2-r)	$\mathcal{O}(N_{\mathrm{SCFA,1}} K^2 N^2 L^2 + N_{\mathrm{SCFA,2}} K^{3.25} N^{5.25} L^4)$
ILR	(P2-r)	$\mathcal{O}(K^{4.25} N^{6.25} L^4)$
ES	(P2-r)	$\mathcal{O}\left((2^{KN} K^{3.25} N^{5.25} L^4\right)$
MM	(P3)	$\mathcal{O}(N_{\mathrm{MM}} K^{3.25} N^{5.25} L^4)$
GSB	(P2-r), (P4)	$\mathcal{O}(K^{4.25} N^{3.25} L^3 + K^{4.25} N^{6.25} L^4)$
SCA	(P5)	$\mathcal{O}(N_{\mathrm{SCA}} K^{3.25} N^{5.25} L^4)$

The simulation results show that $N_{\mathrm{SCFA,1}} < 100,\ N_{\mathrm{SCFA,2}} < 10,\ N_{\mathrm{MM}} < 100,\ N_{\mathrm{SCA}} < 100$ holds for most of the cases. Considering this result, we conclude that for small K, N, L values, the complexity of SCFA is higher compared to ILR, MM, SCA, and GSB. On the other hand, when K, N, L are large, the complexity of SCFA becomes much smaller than those of ILR, MM, SCA, and GSB. In any case, the optimal algorithm ES is the most complex one.

[4] Here we use well-known Arithmetic-Geometric Mean Inequality to show that $x + y \geq 2\sqrt{xy}$.

4.4 Theoretical Bounds on P

In this section, we find lower and upper bounds for the optimum value P_{opt} of the total power spent. The main result is stated in Theorem 4.3.

Theorem 4.3: $P_\ell \leq P_{\text{opt}} \leq P_u$ where

$$P_u = \epsilon_1 N \sum_{k=1}^{K} \log_2(1+\gamma_k) + \epsilon_2 N P_t \tag{4.67}$$

$$P_\ell = \sum_{k=1}^{K} \mathcal{P}_k \tag{4.68}$$

$$\mathcal{P}_k = \min_{S_k} \epsilon_1 \log_2(1+\gamma_k)|S_k| + \epsilon_2 \frac{\gamma_k \sigma^2_{\text{UE},k}}{\lambda_{\max}\left(\widehat{\mathbf{h}}'_k (\widehat{\mathbf{h}}'_k)^H - \gamma_k \mathbf{D}'_k\right)}$$

$S_k = \{n_1, n_2, \ldots, n_r\}$ is the index set of RRHs serving the user k,

$$\begin{aligned} \widehat{\mathbf{h}}'_k &= [\widehat{\mathbf{h}}^T_{n_1} \; \widehat{\mathbf{h}}^T_{n_2} \; \cdots \; \widehat{\mathbf{h}}^T_{n_r}]^T, \\ \mathbf{D}'_k &= \text{diag}\left(\sigma^2_{k,n_1}\mathbf{I}_L, \sigma^2_{k,n_2}\mathbf{I}_L, \ldots, \sigma^2_{k,n_r}\mathbf{I}_L\right). \end{aligned} \tag{4.69}$$

To obtain a feasible solution, $\lambda_{\max}\left(\widehat{\mathbf{h}}'_k (\widehat{\mathbf{h}}'_k)^H - \gamma_k \mathbf{D}'_k\right) > 0$ should satisfy for all k. We evaluate $\mathcal{P}_k$ by applying the minimization over all possible S_k sets.

Proof: The proof is given in Appendix F.

Notice that if $P_\ell > P_u$ for some channel vectors, we can directly say that the problem is infeasible without doing any optimization. In such a case, as it is not possible to serve all users, we may try to find which users can be served. This is referred to as the user admission problem [38] in the literature and out of the scope of this study.

4.5 Simulation Results

In this section, we compare the performances of the algorithms. Throughout the simulations, we assume that $\gamma_k = \gamma$, $\sigma_{\text{UE},k} = \sigma$ and $r_k = \log_2(1+\gamma)$ for all k. We use a realistic channel model including path-loss, shadowing and small-scale fading defined in a 3GPP standard [84]. We consider a circular region in which RRHs and UEs are distributed uniformly.[5] In Table 4.2, the model parameters are presented.

[5] To avoid channel model inconsistencies, configurations where RRH-to-UE distances are all at least 50 meters are considered.

Table 4.2: Model parameters used in simulations

Cell radius	0.5 km
Path-loss (P_L)	$P_L = 128.1 + 37.6 \log_{10} d$ where d is in km
RRH/UE antenna gain	0 dBi
Shadowing model/variance	Log-normal, 10 dB
UE Noise Figure (NF)	9 dB
Bandwidth (BW)	10 MHz
σ^2	$-174 + 10 \log_{10}$ BW + NF $= -95$ dBm
Small-scale fading model	Rayleigh
ϵ_1	$5\text{W} \cdot \text{Hz/bps}$
ϵ_2	2

In this study, we fix the parameters ϵ_1, ϵ_2 which are related to the infrastructure and hardware quality of the network. We also assume that all user equipments are identical ($\sigma_{\text{UE},k} = \sigma,\ \forall k$) and priority of users are equal ($\gamma_k = \gamma,\ \forall k$). All algorithms analyzed can be operated with any combinations of these parameters. One can use a different parameter set to see the corresponding algorithm performances.

To generate channel estimates and channel estimation errors, we assume that pilot signal powers are adjusted according to the channel amplitudes so that the power ratios of $\mathbb{E}(|\Delta\mathbf{h}_{k,n}|^2)/|\mathbf{h}_{k,n}|^2,\ \forall k, n$ are all equal to some known constant γ_{ch}. Here γ_{ch} is a measure of channel estimation quality. Using the channel estimates and γ_{ch}, one can evaluate $\sigma_{k,n}^2,\ \forall k, n$ accordingly.

In simulations, we observe the effect of parameters $\gamma, K, N, L, \gamma_{\text{ch}}, P_t$. We generate channel vectors so that the problem is feasible (it is possible to satisfy all constraints of the problem).[6] We run 1000 Monte-Carlo trials in each case. To make a comparison, we run the ES method when K, N, L are small. When these parameters are large ES will not be depicted due to impractical run-times.

[6] The feasibility of the problem (P2) is equivalent to the feasibility of (P2-r) for a full cooperation case.

4.5.1 Effect of SINR threshold

We know that the total power spent is an increasing function of the SINR threshold γ. This fact can also be verified considering the lower bound expression given in Theorem 3. In Fig. 2-3, we see the performances of the algorithms as γ varies. We take $P_t = 10\text{W}, \gamma_{\text{ch}} = 0.01$ in both cases and consider the results for triples $(K, N, L) = (3, 3, 2), (8, 4, 8)$. The results show that SCFA outperforms other algorithms (except for ES which is the optimal one) for all γ values.

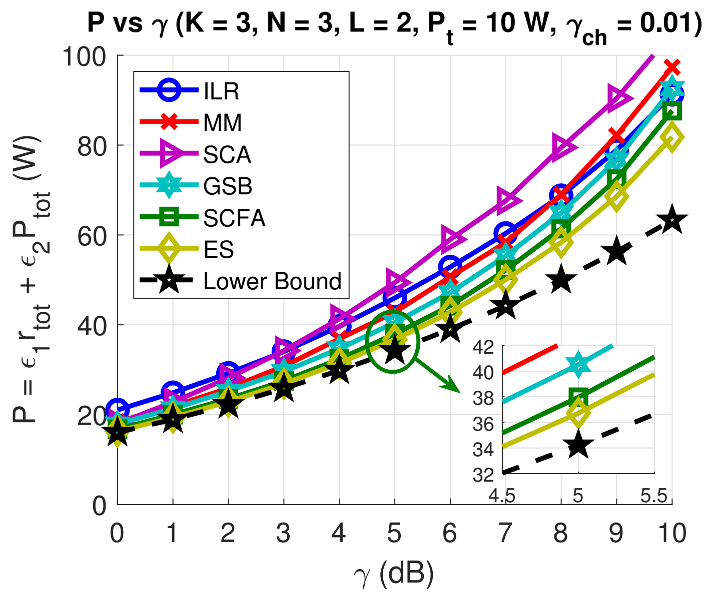

Figure 4.1: P vs γ. $K = 3, N = 3, L = 2, P_t = 10\text{W}, \gamma_{\text{ch}} = 0.01$.

In Fig. 4.1, we observe that ES requires slightly less power than SCFA. The power difference between SCFA and ES is about 1 W for $\gamma = 5$ dB. We also note that the performance of SCFA is very close to the theoretical lower bound for small γ values. The power difference between SCFA and the bound is roughly 10 percent for $\gamma = 5$ dB. As γ increases, the lower bound becomes too optimistic. This is because the lower bound can be achieved when the inter-user interference is perfectly eliminated which becomes harder for large SINR thresholds.

In Fig. 4.2, we also see that SCFA outperforms other methods and its performance is close to the lower bound at small SINR thresholds. Considering the results, we can say that the performance of SCFA is satisfactory even when there is imperfect channel knowledge.

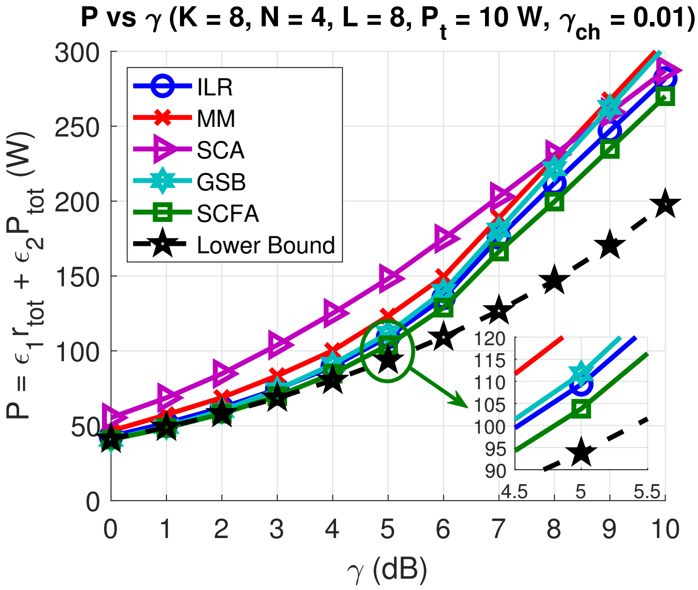

Figure 4.2: P vs γ. $K = 8, N = 4, L = 8, P_t = 10\text{W}, \gamma_{\text{ch}} = 0.01$.

4.5.2 Effect of Number of Users

As the number of users increases, we expect higher power consumption to satisfy all SINR constraints.

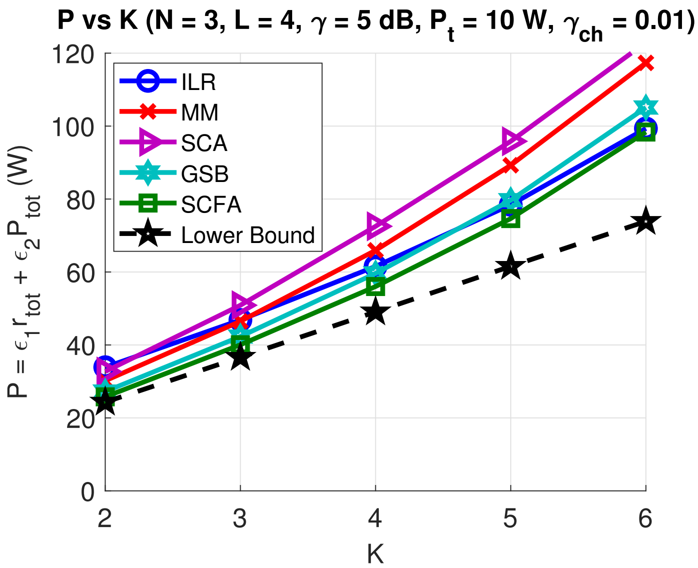

Figure 4.3: P vs K. $N = 3, L = 4, \gamma = 5$ dB, $P_t = 10\text{W}, \gamma_{\text{ch}} = 0.01$.

In Fig. 4.3, we observe the effect of the number of users. We see that SCFA outperforms other methods for all K values. The results show that the power difference between SCFA and the bound is very low for small K values. The difference becomes large as K increases. The reason is similar to that of the large γ case. To achieve the bound, the interference due to other users should be eliminated. As K increases it becomes harder to eliminate this interference and hence the power differences between the methods and the bound become larger.

4.5.3 Effect of Number of RRHs and Number of RRH Antennas

When the number of RRHs and/or the number of RRH antennas increases, the dimension of the augmented beamformer vector **w** becomes higher which enables a better resource allocation and provides a lower power consumption.

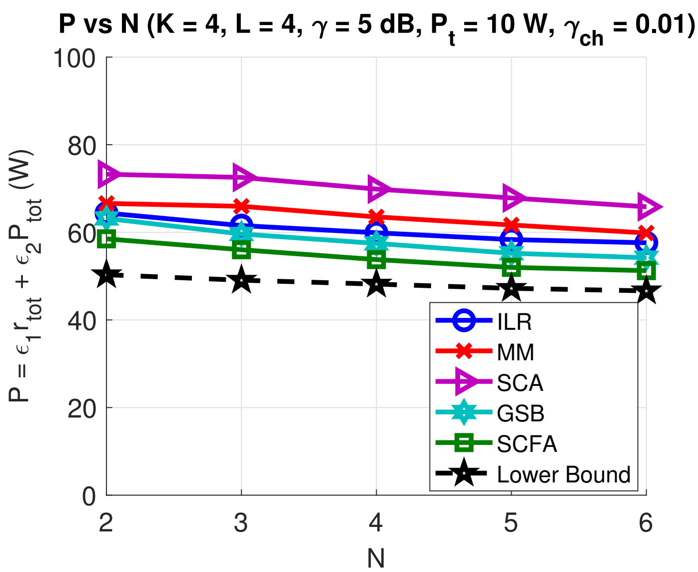

Figure 4.4: P vs N. $K = 4, L = 4, \gamma = 5$ dB, $P_t = 10$W, $\gamma_{\text{ch}} = 0.01$.

Fig. 4.4-4.5 show the effect of the number of RRHs and the number of RRH antennas. As in the previous cases, SCFA performance is better compared to other methods for all N and L values. We observe that the power values of all methods are lower bounded as N or L increases. This is because for a fixed K, the optimal strategy uses some set of links between RRHs and UEs, and if there are sufficient links in the system, adding more links does not improve the performance much. We also observe that for large N or L, the performance of SCFA becomes very close to the bound. This shows that the bound is very tight and SCFA performance is near-optimal at these values.

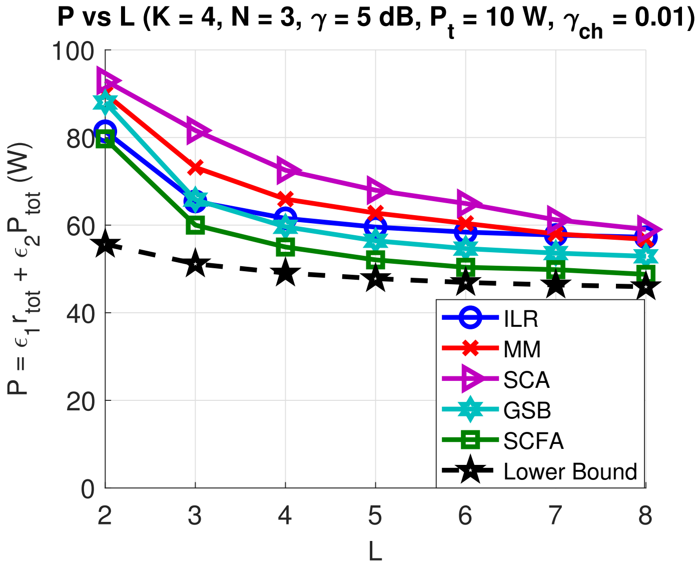

Figure 4.5: P vs L. $K = 4, N = 3, \gamma = 5$ dB, $P_t = 10$W, $\gamma_{\text{ch}} = 0.01$.

4.5.4 Effect of Channel Estimation Quality

We know by (4.5) that a larger channel estimation error corresponds to a lower SINR which results in higher power consumption.

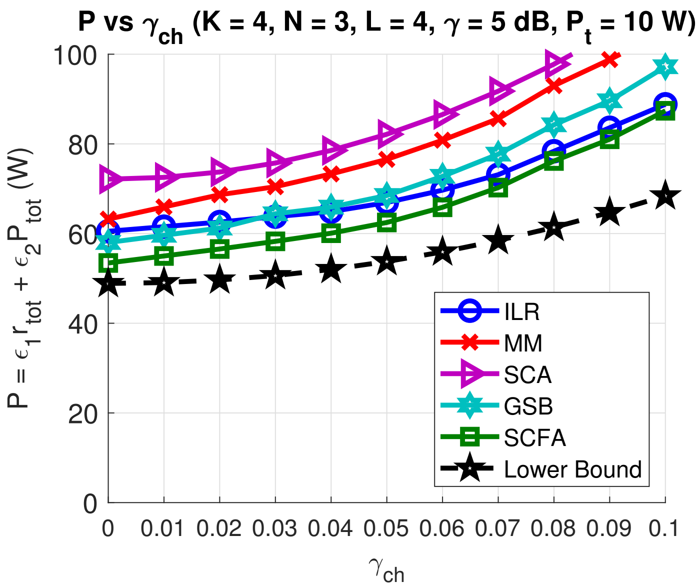

Figure 4.6: P vs γ_{ch}. $K = 4, N = 3, L = 4, \gamma = 5$ dB, $P_t = 10$W.

Fig. 4.6-4.7 present the effect of channel estimation quality. We see that when the channel estimation quality is poor, the power required to satisfy the constraints of the problem becomes large. In $(K, N, L) = (4, 3, 4)$ case, for all methods, there is a

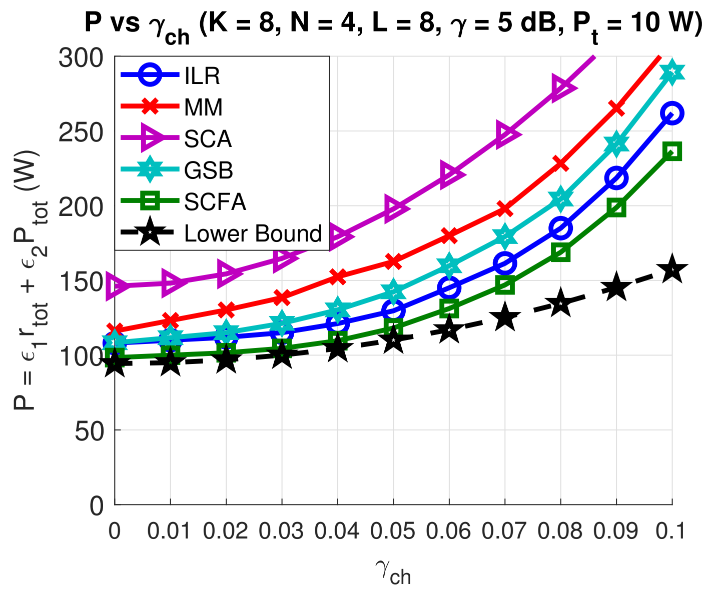

Figure 4.7: P vs γ_{ch}. $K = 8, N = 4, L = 8, \gamma = 5$ dB, $P_t = 10$W.

roughly 50 percent increase in the power between $\gamma_{\text{ch}} = 0$ (perfect CSI) and $\gamma_{\text{ch}} = 0.1$. The increase in the power becomes larger than 100 percent for $(K, N, L) = (8, 4, 8)$ case for all methods. This shows that channel estimation quality has a significant effect on power consumption. On the other hand, employing the robustness of the algorithm designs, increasing the channel estimation error variance by a factor of 10 yields only 2 times higher power consumption. We also observe that the performances of all methods are far away from the bound when the channel estimation quality is not good enough. This shows that inter-user interference cannot be eliminated when the channel estimation quality is poor.

4.5.5 Effect of per-RRH Power Transmit Constraint

RRH power transmit constraint is one of the limiting factors of performance. The lower bound derivation does not include the effect of power transmit constraints and hence we expect a constant lower bound as P_t varies. On the other hand, when P_t is small, it becomes a limiting factor and hence it affects the performance of the algorithms.

Fig. 4.8-4.9 show the effect of per-RRH transmit power constraint. There exists a value for P_t after which the performances of all methods remain constant. After that value, the power spent by each RRH becomes low enough to satisfy transmit power constraints, hence further increasing P_t does not affect the performance.

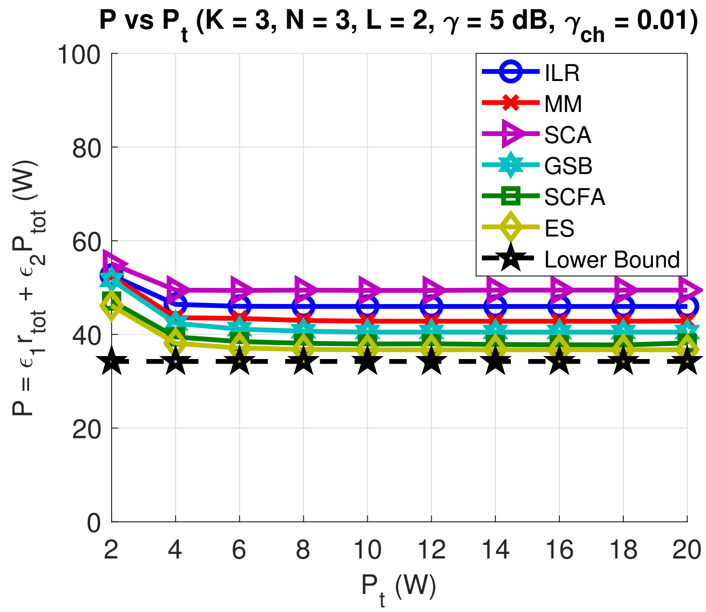

Figure 4.8: P vs P_t. $K = 3, N = 3, L = 2, \gamma = 5$ dB, $\gamma_{\text{ch}} = 0.01$.

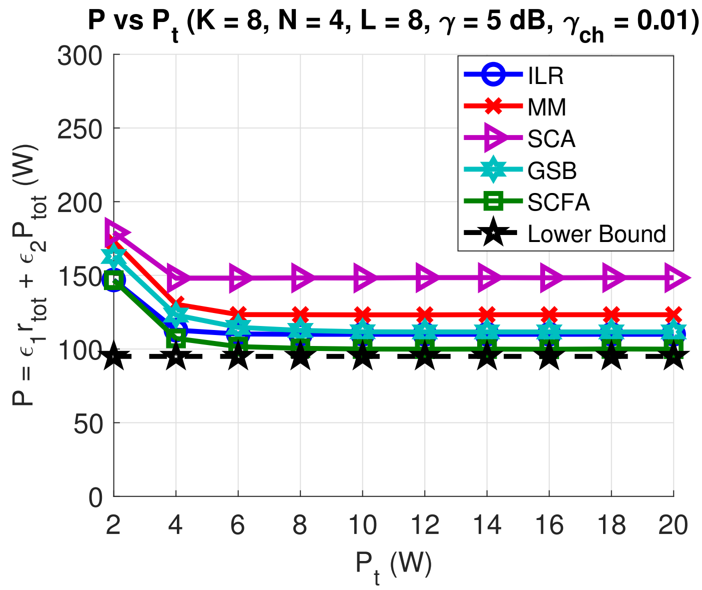

Figure 4.9: P vs P_t. $K = 8, N = 4, L = 8, \gamma = 5$ dB, $\gamma_{\text{ch}} = 0.01$.

4.5.6 Average Run-Time Comparison

In this part, we aim to verify the average complexity values by measuring the average run times of the algorithms.

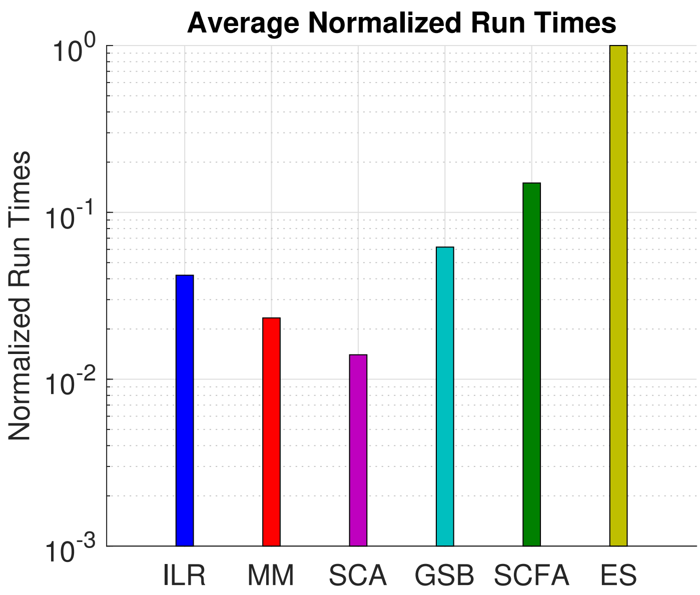

Figure 4.10: Average Complexity Comparison $(K, N, L) = (3, 3, 2)$.

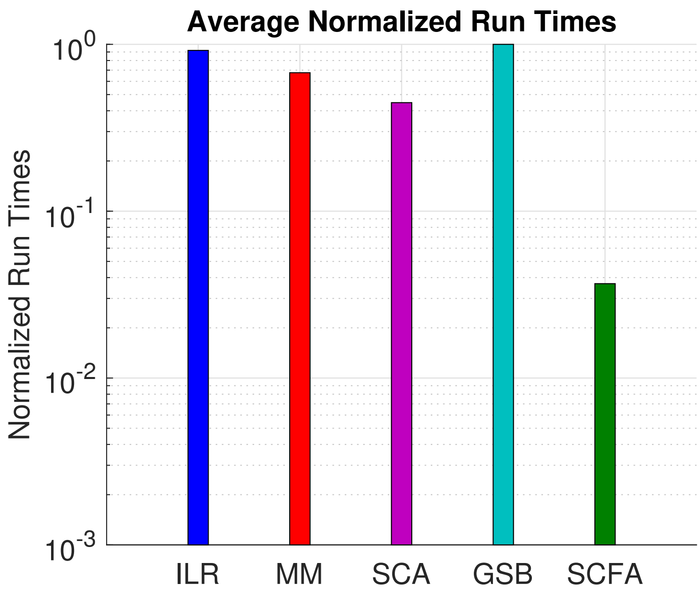

Figure 4.11: Average Complexity Comparison $(K, N, L) = (8, 4, 8)$.

Fig. 4.10-4.11 present the average normalized[7] run-times of each method for $(K, N, L) = (3, 3, 2)$ and $(K, N, L) = (8, 4, 8)$ where we calculate the run-times by averaging the results over all previously described simulations with given (K, N, L) triples.[8] We see that although the performance of SCFA is the best, its computational complex-

[7] We normalize the run-times so that the maximum run-time is equal to 1.
[8] We use Matlab 2020b to run all algorithms.

ity is higher compared to all methods other than ES for $(K, N, L) = (3, 3, 2)$ case. Nevertheless, its complexity is much lower than that of the optimal algorithm ES. On the other hand, the complexity of SCFA becomes much less than those of ILR, MM, SCA, and GSB for $(K, N, L) = (8, 4, 8)$ case.[9] This fact is also verified in the Complexity Comparison section.

4.6 Conclusions

In this study, we analyze the robust beamforming design problem for downlink C-RAN with imperfect channel state information. We consider both the fronthaul power which is related to fronthaul data transfer from CP to RRHs, and total power spent in RRHs to transmit user data to UEs. The total power spent in the C-RAN cluster is minimized under user SINR and per-RRH power transmit constraints. The original problem includes discontinuous terms and hence the optimization is challenging. To do a proper beamforming design, we transform the problem into a smooth constraint-free function minimization problem, and optimization is performed using gradient descent iteratively. The initial point of the algorithm is found by the solution of the full cooperation case which can be optimally solved by convex optimization. As a comparison, we also consider a heuristic search method applying successive convex optimizations to the equivalent combinatorial convex version of the original problem, and sparse beamforming techniques applying ℓ_0 norm approximations. To make optimality analysis, we find a novel theoretical performance bound.

The detailed simulations show that the proposed method SCFA provides an efficient solution. Its performance is better than those of other non-optimal algorithms analyzed, and the power values found for SCFA are close to the lower bound and to the optimal but impractical algorithm ES. For some cases (small K or large N or large L), the power values of SCFA and the bound becomes very close. This proves that the bound that we derived is very tight and SCFA performance is near-optimal at those values of network parameters.

[9] We cannot run ES for large K, N, L due to its high computational complexity.

CHAPTER 5

USER ADMISSION FOR C-RAN WITH WIRED FRONTHAUL

5.1 Problem Definition

In this chapter, we jointly optimize the number of UEs served, total fronthaul data, and total transmit power in downlink C-RAN with wired fronthaul [17]. In this study, we assume imperfect channel knowledge in beamformer design. We first find a theoretical performance bound for the design problem. Then we propose a method based on the bound derivation that jointly optimizes all target parameters.

Throughout this chapter, we use the system model described in Section 2.4.1. We also assume that $\sigma_{\text{UE},k} = \sigma,\ \forall k$, i.e., the average noise powers in all UEs are equal to each other. Using the received signal equation given in (2.5), the received SINR for the k-th UE can be expressed as

$$\text{SINR}_k = \frac{P_d}{P_m + P_{\text{int}} + P_{\text{noise}}} \tag{5.1}$$

where

$$\begin{aligned} P_d &= \mathbb{E}[|\widehat{\mathbf{h}}_k^H \mathbf{w}_k s_k|^2],\ \ P_m = \mathbb{E}[|\Delta\mathbf{h}_k^H \mathbf{w}_k s_k|^2] \\ P_{\text{int}} &= \mathbb{E}[|\mathbf{h}_k^H \sum_{\ell \neq k} \mathbf{w}_\ell s_\ell|^2],\ \ P_{\text{noise}} = \mathbb{E}[|z_{\text{UE},k}|^2]. \end{aligned} \tag{5.2}$$

Using the fact that $\mathbb{E}\left[s_k^* s_\ell\right] = \delta[k-\ell]$ and statistics of the channel error and noise terms, we find that

$$\begin{aligned} P_d &= \text{tr}(\widehat{\mathbf{H}}_k \mathbf{W}_k),\ P_m = \text{tr}(\mathbf{D}_k \mathbf{W}_k), \\ P_{\text{int}} &= \sum_{\ell \neq k} \text{tr}(\widetilde{\mathbf{H}}_k \mathbf{W}_\ell),\ P_{\text{noise}} = \sigma^2 \end{aligned} \tag{5.3}$$

where for all k, we have

$$\widehat{\mathbf{H}}_k = \widehat{\mathbf{h}}_k \widehat{\mathbf{h}}_k^H, \;\; \widetilde{\mathbf{H}}_k = \mathbb{E}[\mathbf{h}_k \mathbf{h}_k^H] = \widehat{\mathbf{H}}_k + \mathbf{D}_k, \;\; \mathbf{W}_k = \mathbf{w}_k \mathbf{w}_k^H$$
$$\mathbf{D}_k = \mathbb{E}[\Delta \mathbf{h}_k \Delta \mathbf{h}_k^H] = \text{diag}\left(\sigma_{k,1}^2 \mathbf{I}_L, \sigma_{k,2}^2 \mathbf{I}_L, \ldots, \sigma_{k,N}^2 \mathbf{I}_L\right). \tag{5.4}$$

Using (5.1) and (5.3), we can write

$$\text{SINR}_k = \frac{\text{tr}(\widehat{\mathbf{H}}_k \mathbf{W}_k)}{\sum_{\ell \neq k} \text{tr}(\widetilde{\mathbf{H}}_k \mathbf{W}_\ell) + \text{tr}(\mathbf{D}_k \mathbf{W}_k) + \sigma^2}, \quad \forall k. \tag{5.5}$$

Using the idea given in [43], we can show that the rate $\log_2(1 + \text{SINR}_k)$ is achievable for the k-th UE. (See Appendix B for a similar proof.) Hence, the SINR that we defined can be used as a design criterion. A certain SINR is needed to decode the received signals in the UEs. We assume that a UE k is successfully served if and only if $\text{SINR}_k \geq \gamma_k$ where γ_k's are pre-determined SINR thresholds.

In a C-RAN cluster, UE data is first sent by CP to RRHs via fronthaul links. As a measure of fronthaul data transfer, we count the total number of UE data streams to be transmitted. Let S_k be the set of RRHs serving the UE k. As an example, for a system with 4 RRHs and 4 UEs, if $S_1 = \{1, 2\}, S_2 = \{1, 2, 4\}, S_3 = \{3\}, S_4 = \{3, 4\}$ each RRH sends 2 UE data streams, which makes the total number of fronthaul streams 8. We know that the power required to carry the UE data through fronthaul links is an increasing function of the total fronthaul data rate. In general, we aim to minimize the total power spent in the system that is one of the major costs of an operator. Hence a natural optimization criterion might be minimizing the total number of fronthaul streams.

In general, it is desired to serve a large number of UEs while keeping the fronthaul data transfer and total transmit power as small as possible. Furthermore, there exists a natural transmit power limit in the RRHs. Considering all three variables and per-RRH power constraint, we form a mixed expression f and define the problem by

$$\begin{aligned} &\text{(P6)} \quad \max_{\mathbf{w}_{k,n}} \; f = K_s - \epsilon_1 L_u - \epsilon_2 \frac{P_{\text{tot}}}{\sigma^2} \\ &K_s = |\{k : \text{SINR}_k \geq \gamma_k\}|, \; L_u = |\{(k, n) : \mathbf{w}_{k,n} \neq \mathbf{0}\}| \\ &\text{s.t. } P_n = \sum_{k=1}^{K} \|\mathbf{w}_{k,n}\|^2 \leq P_t, \; \forall n, \;\; P_{\text{tot}} = \sum_{n=1}^{N} P_n \end{aligned} \tag{5.6}$$

where K_s is the number of UEs served, L_u is the number of fronthaul links used, P_{tot} is the total transmit power, and P_n is the total transmit power for n-th RRH. P_t denotes the maximal power that can be transmitted by each RRH. ϵ_1 and ϵ_2 are two positive weights that determine the relative significance of the number of fronthaul links used and the total transmit power. The designer can adjust ϵ_1 and ϵ_2 for specific cases.

Some works are analyzing a subset of terms considered in (P6). In [34], [37], [41], [15] cooperation strategy and total transmit power are optimized by fixing the number of UEs served. [38] analyzes the UE selection problem under very limited cooperation strategy options. In a realistic scenario, all these variables are important and should be jointly optimized. A natural way for joint optimization is to define a suitable linear combination of these variables. To make all terms unitless we divide the total transmit power by average noise power. In some works [15], [38], fronthaul capacity is assumed to be limited and the corresponding term is used as a constraint. As a second approach, it is assumed that full cooperation is possible but fronthaul data transfer is minimized to decrease the total power spent in the system [15], [37], [52]. In this study, we follow the second approach by adding the term L_u to our cost function to be maximized.

5.2 Equivalent Combinatorial Search Problem

(P6) can be transformed into a combinatorial search problem that can be optimally solved with a finite number of convex sub-problems. Firstly, to analyze the cooperation between the RRHs, we define a binary network link matrix $\mathbf{C}$ with dimensions $K \times N$. This matrix is also defined in Chapter 3 and 4. If the n-th RRH sends k-th UE data, then we say that there is a link between the n-th RRH and the k-th UE and set $c_{k,n} = 0$, $\mathbf{w}_{k,n} \neq \mathbf{0}$. Otherwise $c_{k,n} = 1$, $\mathbf{w}_{k,n} = \mathbf{0}$. Therefore either $c_{k,n} = 0$ or $\mathbf{w}_{k,n} = \mathbf{0}$, and hence $c_{k,n}\|\mathbf{w}_{k,n}\|^2 = 0$, $\forall k, n$. Hence, we can write

$$\sum_{n=1}^{N} c_{k,n}\|\mathbf{w}_{k,n}\|^2 = \sum_{n=1}^{N} c_{k,n}\, \mathrm{tr}\left(\mathbf{B}_n \mathbf{W}_k\right) = 0, \quad \forall k \tag{5.7}$$

where $\mathbf{B}_n$ is an $NL \times NL$ diagonal matrix defined as

$$\mathbf{B}_n = \text{diag}(\overbrace{0, 0, \ldots, 0}^{(n-1)L}, \overbrace{1, 1, \ldots, 1}^{L}, \overbrace{0, 0, \ldots, 0}^{(N-n)L}),\ \forall n. \tag{5.8}$$

The terms P_n and P_{tot} can be written as

$$P_n = \sum_{k=1}^{K} \text{tr}(\mathbf{B}_n \mathbf{W}_k),\ \ P_{\text{tot}} = \sum_{k=1}^{K} \text{tr}(\mathbf{W}_k). \tag{5.9}$$

(P6) is a problem involving K_s and L_u that are discontinuous functions of $\mathbf{w}_{k,n}$'s. When we take ϵ_1 and ϵ_2 positive but very small, we obtain the problem in [37], proved to be NP-hard. To find a solution, we can consider the problem for a fixed $\mathbf{C}$ denoted by (P7). If we solve (P7) for all possible $\mathbf{C}$ matrices, then we can find the optimal solution of (P6) by finding the optimal $\mathbf{C}$ that maximizes f. When we fix $\mathbf{C}$, terms K_s and L_u become also fixed, and the problem reduces to finding optimal beamformers minimizing the total transmit power. (P7) can be expressed by

$$\text{(P7)} \quad \min_{\{\mathbf{W}_k\}_{k=1}^{K}} \ \sum_{k=1}^{K} \text{tr}(\mathbf{W}_k), \tag{5.10}$$

$$\text{s.t.} \quad \text{SINR}_k \geq \gamma_k \left(1 - \prod_{m=1}^{N} c_{k,m}\right),\ \ \forall k, \tag{5.11}$$

$$\sum_{m=1}^{N} c_{k,m}\, \text{tr}\left(\mathbf{B}_m \mathbf{W}_k\right) = 0,\ \ \forall k, \tag{5.12}$$

$$\sum_{\ell=1}^{K} \text{tr}(\mathbf{B}_n \mathbf{W}_\ell) \leq P_t,\ \ \forall n, \tag{5.13}$$

$$\text{rank}(\mathbf{W}_k) = 1,\ \ \mathbf{W}_k \succeq 0,\ \ \forall k. \tag{5.14}$$

As it is not possible to serve a UE with no link, we adjust the SINR threshold in (5.11) so that if a UE k has no link, then the corresponding threshold is equal to 0. (5.12) includes the relation between the $\mathbf{C}$ matrix and beamformers, and (5.13) shows per-RRH power constraints. Finally, (5.14) includes a rank constraint, which makes the problem non-convex.

(P7) can be solved using convex optimization with semi-definite relaxation by omitting the rank constraint. Using the idea in [54], by a similar proof given in Appendix A and C, it can be shown that the solution of the relaxed problem satisfies $\text{rank}(\mathbf{W}_k) = 1$, $\forall k$ and hence it optimally solves (P7). As a result, to find the optimal solution of (P6), we need to solve (P7) for all possible $\mathbf{C}$ matrices and determine the one with the maximum f value. This is a combinatorial search problem that requires a lot of convex optimizations. To find a practical solution, one way is to apply a heuristic search over $\mathbf{C}$ matrices. In general, the performance of this approach enhances as the number of trials increases.

5.3 Bound Based Link Selection (BBLS) Method

To find a practical and effective solution for (P6), we propose a novel bound based link selection (BBLS) method inspired by the derivation of a theoretical upper bound. Firstly, we find a theoretical upper bound for f under the constraints defined in (P6). Using the fact that

$$\mathrm{tr}(\widetilde{\mathbf{H}}_k \, \mathbf{W}_\ell) \geq 0, \; \forall k, \ell \tag{5.15}$$

we get

$$\mathbf{w}_k^H \left(\widehat{\mathbf{h}}_k \, \widehat{\mathbf{h}}_k^H - \gamma_k \mathbf{D}_k \right) \mathbf{w}_k \geq \gamma_k \sigma^2. \tag{5.16}$$

Since $S_k = \{n_1, n_2, \ldots, n_r\}$ is the index set of RRHs serving the UE k, we have $\mathbf{w}_{kn} = \mathbf{0}$ for all $n \notin S_k$. Therefore, we can write

$$\mathbf{w}_k^H \left(\widehat{\mathbf{h}}_k \, \widehat{\mathbf{h}}_k^H - \gamma_k \mathbf{D}_k \right) \mathbf{w}_k = (\mathbf{w}_k')^H \left(\widehat{\mathbf{h}}_k' (\widehat{\mathbf{h}}_k')^H - \gamma_k \mathbf{D}_k' \right) \mathbf{w}_k' \tag{5.17}$$

where $\mathbf{w}_k' = [\mathbf{w}_{k,n_1}^T \; \mathbf{w}_{k,n_2}^T \; \cdots \; \mathbf{w}_{k,n_r}^T]^T$ and $\widehat{\mathbf{h}}_k'$, $\mathbf{D}_k'$ are defined accordingly. Using Cauchy-Schwarz Inequality [85], we get

$$\frac{(\mathbf{w}_k')^H \left(\widehat{\mathbf{h}}_k' (\widehat{\mathbf{h}}_k')^H - \gamma_k \mathbf{D}_k' \right) \mathbf{w}_k'}{(\mathbf{w}_k')^H \mathbf{w}_k'} \leq \lambda_{\text{max}} \left(\widehat{\mathbf{h}}_k' (\widehat{\mathbf{h}}_k')^H - \gamma_k \mathbf{D}_k' \right) \tag{5.18}$$

where $\lambda_{\text{max}}(\cdot)$ denotes the maximum eigenvalue of the matrix argument. To satisfy (5.18) we need $\lambda_{\text{max}} \left(\widehat{\mathbf{h}}_k' (\widehat{\mathbf{h}}_k')^H - \gamma_k \mathbf{D}_k' \right) > 0$. If this condition holds, then we obtain that

$$\frac{P_{\text{tot}}}{\sigma^2} \geq \frac{1}{\sigma^2} \sum_{k=1}^{K} (\mathbf{w}_k')^H \mathbf{w}_k' \geq \sum_{k=1}^{K} \frac{\gamma_k}{\lambda_{\text{max}} \left(\widehat{\mathbf{h}}_k' (\widehat{\mathbf{h}}_k')^H - \gamma_k \mathbf{D}_k' \right)}. \tag{5.19}$$

Using (5.19), we obtain that

$$f \leq \sum_{k=1}^{K} \max_{S_k} f_k = \max_{S_1, S_2, \ldots, S_K} \sum_{k=1}^{K} f_k \tag{5.20}$$

where

$$f_k = \text{sgn}(|S_k|) - \epsilon_1 |S_k| - \epsilon_2 \frac{\gamma_k}{\lambda_{\max}\left(\widehat{\mathbf{h}}_k' (\widehat{\mathbf{h}}_k')^H - \gamma_k \mathbf{D}_k'\right)}. \tag{5.21}$$

In (5.21), $\text{sgn}(\cdot)$ denotes the sign function. Motivated by this bound expression we propose a novel BBLS method where the details are given in Algorithm 5.1.

Algorithm 5.1: (Bound Based Link Selection, BBLS)

---

1) For each k and possible S_k sets, evaluate f_k's and find the corresponding **C** matrix.

2) Sort $f_1 + f_2 + \cdots + f_K$ values in descending order. Sort the corresponding **C** matrices accordingly.

3) Solve (P7) for each **C** in the list until obtaining a feasible solution or reaching the maximum number of trials N_{trial}.

We know that the maximum value of the sum $f_1 + f_2 + \cdots + f_K$ is equal to the upper bound given in (5.20). On the other hand, the corresponding cooperation matrix may not yield a feasible solution as the bound may not be perfectly tight. Therefore, we try other **C** matrices yielding the largest sum of f_k's. Notice that there are $K \cdot 2^N$ many possible trials; however, the simulation results show that $N_{\text{trial}} = NK$ is enough to obtain a feasible solution in general.

5.4 Other Methods

In this section, we discuss heuristic search and norm approximation methods for comparison. We know that the optimal solution of (P6) can be obtained by solving (P7) for all 2^{NK} possible **C** matrices. This approach is impractical due to a large number of trials. As a practical solution, we can iteratively find a proper **C** matrix with a heuristic sequence of trials. Starting from a feasible case, we can add or remove links iteratively to optimize f. Link selection can be done according to the beamformer norms. We consider ILR [41] and ILA [15] algorithms.

The term L_u can be written as the ℓ_0 norm of a vector including beamformer norms. In norm approximation techniques, we approximate ℓ_0 norm by ℓ_1 or ℓ_2 norm. After the approximation, the resulting expression can be optimized by successive convex approximations or SOCP. We consider MM [49]-[51] using ℓ_0/ℓ_1 norm approximation and GSB [52], [53] applying ℓ_0/ℓ_2 norm approximation. In MM method, we use the approximation

$$L_u \approx \sum_{k=1}^{K}\sum_{n=1}^{N} \frac{\|\mathbf{w}_{k,n}\|^2}{\|\mathbf{w}_{k,n}^{(t)}\|^2+\tau} \cdot \frac{1}{\ln(1+\tau^{-1})} \tag{5.22}$$

where $\tau > 0$ is a small number and $\mathbf{w}_{k,n}^{(t)}$ is the beamformer found at the previous iteration. In GSB method, we first write

$$\epsilon_1 L_u + \epsilon_2 \frac{P_{\text{tot}}}{\sigma^2} = \sum_{k=1}^{K}\sum_{n=1}^{N} g_{\text{GSB}}(k,n) \tag{5.23}$$

$$\text{where} \quad g_{\text{GSB}}(k,n) = \begin{cases} 0, & \text{if } \mathbf{w}_{k,n} = \mathbf{0} \\ \epsilon_1 + \epsilon_2 \frac{\|\mathbf{w}_{k,n}\|^2}{\sigma^2}, & \text{if } \mathbf{w}_{k,n} \neq \mathbf{0}. \end{cases} \tag{5.24}$$

Then, we find a homogeneous convex lower bound as

$$g_{\text{GSB}}(k,n) \geq 2\sqrt{\frac{\epsilon_1\epsilon_2}{\sigma^2}}\|\mathbf{w}_{k,n}\|. \tag{5.25}$$

Using (5.25), we obtain the approximation

$$\epsilon_1 L_u + \epsilon_2 \frac{P_{\text{tot}}}{\sigma^2} \approx \sum_{k=1}^{K}\sum_{n=1}^{N} 2\sqrt{\frac{\epsilon_1\epsilon_2}{\sigma^2}}\|\mathbf{w}_{k,n}\|. \tag{5.26}$$

Notice that MM and GSB are also considered in Chapter 4. In MM, we optimize the approximated expression by successive convex approximations with semi-definite relaxation. In GSB, the optimization is performed using SOCP and iterative link removals by solving (P7). The links are prioritized according to the product of beamformer norms found from the SOCP solution and channel amplitudes. Link removal is performed according to the priority of links.

In all four methods, we first find the maximal set of UEs, which can be served by solving a series of (P7). We use channel amplitudes for the prioritization of UEs.

5.5 Numerical Results

In this section, we compare the performances of all algorithms under various cases. Throughout the simulations, we assume that $\gamma_k = \gamma, \quad \forall k$. We use a realistic channel model including path-loss ($P_L = 128.1 + 37.6 \log_{10} d$ where d is in km), log-normal shadowing (10 dB variance) and Rayleigh small-scale fading defined in a 3GPP standard [84]. We consider a circular region with a diameter of 1 km in which RRHs and UEs are distributed uniformly. To avoid channel model inconsistencies, configurations, where RRH-to-UE distances are all at least 50 meters, are considered. RRH and UE antenna gains are chosen as 0 dBi, the UE noise figure is taken as 9 dB, and the system bandwidth is 10 MHz. These parameters are similar to those taken in Chapter 4.

To generate channel estimates and channel estimation errors, we assume that pilot signal powers are adjusted according to the channel amplitudes so that the power ratios of $\mathbb{E}(|\Delta \mathbf{h}_{k,n}|^2)/|\mathbf{h}_{k,n}|^2, \ \forall k, n$ are all equal to some known constant γ_{ch}. Here γ_{ch} is a measure of channel estimation quality. Using the channel estimates and γ_{ch}, one can evaluate $\sigma_{k,n}^2, \ \forall n, k$ accordingly.

Table 5.1: Network parameters used in simulations

	K	N	L	γ (dB)	γ_{ch}	P_t (W)	ϵ_1	$\epsilon_2' = \epsilon_2\eta$
Interval	$[2, 8]$	$[2, 8]$	$[2, 8]$	$[0, 10]$	$[0.01, 0.1]$	$[10, 100]$	$[0.1, 0.5]$	$[0.1, 0.5]$
Step-Size	1	1	1	1	0.01	10	0.1	0.1

In simulations, we consider various values of the parameters $K, N, L, \gamma, \gamma_{\text{ch}}, P_t, \epsilon_1, \epsilon_2$. We choose $7, 7, 7, 11, 10, 10, 5, 5$ equally spaced numbers from intervals with given step-size values in Table 5.1, respectively. We run 1000 Monte Carlo trials for each selection. We only take (K, N, L) triples with $NL \geq K$ for proper transmission. $\epsilon_2' = \epsilon_2 \cdot \eta$ where $\eta = 10^{10.86}$ is the average RRH-to-UE linear path-loss.

In Fig. 5.1, we see the average f values of the algorithms as γ varies. The averaging is performed over all possible 83750000 combinations of parameters given in Table 5.1. The bound values are obtained through (5.20)-(5.21) by evaluating all $K \cdot 2^N$

possible sum of f_k's. We observe that the proposed method BBLS outperforms all other methods. The performance of BBLS is close to the upper bound for small and large γ values. For small γ values, it is easier to satisfy UE SINR constraints and hence BBLS can find a feasible solution after a few iterations. For large γ values, the problem becomes infeasible in most cases. (The optimal value of f is zero as $\gamma \to \infty$.) In both cases, BBLS can find a link configuration close to the one corresponding to the upper bound derivation.

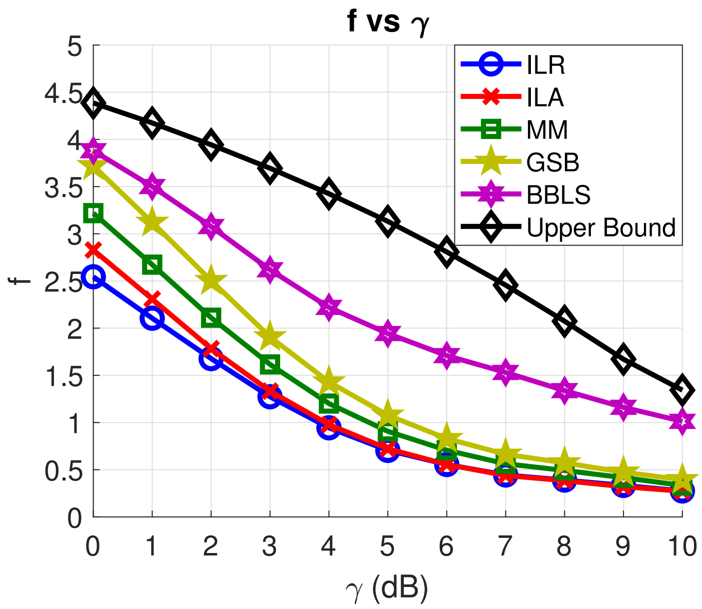

Figure 5.1: Average f vs γ.

In Fig. 5.2-5.3, we observe the performance comparison in terms of the average number of UEs served, the average number of links used, average transmit power, and average normalized run-times, respectively. We see that performance of BBLS is significantly better than those of the other four algorithms in terms of the number of UEs served. The performance gain of BBLS compared to other algorithms is positive but smaller for the average number of links used and average transmit power. The results show that BBLS can serve a 17.6 percent larger number of UEs with 8 percent fewer links and 6.4 percent less transmit power. We also see that BBLS is at least 2 times faster than the other four algorithms. We use SeDuMi [82] convex optimization tool to solve (P7) and to find a solution for MM method, CVX [81] software to solve the SOCP problem in GSB, and MATLAB 2020b to measure run-times.

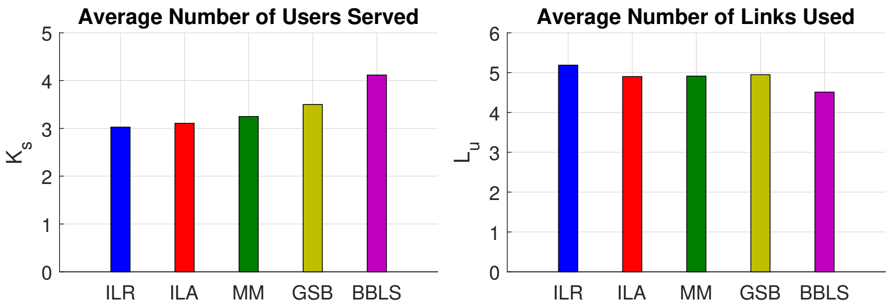

Figure 5.2: Average Number of UEs Served (Left) and Average Number of Links Used (Right).

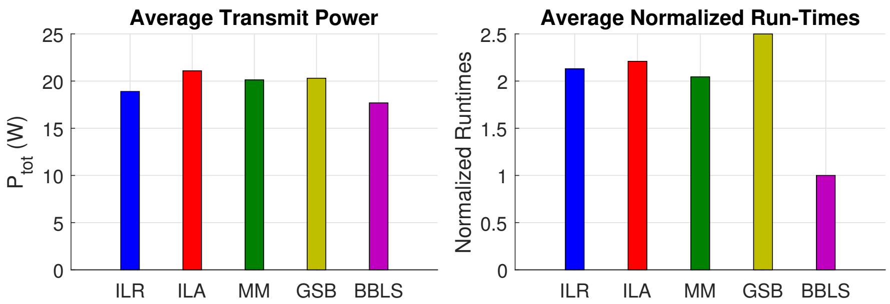

Figure 5.3: Average Transmit Power (Left) and Average Normalized Run-Times (Right).

5.6 Conclusions

In this study, we analyze the beamforming design problem for downlink C-RAN with wired fronthaul. We use a mixed expression to be maximized including the number of UEs served, the number of fronthaul links used, and total transmit power. We propose a novel method BBLS, which is based on the derivation of a theoretical upper bound, and compare it with two heuristic search methods ILR, ILA, and two norm approximation methods MM and GSB. The numerical results show that the proposed method performs better than the other four algorithms in terms of all target parameters. Furthermore, its run-time is also lower than those of other methods, and hence it can effectively solve the problem.

CHAPTER 6

A THEORETICAL PERFORMANCE BOUND FOR C-RAN WITH WIRELESS FRONTHAUL

6.1 Problem Definition

In this chapter, we consider a downlink C-RAN system with wireless fronthaul where the transmissions of fronthaul and access links are in the same frequency band but in different time-slots [18]. We assume that there is a partial channel knowledge where the second-order statistics of the channel error are perfectly known. We optimize fronthaul and access link beamformers with AF type relaying in RRHs. Optimization is performed to minimize total power spent under user SINR constraints.

In this work, our main aim is to find a theoretical lower bound for total power spent in the system. In showing the tightness of a lower bound, existence of an algorithm that comes close to the bound is sufficient since no algorithm can perform better than a lower bound. To show that the given bound is tight enough, we consider four different design methods with different complexities. The first method is Alternating Optimization (AO), which consecutively solves a series of beamforming design problems using convex optimization with an SDR approach. Both fronthaul and access link beamformers are designed using convex optimizations. The performance of this method is close to the bound but its complexity is high in general. The second method is a modified version of AO which is called Total SNR Maximization (TSM), where fronthaul beamformer design is based on the maximization of total SNR at RRHs. The access link beamformers are found as in AO. The third and fourth methods are proposed as a mixture of standard beamforming design methods which are maximal ratio combining (MRC), zero-forcing (ZF), and singular value decomposition (SVD).

The third method is a combination of MRC and ZF so it is named MRC-ZF. In this method, CP beamformers (related to fronthaul link) are found using MRC whereas RRH beamformers (related to access link) are found using ZF. The fourth method is called SVD-ZF and the corresponding CP and RRH beamformers are designed accordingly. MRC-ZF and SVD-ZF can directly find beamformers without using convex optimization and hence they are simpler compared to AO and TSM. They are considered to make a comparison between the well-known beamforming methods and the high-complexity convex optimization-based methods.

We use the system model given in Section 2.4.2. We assume that $\sigma_{\text{RRH},n} = \sigma_{\text{RRH}},\ \forall n$ and $\sigma_{\text{UE},k} = \sigma_{\text{UE}},\ \forall k$. Using the equation in (2.12), we define

$$\text{SINR}_k = \frac{P_d}{P_{I,1} + P_{I,2} + P_n} \tag{6.1}$$

where

$$\begin{aligned} P_d &= \mathbb{E}\left\{\left|\widehat{\mathbf{h}}_k^H \mathbf{W}\widehat{\mathbf{G}}^H \mathbf{v}_k s_k\right|^2\right\}, & P_{I,1} &= \mathbb{E}\left\{\left|\left(\mathbf{h}_k^H \mathbf{W}\mathbf{G}^H \mathbf{v}_k - \widehat{\mathbf{h}}_k^H \mathbf{W}\widehat{\mathbf{G}}^H \mathbf{v}_k\right) s_k\right|^2\right\} \\ P_{I,2} &= \mathbb{E}\left\{\left|\sum_{\ell\neq k} \mathbf{h}_k^H \mathbf{W}\mathbf{G}^H \mathbf{v}_\ell s_\ell\right|^2\right\}, & P_n &= \mathbb{E}\left\{\left|\mathbf{h}_k^H \mathbf{W}\mathbf{z}_{\text{RRH}} + z_{\text{UE},k}\right|^2\right\}. \end{aligned} \tag{6.2}$$

In Appendix G, using the fact that $\mathbb{E}\left[s_k^* s_\ell\right] = \delta[k-\ell]$ and statistics of the channel error matrices/vectors and noise terms, we find that

$$\text{SINR}_k = \frac{\left|\widehat{\mathbf{h}}_k^H \mathbf{W}\widehat{\mathbf{G}}^H \mathbf{v}_k\right|^2}{\sum_{\ell=1}^{K} \text{tr}\left(\mathbf{D}_k \mathbf{W}\mathbf{C}_\ell \mathbf{W}^H\right) - \left|\widehat{\mathbf{h}}_k^H \mathbf{W}\widehat{\mathbf{G}}^H \mathbf{v}_k\right|^2 + \sigma_{\text{RRH}}^2 \,\text{tr}\left(\mathbf{D}_k \mathbf{W}\mathbf{W}^H\right) + \sigma_{\text{UE}}^2} \tag{6.3}$$

where

$$\begin{aligned} \mathbf{D}_k &= \widehat{\mathbf{h}}_k \widehat{\mathbf{h}}_k^H + \mathbf{\Sigma}_{2,k}, \\ \mathbf{C}_k &= \widehat{\mathbf{G}}^H \mathbf{v}_k \mathbf{v}_k^H \widehat{\mathbf{G}} + (\mathbf{v}_k^H \mathbf{v}_k)\mathbf{\Sigma}_1, \\ \mathbf{\Sigma}_1 &= \text{diag}\left(\sigma_{1,1}^2 \mathbf{I}_L, \sigma_{1,2}^2 \mathbf{I}_L, \ldots, \sigma_{1,N}^2 \mathbf{I}_L\right), \\ \mathbf{\Sigma}_{2,k} &= \text{diag}\left(\sigma_{2,k,1}^2 \mathbf{I}_L, \sigma_{2,k,2}^2 \mathbf{I}_L, \ldots, \sigma_{2,k,N}^2 \mathbf{I}_L\right). \end{aligned} \tag{6.4}$$

By a similar proof as given in Appendix B, we can show that the rate $\log_2(1+\text{SINR}_k)$ is achievable for the k-th UE. Hence, the SINR that we defined can be used as a design criterion. Another design term that can be optimized is the total power spent in the system. The total power P has two components P_{CP} and P_{RRH} which correspond to the power transmitted by CP and RRHs, respectively. Considering that CP transmits $\sum_{k=1}^{K} \mathbf{v}_k s_k$ and n-th RRH transmits $\mathbf{y}_n$ for all n, we can write

$$\begin{aligned}
P_{\text{CP}} &= \mathbb{E}\left[\left|\sum_{k=1}^{K} \mathbf{v}_k s_k\right|^2\right] = \sum_{k=1}^{K} \mathbf{v}_k^H \mathbf{v}_k, \\
P_{\text{RRH}} &= \sum_{n=1}^{N} \mathbb{E}\left[\left|\mathbf{W}_n \left(\mathbf{G}_n^H \sum_{k=1}^{K} \mathbf{v}_k s_k + \mathbf{z}_n\right)\right|^2\right] \\
&= \sum_{k=1}^{K} \mathbf{v}_k^H \mathbb{E}\left[\mathbf{G}\mathbf{W}^H \mathbf{W}\mathbf{G}^H\right] \mathbf{v}_k + \sigma_{\text{RRH}}^2 \operatorname{tr}\left(\mathbf{W}^H \mathbf{W}\right) \\
&= \sum_{k=1}^{K} \mathbf{v}_k^H \left[\widehat{\mathbf{G}}\mathbf{W}^H \mathbf{W}\widehat{\mathbf{G}}^H + \operatorname{tr}\left(\mathbf{W}^H \mathbf{W}\boldsymbol{\Sigma}_1\right) \mathbf{I}_M\right] \mathbf{v}_k + \sigma_{\text{RRH}}^2 \operatorname{tr}\left(\mathbf{W}^H \mathbf{W}\right).
\end{aligned} \tag{6.5}$$

We optimize the total power $P = P_{\text{CP}} + P_{\text{RRH}}$ which can be evaluated as

$$P = \sum_{k=1}^{K} \operatorname{tr}\left(\boldsymbol{\tau}_{\mathbf{0}} \mathbf{v}_k \mathbf{v}_k^H\right) + \sigma_{\text{RRH}}^2 \operatorname{tr}\left(\mathbf{W}^H \mathbf{W}\right) \tag{6.6}$$

where $\boldsymbol{\tau}_{\mathbf{0}} = \mathbf{I}_M + \widehat{\mathbf{G}}\mathbf{W}^H \mathbf{W}\widehat{\mathbf{G}}^H + \operatorname{tr}\left(\mathbf{W}^H \mathbf{W}\boldsymbol{\Sigma}_1\right) \mathbf{I}_M$.

In this study, we aim to minimize total power P under SINR constraints $\text{SINR}_k \geq \gamma_k$ where $\{\gamma_k\}_{k=1}^{K}$ are given SINR thresholds. By a similar proof done in Appendix B, it can be shown that the SINR constraints provide that the rate $\log_2(1+\gamma_k)$ is achievable for the k-th user. This type of problem is studied under QoS in the literature where we minimize the power spent in the system by satisfying a certain rate (or SINR) for each user. User rates can be adjusted according to the priority of users by changing the corresponding threshold values. The main optimization problem (P8) can be formulated as

$$\text{(P8)} \qquad \min_{\mathbf{W}, \{\mathbf{v}_k\}_{k=1}^{K}} P \quad \text{such that} \quad \text{SINR}_k \geq \gamma_k, \quad \forall k = 1, 2, \ldots, K. \tag{6.7}$$

6.2 A Theoretical Performance Bound

In this section, we find a novel performance bound for (P8). We find a lower bound for the total mean power P under SINR constraints. To obtain the result, we prove several lemmas.

Lemma 6.1: For all k, we have

$$\left|\widehat{\mathbf{h}}_k^H \mathbf{W}\widehat{\mathbf{G}}^H \mathbf{v}_k\right|^2 \geq \gamma_k\Big(\operatorname{tr}\left(\mathbf{D}_k \mathbf{W}\mathbf{C}_k \mathbf{W}^H\right) - \left|\widehat{\mathbf{h}}_k^H \mathbf{W}\widehat{\mathbf{G}}^H \mathbf{v}_k\right|^2 + \sigma_{\text{RRH}}^2 \operatorname{tr}\left(\mathbf{D}_k \mathbf{W}\mathbf{W}^H\right) + \sigma_{\text{UE}}^2\Big). \tag{6.8}$$

Proof. Using SINR constraints and the fact $\operatorname{tr}\left(\mathbf{D}_k \mathbf{W}\mathbf{C}_\ell \mathbf{W}^H\right) \geq 0 \ \forall k \neq \ell$, we reach the result.

Lemma 6.2: For all k, we get

$$\begin{aligned}\operatorname{tr}\left(\mathbf{D}_k \mathbf{W}\mathbf{C}_k \mathbf{W}^H\right) - \left|\widehat{\mathbf{h}}_k^H \mathbf{W}\widehat{\mathbf{G}}^H \mathbf{v}_k\right|^2 &= \operatorname{tr}\left(\mathbf{\Sigma}_{2,k}(\mathbf{W}\,\widehat{\mathbf{G}}^H\, \mathbf{v}_k)(\mathbf{W}\,\widehat{\mathbf{G}}^H\, \mathbf{v}_k)^H\right) \\ &+ \mathbf{v}_k^H \mathbf{v}_k \left[\operatorname{tr}\left((\widehat{\mathbf{h}}_k^H\, \mathbf{W})^H(\widehat{\mathbf{h}}_k^H\, \mathbf{W})\mathbf{\Sigma}_1\right) + \operatorname{tr}\left(\mathbf{W}^H \mathbf{W}\mathbf{\Sigma}_{2,k}\mathbf{\Sigma}_1\right)\right].\end{aligned} \tag{6.9}$$

Proof. By numerical manipulations and using the facts $\mathbf{W}\mathbf{\Sigma}_1 = \mathbf{\Sigma}_1 \mathbf{W}$ and $\mathbf{W}\mathbf{\Sigma}_{2,k} = \mathbf{\Sigma}_{2,k}\mathbf{W}$ we can complete the proof.

Lemma 6.3: For all k, we obtain that

$$\begin{aligned}\operatorname{tr}\left(\mathbf{D}_k \mathbf{W}\mathbf{C}_k \mathbf{W}^H\right) - \left|\widehat{\mathbf{h}}_k^H \mathbf{W}\widehat{\mathbf{G}}^H \mathbf{v}_k\right|^2 &\geq \lambda_{\min}\left(\mathbf{\Sigma}_{2,k}\right) \left\|\mathbf{W}\,\widehat{\mathbf{G}}^H\, \mathbf{v}_k\right\|^2 \\ &+ \mathbf{v}_k^H \mathbf{v}_k \left[\lambda_{\min}\left(\mathbf{\Sigma}_1\right) \left\|\widehat{\mathbf{h}}_k^H\, \mathbf{W}\right\|^2 + \lambda_{\min}\left(\mathbf{\Sigma}_{2,k}\mathbf{\Sigma}_1\right) \|\mathbf{W}\|^2\right].\end{aligned} \tag{6.10}$$

Proof. Using Von-Neumann's Inequality [86], for any two $c \times c$ Hermitian positive semi-definite matrices $\mathbf{A}$ and $\mathbf{B}$ we have $\operatorname{tr}\left(\mathbf{A}\mathbf{B}\right) \geq \sum_{i=1}^{c} \lambda_i(\mathbf{A})\lambda_{c-i+1}(\mathbf{B}) \geq \lambda_c(\mathbf{A})\lambda_1(\mathbf{B}) = \lambda_{\min}\left(\mathbf{A}\right) \|\mathbf{B}\|$. Using this fact and (6.9), we get the desired result.

Lemma 6.4: For each k, we have

$$\operatorname{tr}\left(\mathbf{D}_k \mathbf{W}\mathbf{W}^H\right) = \operatorname{tr}\left((\widehat{\mathbf{h}}_k\, \widehat{\mathbf{h}}_k^H + \mathbf{\Sigma}_{2,k})\mathbf{W}\mathbf{W}^H\right) \geq \left\|\widehat{\mathbf{h}}_k\, \mathbf{W}\right\|^2 + \lambda_{\min}\left(\mathbf{\Sigma}_{2,k}\right) \|\mathbf{W}\|^2. \tag{6.11}$$

Proof. As in the proof of Lemma 6.3, we can prove Lemma 6.4 using Von-Neumann's Inequality.

Lemma 6.5: For all k, we get

$$\begin{aligned}\left|\widehat{\mathbf{h}}_k^H \mathbf{W}\widehat{\mathbf{G}}^H \mathbf{v}_k\right|^2 &\geq \gamma_k \Big[\lambda_{\min}\left(\mathbf{\Sigma}_{2,k}\right) \left\|\mathbf{W}\,\widehat{\mathbf{G}}^H\, \mathbf{v}_k\right\|^2 + \lambda_{\min}\left(\mathbf{v}_k^H \mathbf{v}_k \mathbf{\Sigma}_1 + \sigma_{\text{RRH}}^2 \mathbf{I}_{NL}\right) \left\|\widehat{\mathbf{h}}_k^H\, \mathbf{W}\right\|^2 \\ &+ \lambda_{\min}\left(\mathbf{v}_k^H \mathbf{v}_k \mathbf{\Sigma}_{2,k}\mathbf{\Sigma}_1 + \sigma_{\text{RRH}}^2 \mathbf{\Sigma}_{2,k}\right) \|\mathbf{W}\|^2 + \sigma_{\text{UE}}^2\Big] \\ &= \gamma_k \Big[\sigma_{2,k}^2 \left\|\mathbf{W}\,\widehat{\mathbf{G}}^H\, \mathbf{v}_k\right\|^2 \\ &+ (\mathbf{v}_k^H \mathbf{v}_k \sigma_1^2 + \sigma_{\text{RRH}}^2) \left(\left\|\widehat{\mathbf{h}}_k^H\, \mathbf{W}\right\|^2 + \sigma_{2,k}^2 \|\mathbf{W}\|^2\right) + \sigma_{\text{UE}}^2\Big]\end{aligned} \tag{6.12}$$

where $\sigma_1^2 = \min\limits_n \sigma_{1,n}^2$ and $\sigma_{2,k}^2 = \min\limits_n \sigma_{2,k,n}^2$.

Proof. Lemma 6.5 is a direct result of Lemma 6.1, 6.3, 6.4.

Lemma 6.6:

$$\begin{aligned} P &\geq \sum_{k=1}^{K} \left(\mathbf{v}_k^H \mathbf{v}_k + \left\| \mathbf{W} \widehat{\mathbf{G}}^H \mathbf{v}_k \right\|^2 + \mathbf{v}_k^H \mathbf{v}_k \lambda_{\min} \left(\mathbf{\Sigma}_1 \right) \|\mathbf{W}\|^2 \right) + \sigma_{\text{RRH}}^2 \operatorname{tr} \left(\mathbf{W}^H \mathbf{W} \right) \\ &\geq \sum_{k=1}^{K} \underbrace{\left(\mathbf{v}_k^H \mathbf{v}_k + \left\| \mathbf{W} \widehat{\mathbf{G}}^H \mathbf{v}_k \right\|^2 + \mathbf{v}_k^H \mathbf{v}_k \sigma_1^2 \|\mathbf{W}\|^2 + \frac{\sigma_{\text{RRH}}^2}{K} \|\mathbf{W}\|^2 \right)}_{P_k}. \end{aligned} \tag{6.13}$$

Proof. It can be proved using Von-Neumann's Inequality and some algebraic manipulations.

We will find a lower bound for P_k for all k using (6.12). To simplify the notations, we define

$$\begin{gathered} x_1 = \left| \widehat{\mathbf{h}}_k^H \mathbf{W} \widehat{\mathbf{G}}^H \mathbf{v}_k \right|^2,\ x_2 = \left\| \mathbf{W} \widehat{\mathbf{G}}^H \mathbf{v}_k \right\|^2,\ x_3 = \left\| \widehat{\mathbf{h}}_k^H \mathbf{W} \right\|^2, \\ x_4 = \|\mathbf{W}\|^2,\ x_5 = \mathbf{v}_k^H \mathbf{v}_k,\ y = P_k, \\ c_1 = \gamma_k,\ c_2 = \sigma_{2,k}^2,\ c_3 = \sigma_1^2, c_4 = \sigma_{\text{RRH}}^2,\ c_5 = \sigma_{\text{UE}}^2,\ c_6 = \frac{\sigma_{\text{RRH}}^2}{K}, \\ d_1 = \left\| \widehat{\mathbf{h}}_k \right\|^2, d_2 = \left\| \widehat{\mathbf{G}} \right\|^2. \end{gathered}$$

(6.12) and (6.13) can be written in terms of new variables as

$$x_1 \geq c_1 \left[c_2 x_2 + (c_3 x_5 + c_4)(x_3 + c_2 x_4) + c_5 \right],\ y = x_2 + x_5 + c_3 x_4 x_5 + c_6 x_4. \tag{6.14}$$

Lemma 6.7: For all k, we obtain that

$$\left\| \widehat{\mathbf{h}}_k \right\|^2 \left\| \mathbf{W} \widehat{\mathbf{G}}^H \mathbf{v}_k \right\|^2 \geq \left| \widehat{\mathbf{h}}_k^H \mathbf{W} \widehat{\mathbf{G}}^H \mathbf{v}_k \right|^2 \implies x_2 d_1 \geq x_1. \tag{6.15}$$

$$\|\mathbf{W}\|^2 \left\| \widehat{\mathbf{h}}_k \right\|^2 \geq \left\| \widehat{\mathbf{h}}_k^H \mathbf{W} \right\|^2 \implies x_4 d_1 \geq x_3. \tag{6.16}$$

$$\left\| \widehat{\mathbf{h}}_k^H \mathbf{W} \right\|^2 \|\mathbf{v}_k\|^2 \left\| \widehat{\mathbf{G}} \right\|^2 \geq \left\| \widehat{\mathbf{h}}_k^H \mathbf{W} \right\|^2 \left\| \mathbf{v}_k^H \widehat{\mathbf{G}} \right\|^2 \geq \left| \widehat{\mathbf{h}}_k^H \mathbf{W} \widehat{\mathbf{G}}^H \mathbf{v}_k \right|^2 \implies x_3 x_5 d_2 \geq x_1. \tag{6.17}$$

Proof. By Cauchy-Schwarz Inequality [85] and submultiplicativity of ℓ_2-norm, we get the result.

Lemma 6.8:

$$y \geq \frac{1}{a} \left(b + c_3 c_5 + 2\sqrt{c_3 c_5 b + c_5 (d_2 + c_6) a} \right), \tag{6.18}$$

where $a = \dfrac{d_1 d_2}{c_1} - c_2 d_2 - c_3 d_1 - c_2 c_3,\ b = c_4 (d_1 + c_2)$.

Proof. The proof is given in Appendix H.

Theorem 6.1: (Performance Bound for (P8))

$$P \geq \sum_{k=1}^{K} \frac{\widetilde{\mathbf{H}}_k \, \sigma_{\mathrm{RRH}}^2 + \widetilde{\mathbf{G}} \, \sigma_{\mathrm{UE}}^2 + 2\sigma_{\mathrm{RRH}}\sigma_{\mathrm{UE}}\sqrt{\widetilde{\mathbf{H}}_k \, \widetilde{\mathbf{G}} + \dfrac{\Delta_k}{K}}}{\Delta_k}, \ \ \Delta_k > 0, \ \forall k \tag{6.19}$$

where $\widetilde{\mathbf{H}}_k = \left\| \widehat{\mathbf{h}}_k \right\|^2 + \sigma_{2,k}^2, \ \widetilde{\mathbf{G}} = \left\| \widehat{\mathbf{G}} \right\|^2 + \sigma_1^2, \ \Delta_k = \left(1 + \dfrac{1}{\gamma_k}\right) \left\| \widehat{\mathbf{h}}_k \right\|^2 \left\| \widehat{\mathbf{G}} \right\|^2 - \widetilde{\mathbf{H}}_k \, \widetilde{\mathbf{G}} \, .$

(6.20)

Proof. The bound expression can be obtained using Lemma 6.8 and calculating the parameters a, b, c_3, c_5, c_6, d_2 in terms of channel estimates, channel error, and noise parameters.

It is easy to show that $a = \Delta_k$. In Appendix H, we also show that $a > 0$ (equivalently $\Delta_k > 0, \ \forall k$) is a necessary (but not sufficient) feasibility condition which has to be satisfied to obtain a proper solution for (P8). It it easy to show that the lower bound is an increasing function of $\sigma_{\mathrm{RRH}}, \sigma_{\mathrm{UE}}, \sigma_1, \sigma_{2,k}, \gamma_k$ and a decreasing function of $\left\| \widehat{\mathbf{h}}_k \right\|$ and $\left\| \widehat{\mathbf{G}} \right\|$, as expected.

6.3 Convex Optimization Methods

In the previous section, we have found a performance bound for the problem (P8). To observe the tightness of the proposed lower bound, we consider different methods to solve the joint beamformer design problem. The access and fronthaul link beamformers are in multiplicative form in the original problem and hence direct optimization is difficult. In this section, we present two convex optimization-based methods to solve (P8). Both methods apply successive convex optimizations with the SDR idea. Firstly, we will show that each one of the fronthaul and access link beamformers can be optimized using convex optimization with SDR when the other one is fixed. Using this observation, we will propose two methods with different complexities.

6.3.1 Access Link Beamformer Design

Let $\mathbf{v}_k$'s be given. In this case, the matrices $\mathbf{D}_k$ and $\mathbf{C}_\ell$ become constant. For any matrices $\mathbf{X}, \mathbf{Y}, \mathbf{Z}$ with suitable dimensions, we have [87]

$$\operatorname{tr}\left(\mathbf{X}^H \mathbf{Y} \mathbf{X} \mathbf{Z}\right) = \left(\operatorname{vec}(\mathbf{X})\right)^H \left(\mathbf{Z}^T \otimes \mathbf{Y}\right) \operatorname{vec}(\mathbf{X}). \tag{6.21}$$

Using this property, we get

$$\begin{aligned}
\left|\widehat{\mathbf{h}}_k^H \mathbf{W} \widehat{\mathbf{G}}^H \mathbf{v}_k\right|^2 &= \left(\operatorname{vec}(\mathbf{W})\right)^H \mathbf{T}_k \operatorname{vec}(\mathbf{W}), \\
\operatorname{tr}\left(\mathbf{D}_k \mathbf{W} \mathbf{C}_\ell \mathbf{W}^H\right) &= \left(\operatorname{vec}(\mathbf{W})\right)^H \mathbf{F}_{\ell,k} \operatorname{vec}(\mathbf{W}), \\
\operatorname{tr}\left(\mathbf{D}_k \mathbf{W} \mathbf{W}^H\right) &= \left(\operatorname{vec}(\mathbf{W})\right)^H \mathbf{E}_k \operatorname{vec}(\mathbf{W}), \\
\operatorname{tr}\left(\mathbf{W}^H \mathbf{W}\right) &= \left(\operatorname{vec}(\mathbf{W})\right)^H \operatorname{vec}(\mathbf{W}), \\
\operatorname{tr}\left(\boldsymbol{\tau}_0 \mathbf{v}_k \mathbf{v}_k^H\right) &= \mathbf{v}_k^H \mathbf{v}_k + \operatorname{tr}\left(\mathbf{W}^H \mathbf{W} \widehat{\mathbf{G}}^H \mathbf{v}_k \mathbf{v}_k^H \widehat{\mathbf{G}}\right) + \operatorname{tr}\left(\mathbf{W}^H \mathbf{W} \boldsymbol{\Sigma}_1\right) \mathbf{v}_k^H \mathbf{v}_k \\
&= \mathbf{v}_k^H \mathbf{v}_k + \left(\operatorname{vec}(\mathbf{W})\right)^H \Big((\widehat{\mathbf{G}}^H \mathbf{v}_k \mathbf{v}_k^H \widehat{\mathbf{G}})^T \otimes \mathbf{I}_{NL} \\
&\quad + (\mathbf{v}_k^H \mathbf{v}_k)(\boldsymbol{\Sigma}_1 \otimes \mathbf{I}_{NL}) \Big) \operatorname{vec}(\mathbf{W}) \\
&= \mathbf{v}_k^H \mathbf{v}_k + \left(\operatorname{vec}(\mathbf{W})\right)^H \mathbf{J}_k \operatorname{vec}(\mathbf{W}).
\end{aligned} \tag{6.22}$$

where $\mathbf{T}_k = (\widehat{\mathbf{G}}^H \mathbf{v}_k \mathbf{v}_k^H \widehat{\mathbf{G}})^T \otimes (\widehat{\mathbf{h}}_k \widehat{\mathbf{h}}_k^H),\ \mathbf{F}_{\ell,k} = \mathbf{C}_\ell^T \otimes \mathbf{D}_k,\ \mathbf{E}_k = \mathbf{I}_{NL} \otimes \mathbf{D}_k,\ \mathbf{J}_k = \mathbf{C}_k^T \otimes \mathbf{I}_{NL}$.

The matrix $\mathbf{W}$ is block diagonal and it includes NL^2 many unknowns. Other $(N^2 - N)L^2$ entries are zero. There exists a matrix $\mathbf{U} :\ N^2L^2 \times NL^2$ and a vector of unknown variables $\mathbf{w}_0 :\ NL^2 \times 1$ such that $\operatorname{vec}(\mathbf{W}) = \mathbf{U}\mathbf{w}_0$. Here, each column of $\mathbf{U}$ includes a single 1 and other entries are equal to 0. We put the 1's at the entries corresponding to the unknown variables in $\operatorname{vec}(\mathbf{W})$. After this observation, we can write P and SINR constraints in terms of $\mathbf{w}_0$ as

$$P = a_1 + \mathbf{w}_0^H \mathbf{B}_1 \mathbf{w}_0, \quad \mathbf{w}_0^H \mathbf{A}_{k,1} \mathbf{w}_0 \geq \gamma_k \sigma_{\text{UE}}^2,\ \forall k \tag{6.23}$$

where

$$\begin{aligned}
a_1 = \sum_{k=1}^{K} \mathbf{v}_k^H \mathbf{v}_k, \quad \mathbf{B}_1 &= \mathbf{U}^H \left(\sigma_{\text{RRH}}^2 \mathbf{I}_{N^2L^2} + \sum_{k=1}^{K} \mathbf{J}_k \right) \mathbf{U} \\
\mathbf{A}_{k,1} &= \mathbf{U}^H \left[(1+\gamma_k)\mathbf{T}_k - \gamma_k \sum_{\ell=1}^{K} \mathbf{F}_{\ell,k} - \gamma_k \sigma_{\text{RRH}}^2 \mathbf{E}_k \right] \mathbf{U},\ \forall k.
\end{aligned} \tag{6.24}$$

Finally we define $\boldsymbol{\mathcal{W}} = \mathbf{w}_0\mathbf{w}_0^H$ satisfying $\boldsymbol{\mathcal{W}} \succeq 0$ and $\mathrm{rank}(\boldsymbol{\mathcal{W}}) = 1$. Using the variable $\boldsymbol{\mathcal{W}}$, we can formulate the problem as

$$\begin{aligned} \text{(P9)} \quad & \min_{\boldsymbol{\mathcal{W}}} \ \mathrm{tr}\left[\mathbf{B}_1\boldsymbol{\mathcal{W}}\right] \\ \text{such that} \quad & \mathrm{tr}\left[\mathbf{A}_{k,1}\boldsymbol{\mathcal{W}}\right] \geq \gamma_k\sigma_{\mathrm{UE}}^2,\ \forall k,\ \boldsymbol{\mathcal{W}} \succeq 0,\ \mathrm{rank}(\boldsymbol{\mathcal{W}}) = 1. \end{aligned} \tag{6.25}$$

In (P9), cost and all constraints except the rank constraint are convex. By omitting the rank constraint, it can be solved with SDR using standard convex optimization tools such as CVX [81], SeDuMi [82], Mosek [88].

6.3.2 Fronthaul Link Beamformer Design

In this part, we consider the case where $\mathbf{W}$ is fixed. In this case, we can write

$$\begin{aligned} \left|\widehat{\mathbf{h}}_k^H\mathbf{W}\widehat{\mathbf{G}}^H\mathbf{v}_k\right|^2 &= \mathbf{v}_k^H\mathbf{A}_{k,2}\mathbf{v}_k, \\ \mathrm{tr}\left(\mathbf{D}_k\mathbf{W}\mathbf{C}_\ell\mathbf{W}^H\right) = \mathrm{tr}\left(\mathbf{W}^H\mathbf{D}_k\mathbf{W}\left(\widehat{\mathbf{G}}^H\mathbf{v}_\ell\mathbf{v}_\ell^H\,\widehat{\mathbf{G}} + (\mathbf{v}_\ell^H\mathbf{v}_\ell)\boldsymbol{\Sigma}_1\right)\right) &= \mathbf{v}_\ell^H\mathbf{B}_{k,2}\mathbf{v}_\ell \end{aligned} \tag{6.26}$$

where $\mathbf{A}_{k,2} = \widehat{\mathbf{G}}\,\mathbf{W}^H\,\widehat{\mathbf{h}}_k\,\widehat{\mathbf{h}}_k^H\,\mathbf{W}\,\widehat{\mathbf{G}}^H$, $\mathbf{B}_{k,2} = \widehat{\mathbf{G}}\,\mathbf{W}^H\mathbf{D}_k\mathbf{W}\,\widehat{\mathbf{G}}^H + \mathrm{tr}(\mathbf{W}^H\mathbf{D}_k\mathbf{W}\boldsymbol{\Sigma}_1)\mathbf{I}_M$. Let $\mathbf{V}_k = \mathbf{v}_k\mathbf{v}_k^H$ and $a_{k,2} = \sigma_{\mathrm{RRH}}^2\,\mathrm{tr}\left(\mathbf{D}_k\mathbf{W}\mathbf{W}^H\right) + \sigma_{\mathrm{UE}}^2$. Using (6.6) and (6.26), we formulate the problem as

$$\begin{aligned} \text{(P10)} \quad & \min_{\{\mathbf{V}_k\}_{k=1}^K} \ \sum_{k=1}^K \mathrm{tr}\left(\boldsymbol{\tau}_{\mathbf{0}}\mathbf{V}_k\right) \\ \text{such that} \quad & \frac{\mathrm{tr}\left(\mathbf{A}_{k,2}\mathbf{V}_k\right)}{\sum_{\ell=1}^K \mathrm{tr}\left(\mathbf{B}_{k,2}\mathbf{V}_\ell\right) - \mathrm{tr}\left(\mathbf{A}_{k,2}\mathbf{V}_k\right) + a_{k,2}} \geq \gamma_k,\ \ \forall k, \\ & \mathbf{V}_k \succeq 0,\ \ \mathrm{rank}(\mathbf{V}_k) = 1,\ \ \forall k. \end{aligned} \tag{6.27}$$

(P10) can also be solved using convex optimization tools by omitting the rank constraints.

6.3.3 Rank-1 Approximation for SDR

In both fronthaul and access link beamformer designs, we find a solution by omitting the rank constraint. If the result is rank-1, the solution becomes optimal. In Appendix I, we prove that the optimal solution of the relaxed version of (P9) satisfies rank($\boldsymbol{\mathcal{W}}$) $\leq K$ and the optimal solution of the relaxed version of (P10) is always rank-1, i.e., rank($\mathbf{V}_k$) $= 1, \forall k$. When the solution found after SDR is not rank-1, we apply a widely used randomization method [19], [20], [29]. Let $\mathbf{X}$ be the matrix found after convex optimization. We want to find a vector $\mathbf{x}$ satisfying $\mathbf{X} = \mathbf{x}\mathbf{x}^H$ which is not possible if rank($\mathbf{X}$) > 1. In such a case, we select $\mathbf{x} = \mathbf{E}\boldsymbol{\Lambda}^{1/2}\mathbf{y}$ where $\mathbf{X} = \mathbf{E}\boldsymbol{\Lambda}\mathbf{E}^H$ is the eigenvalue decomposition of $\mathbf{X}$ and $\mathbf{y}$ is a zero-mean real Gaussian random vector with unity covariance matrix.

6.3.4 Alternating Optimization (AO) Method

We know that each one of the fronthaul and access link beamformers can be found using convex optimization with the SDR approach by fixing the other. Using this idea, we can find a solution for (P8) by alternating optimization of fronthaul and access link beamformers. In general, alternating optimization methods converge to local optimum points. The choice of initial point affects the performance. We consider the CP-to-RRH transmissions and use the total SNR at RRHs to find a suitable initial point. Let $\text{SNR}_{k,n}$ be the SNR of k-th user at n-th RRH, i.e., $\text{SNR}_{k,n} = \frac{\|\widehat{\mathbf{G}}_n^H \mathbf{v}_k\|^2}{\sigma^2_{\text{RRH}}}$. The total SNR is given by $\text{SNR}_{\text{tot}} = \sum_{n=1}^{N}\sum_{k=1}^{K} \text{SNR}_{k,n} = \operatorname{tr}\left(\mathbf{V}^H\mathbf{G}_0\mathbf{V}\right)$ where $\mathbf{G}_0 = \frac{1}{\sigma^2_{\text{RRH}}}\sum_{n=1}^{N} \widehat{\mathbf{G}}_n \widehat{\mathbf{G}}_n^H$ and $\mathbf{V} = [\mathbf{v}_1\ \mathbf{v}_2\ \cdots\ \mathbf{v}_K]$. We know that $P_{\text{CP}} = \operatorname{tr}\left(\mathbf{V}^H\mathbf{V}\right)$. Furthermore, in order to send the user data from CP to RRHs properly, we need $M \geq K$ and rank($\mathbf{V}$) $= K$. To satisfy these constraints, we choose $\mathbf{V}$ such that $\mathbf{V}^H\mathbf{V} = \sqrt{\frac{P_{\text{CP}}}{K}}\mathbf{I}_K$. We aim to find $\mathbf{V}$ maximizing SNR_{tot}. By Von-Neumann's Inequality, we have

$$\begin{aligned}\operatorname{tr}\left(\mathbf{V}\mathbf{V}^H\mathbf{G}_0\right) &\leq \sum_{i=1}^{M} \lambda_i\left(\mathbf{V}\mathbf{V}^H\right)\lambda_i\left(\mathbf{G}_0\right) \\ &= \sum_{i=1}^{K} \lambda_i\left(\mathbf{V}\mathbf{V}^H\right)\lambda_i\left(\mathbf{G}_0\right) = \frac{P_{\text{CP}}}{K}\sum_{i=1}^{K}\lambda_i\left(\mathbf{G}_0\right).\end{aligned} \tag{6.28}$$

Notice that the K largest eigenvalues of $\mathbf{V}\mathbf{V}^H$ are equal to $\frac{P_{\text{CP}}}{K}$ and other $M - K$ are equal to zero. The equality holds when we have

$$\mathbf{v}_k = \sqrt{\frac{P_{\text{CP}}}{K}} e_k\left(\mathbf{G}_0\right), \ \forall k. \tag{6.29}$$

To find a suitable initial point we select the CP beamformers as in (6.29). On the other hand, the selection of initial P_{CP} is also required. To perform this task, we use Algorithm 8.

Algorithm 6.1: (Initialization for Alternating Optimization)

Set $P_{\text{CP}}^{(0)} = 1,\ \mu_0 = 1.05,\ t_{\text{max},0} = 100$. For $t = 0, 1, 2, \ldots, t_{\text{max},0}$ repeat the following steps:

- Form $\mathbf{v}_k^{(t)} = \sqrt{\frac{P_{\text{CP}}^{(t)}}{K}} e_k\left(\mathbf{G}_0\right),\ \forall k$. Solve (P1) to find $\mathbf{W}^{(t)}$.

- If the problem is feasible, then set the initial value of $\mathbf{W}$ as $\mathbf{W}^{(t)}$ and terminate.

- Set $P_{\text{CP}}^{(t+1)} = \mu_0 P_{\text{CP}}^{(t)}$.

Algorithm 6.1 is used to find the initial value of $\mathbf{W}$. Starting from this value, we apply alternating optimization by solving (P9) and (P10) iteratively. At each iteration, P decreases since both (P9) and (P10) minimizes P when one of fronthaul and access link beamformers is fixed. As the power is limited below ($P \geq 0$) we conclude by Monotone Convergence Theorem [89] that this method is convergent. When the rate of change of P is small enough we stop the iteration and find the final solution. The method is summarized in Algorithm 6.2.

Algorithm 6.2: (Alternating Optimization)

Using Algorithm 6.1, find the initial value $\mathbf{W}^{(0)}$. Define $t_{\text{max},1} = 100,\ \eta = 10^{-3}$. For $t = 0, 1, \ldots, t_{\text{max},1}$, repeat the following steps:

- Solve (P10) to find $\mathbf{v}_k^{(t)},\ \forall k$. Solve (P9) to find $\mathbf{W}^{(t)}$.

- If $|P^{(t)} - P^{(t-1)}| < \eta P^{(t)}$, then terminate.

6.3.5 Total SNR Max (TSM) Method

Algorithm 6.1 is used to find an initial point for the AO method. By extending Algorithm 6.1, we propose another iterative method, called the Total SNR Max (TSM) Method, which is computationally less complex compared to AO. Firstly, we make an observation for values of P as P_{CP} increases. Assume that we use (6.29) to form CP beamformers. Starting from a small value, we increase P_{CP} continuously and at each time we find the corresponding RRH beamforming matrix by solving (P9) as in Algorithm 6.1. We observe that in general there exist two iteration indices $0 < t_1 < t_2$ such that the problem is infeasible for $t < t_1$, $P^{(t)}$ is decreasing for $t_1 < t < t_2$, and increasing for $t > t_2$. This shows that optimal value of P is achieved when $t = t_2$. By the motivation of this observation, we propose Algorithm 6.3.

Algorithm 6.3: (Total SNR Max Method)

Set $P_{\text{CP}}^{(0)} = 1$, $P^{(0)} = 0$, $\mu_2 = 1.05$. For $t = 0, 1, \ldots, t_{\text{max},2} = 100$, repeat the following steps:

- Form $\mathbf{v}_k^{(t)} = \sqrt{\frac{P_{\text{CP}}^{(t)}}{K}} e_k\left(\mathbf{G}_0\right), \forall k$.
- Solve (P9) to find $\mathbf{W}^{(t)}$. If the problem is feasible then evaluate $P^{(t)}$ using CP and RRH beamformers. Otherwise, set $P^{(t)} = 0$.
- If $P^{(t)} > P^{(t-1)} > 0$, then terminate, otherwise set $P_{\text{CP}}^{(t+1)} = \mu_2 P_{\text{CP}}^{(t)}$.

This algorithm finds CP beamformers using the approach given in (6.29) by iteratively changing the P_{CP} value. RRH beamforming selection is done as in the AO method.

6.3.6 Complexity of Convex Optimization Methods

In general, we can measure the computational complexity of AO and TSM as the product of the number of iterations and the complexity at each iteration. At each iteration, the main component of complexity is related to the convex optimization and all other operations can be neglected. We use SeDuMi as the convex optimization tool to implement AO and TSM. In both methods, at each iteration, we minimize $\mathbf{c}^H\mathbf{x}$ subject to $\mathbf{A}\mathbf{x} = \mathbf{b}$ where $\mathbf{x} \in \mathbb{C}^n$ is the vector of all unknowns and $\mathbf{A} \in \mathbb{C}^{m\times n}$, $\mathbf{b} \in \mathbb{C}^m$, $\mathbf{c} \in \mathbb{C}^n$ are known vectors/matrices. We know by [82] that the corresponding computational complexity is $\mathcal{O}(n^2m^{2.5} + m^{3.5})$ for SeDuMi. We have

$$\begin{aligned} \text{Fronthaul Link :} \quad & m = K,\ \ n = K + KM^2, \\ \text{Access Link :} \quad & m = K,\ \ n = K + N^2L^4. \end{aligned} \tag{6.30}$$

In AO, both fronthaul and access link beamformer designs are done by convex optimization, meanwhile, TSM uses convex optimization only for the access link. Hence, the corresponding computational complexities are given by

$$\begin{aligned} \text{Complexity of AO :} \quad & \mathcal{O}\left(N_{\text{AO}}K^{2.5}\left[(K + KM^2)^2 + (K + N^2L^4)^2 + 2K\right]\right), \\ \text{Complexity of TSM :} \quad & \mathcal{O}\left(N_{\text{TSM}}K^{2.5}\left[(K + N^2L^4)^2 + K\right]\right) \end{aligned} \tag{6.31}$$

where N_{AO} and N_{TSM} are number of iterations for AO and TSM, respectively. In simulation results, we show that the number of iterations for both methods are similar and the average complexity of AO is larger than that of TSM, as expected.

6.4 Standard Beamforming Methods

In this section, we present two algorithms adapted from well-known beamforming methods. These methods are based on MRC, ZF, and SVD. The purpose of considering these methods is to observe the performance of well-known methods in our joint beamforming design problem. We also make a comparison with the performance bound and relatively complex convex optimization methods described in the previous section. In the first method, called MRC-ZF, we design fronthaul beamformers using the MRC idea. Access link beamformers are chosen as in ZF to cancel the interference due to other user signals. The second method is called SVD-ZF where the fronthaul beamformers are designed by an SVD algorithm. The access link beamformers are chosen to cancel the interference as in MRC-ZF. Because of the nature of the problem, a direct implementation is not possible. We need some adaptations to use MRC, ZF, and SVD.

6.4.1 MRC-ZF

We know that MRC optimizes the signal power by a coherent reception. ZF eliminates the interference and hence enhances the SINR. By the motivation of these beamforming methods, we choose the fronthaul and access link beamformers as

$$\mathbf{v}_k = \left(\widehat{\mathbf{h}}_k^H \mathbf{W} \widehat{\mathbf{G}}^H\right)^H, \ \forall k, \quad \widehat{\mathbf{h}}_k^H \mathbf{W} \widehat{\mathbf{G}}^H \mathbf{v}_\ell = \delta[k-\ell], \ \forall k, \ell. \tag{6.32}$$

In this method, $\mathbf{v}_k$'s are chosen as the conjugate-transpose of the corresponding effective channel $\widehat{\mathbf{h}}_k^H \mathbf{W} \widehat{\mathbf{G}}^H$. The matrix $\mathbf{W}$ is chosen to cancel the interference due to undesired user signals. Notice that both beamformers are chosen in terms of channel estimates only. This approach is used to make the algorithm simpler. Using (6.32), we get

$$\widehat{\mathbf{h}}_k^H \mathbf{W} \widehat{\mathbf{G}}^H \widehat{\mathbf{G}} \mathbf{W}^H \widehat{\mathbf{h}}_\ell = \operatorname{tr}\left(\mathbf{W}^H \widehat{\mathbf{h}}_\ell \widehat{\mathbf{h}}_k^H \mathbf{W} \widehat{\mathbf{G}}^H \widehat{\mathbf{G}}\right) = \delta[k-\ell], \ \forall k, \ell. \tag{6.33}$$

Using the fact that $\operatorname{vec}(\mathbf{W}) = \mathbf{U}\mathbf{w}_0$, we obtain that

$$\mathbf{w}_0^H \mathbf{U}^H \left[(\widehat{\mathbf{G}}^H \widehat{\mathbf{G}})^T \otimes (\widehat{\mathbf{h}}_\ell \widehat{\mathbf{h}}_k^H)\right] \mathbf{U}\mathbf{w}_0 = \delta[k-\ell], \ \forall k, \ell. \tag{6.34}$$

(6.34) is a QCQP type problem including a set of second order matrix equations with NL^2 unknowns and K^2 equations. If $NL^2 \geq K^2$, then we can find a solution using a standard QCQP solver. Let $\mathbf{W}_0$ and $\{\mathbf{v}_{k,0}\}_{k=1}^K$ be some solutions of (6.32). We use $\mathbf{v}_k = \sqrt{a}\mathbf{v}_{k,0}, \ \forall k$ and $\mathbf{W} = \sqrt{b}\mathbf{W}_0$ where a and b are two non-negative real numbers. We use a and b to optimize the power allocation and minimize the total power spent. Using the beamformer expressions, we can write SINR constraints and total mean power as

$$\frac{ab \cdot c_{k,1}}{ab \cdot c_{k,2} - ab \cdot c_{k,1} + b \cdot c_{k,3} + c_{k,4}} \geq \gamma_k, \ \forall k, \ P = a \cdot d_5 + ab \cdot d_6 + b \cdot d_7 \tag{6.35}$$

where

$$
\begin{aligned}
c_{k,1} &= \left| \widehat{\mathbf{h}}_k^H \mathbf{W}_0 \widehat{\mathbf{G}}^H \mathbf{v}_{k,0} \right|^2, \\
c_{k,2} &= \sum_{\ell=1}^{K} \operatorname{tr}\left(\mathbf{D}_k \mathbf{W}_0 \left(\widehat{\mathbf{G}}^H \mathbf{v}_{\ell,0} \mathbf{v}_{\ell,0}^H \widehat{\mathbf{G}} + (\mathbf{v}_{\ell,0}^H \mathbf{v}_{\ell,0}) \boldsymbol{\Sigma}_1 \right) \mathbf{W}_0^H \right), \\
c_{k,3} &= \sigma_{\text{RRH}}^2 \operatorname{tr}\left(\mathbf{D}_k \mathbf{W}_0 \mathbf{W}_0^H \right), \;\; c_{k,4} = \sigma_{\text{RRH}}^2, \;\; d_5 = \sum_{k=1}^{K} \mathbf{v}_{k,0}^H \mathbf{v}_{k,0}, \qquad (6.36) \\
d_6 &= \sum_{k=1}^{K} \mathbf{v}_{k,0}^H \widehat{\mathbf{G}} \mathbf{W}_0^H \mathbf{W}_0 \widehat{\mathbf{G}}^H \mathbf{v}_{k,0} + \operatorname{tr}\left(\mathbf{W}_0^H \mathbf{W}_0 \boldsymbol{\Sigma}_1 \right) \sum_{k=1}^{K} \mathbf{v}_{k,0}^H \mathbf{v}_{k,0}, \\
d_7 &= \sigma_{\text{RRH}}^2 \operatorname{tr}\left(\mathbf{W}_0^H \mathbf{W}_0 \right).
\end{aligned}
$$

Using the SINR constraints in (6.35), we get $a \geq d_{k,1} + \frac{d_{k,2}}{b}$, $(1+\gamma_k)c_{k,1} > \gamma_k c_{k,2}$, $\forall k$ where $d_{k,1} = \frac{\gamma_k c_{k,3}}{(1+\gamma_k)c_{k,1} - \gamma_k c_{k,2}}$, $d_{k,2} = \frac{\gamma_k c_{k,4}}{(1+\gamma_k)c_{k,1} - \gamma_k c_{k,2}}$, $\forall k$. The first condition provides K inequalities for a, b. The second condition should be satisfied for feasibility. The problem of minimizing P in (6.35) under SINR constraints is a two-variable QCQP problem which can be solved directly. The solution steps are explained in Algorithm 6.4.

Algorithm 6.4: (MRC-ZF)

- Find $\mathbf{W}_0$ and $\{\mathbf{v}_{k,0}\}_{k=1}^K$ by solving (6.34) using a QCQP solver.
- Check the feasibility condition. If it is not satisfied, then terminate.
- For all k evaluate $d_{k,1}, d_{k,2}, d_5, d_6, d_7$ using $\mathbf{W}_0$ and $\{\mathbf{v}_{k,0}\}_{k=1}^K$.

For each $k = 1, 2, \ldots, K$ repeat the following steps:

- Find the solution interval $[b_1, b_2] \subseteq [0, \infty)$ of b satisfying $d_{k,1} + \frac{d_{k,2}}{b} \geq d_{\ell,1} + \frac{d_{\ell,2}}{b}$, $\forall \ell \neq k$.
- Evaluate the minimum value $P_{k,0}$ of $P = a \cdot d_5 + ab \cdot d_6 + b \cdot d_7$ for $a = d_{k,1} + \frac{d_{k,2}}{b}$ which is given by $P_{k,0} = d_{k,1} d_5 + d_{k,2} d_6 + d_7 + 2\sqrt{d_{k,1} d_{k,2} d_5 d_6}$.
- Evaluate the values of $P = a \cdot d_5 + ab \cdot d_6 + b \cdot d_7$ for $a = d_{k,1} + \frac{d_{k,2}}{b_1}$, $b = b_1$ and $a = d_{k,1} + \frac{d_{k,2}}{b_2}$, $b = b_2$ as $P_{k,1}$ and $P_{k,2}$.

- Evaluate the global minimum candidate for k as $P_{\text{min},k} = \min(P_{k,0}, P_{k,1}, P_{k,2})$.

Find the solution as $P_{\text{min}} = \min\limits_{k} P_{\text{min},k}$.

Algorithm 6.4 optimally solves the beamforming design problem defined by the MRC-ZF method. Notice that there is a feasibility condition to find a suitable beamformer. By the design method, the algorithm cancels the interference due to undesired user signals. As it uses the channel estimates only, the interference due to the channel mismatch part cannot be canceled. The channel estimation error should be small enough to satisfy the feasibility condition. There is also another condition $NL^2 \geq K^2$ to find a solution for the matrix equation in (6.34). These conditions imply that MRC-ZF can be used if the channel estimation quality is good enough and the number of users is small enough.

6.4.2 SVD-ZF

In the TSM method, fronthaul beamformers are designed by maximizing the total SNR at RRHs. We have shown that the corresponding beamformer is found using SVD of a sum of channel components related to CP-to-RRH channels. We use this approach to design fronthaul beamformers and access link beamformers are found as in MRC-ZF. By the motivation of the SVD and ZF type operations, we name this method SVD-ZF. We first consider the system of equations

$$\mathbf{v}_k = e_k\left(\mathbf{G}_0\right), \ \forall k, \quad \widehat{\mathbf{h}}_k^H \mathbf{W} \widehat{\mathbf{G}}^H \mathbf{v}_\ell = \delta[k-\ell], \ \forall k, \ell. \tag{6.37}$$

The first condition in (6.37) maximizes the total SNR at RRHs and the second condition eliminates the interference. As in MRC-ZF, we only use channel estimates to design beamformers for simplicity. Using the transformation $\text{vec}\left(\mathbf{W}\right) = \mathbf{U}\mathbf{w}_0$, we obtain that

$$\widehat{\mathbf{h}}_k^H \mathbf{W} \widehat{\mathbf{G}}^H e_\ell\left(\mathbf{G}_0\right) = \left(\text{vec}\left([\widehat{\mathbf{G}}^H e_\ell\left(\mathbf{G}_0\right) \widehat{\mathbf{h}}_k^H]^T\right)\right)^T \mathbf{U}\mathbf{w}_0 = \delta[k-\ell], \ \forall k, \ell. \tag{6.38}$$

(6.38) includes a system of linear equations with NL^2 unknowns and K^2 equations. For $NL^2 \geq K^2$, we can find a solution using generalized matrix inversion. As in MRC-ZF we optimize the power allocation to minimize the total power spent. Let $\mathbf{W}_0$

and $\{\mathbf{v}_{k,0}\}_{k=1}^K$ be some solutions of (6.37). We use $\mathbf{v}_k = \sqrt{a}\mathbf{v}_{k,0}, \forall k$ and $\mathbf{W} = \sqrt{b}\mathbf{W}_0$ where a and b are two non-negative real numbers. After this point, we can formulate the problem in terms of a and b as in MRC-ZF and find the optimal values following the same procedure. SVD-ZF is summarized in Algorithm 6.5.

Algorithm 6.5: (SVD-ZF)

- Find $\mathbf{W}_0$ and $\{\mathbf{v}_{k,0}\}_{k=1}^K$ by solving (6.38) using generalized matrix inversion.
- Apply the same procedure done in MRC-ZF to find the solution.

As in MRC-ZF, this method includes a feasibility condition including $\mathbf{W}_0$ and $\{\mathbf{v}_{k,0}\}_{k=1}^K$. We also need $NL^2 \geq K^2$ to find a solution for (6.38). Hence SVD-ZF also requires a good channel estimation quality and a relatively small number of users. One can say that SVD-ZF is computationally less complex compared to MRC-ZF as it does not require a QCQP solver.

6.5 Numerical Results

In this section, we compare the performances of the proposed methods with the performance bound by Monte Carlo simulations. Throughout the simulations, we assume that $\gamma_k = \gamma, \forall k$. We use a realistic channel model including path-loss, shadowing and small-scale fading defined in a 3GPP standard [90]. We consider a circular region in which CP is at the center, RRHs and UEs are distributed uniformly.[1] In Table 6.1, the model parameters are presented.[2]

---

[1] We choose the configurations where CP-to-RRH, CP-to-UE, and RRH-to-UE distances are all at least 50 meters.

[2] In the path-loss formulas in the table, d's are in meters.

Table 6.1: Model parameters used in simulations

Cell radius	1 km
Path-loss for Fronthaul Link ($P_{L,1}$)	$P_{L,1} = 24.6 + 39.1 \log_{10} d$
Path-loss for Access Link ($P_{L,2}$)	$P_{L,2} = 36.8 + 36.7 \log_{10} d$
Antenna gains (CP, RRH, UE)	$(9, 0, 0)$ dBi
Noise figures (RRH, UE)	$(2, 10)$ dB
Bandwidth	10 MHz
Noise power spectral density	-174 dBm/Hz
Small-scale fading model	Rayleigh, $\mathcal{CN}(\mathbf{0}, \mathbf{I})$
Log-normal shadowing variance (CP, RRH)	$(6, 4)$ dB

As in the wired fronthaul case, we assume that we assume that pilot signal powers are adjusted according to the channel amplitudes so that the power ratios of $\mathbb{E}(|\Delta\mathbf{G}_n|^2)/|\mathbf{G}_n|^2$ and $\mathbb{E}(|\Delta\mathbf{h}_{k,n}|^2)/|\mathbf{h}_{k,n}|^2$, $\forall k, n$ are all equal to some known constant γ_{ch}. Here γ_{ch} is a measure of channel estimation quality. Using the channel estimates and γ_{ch}, one can evaluate $\sigma^2_{1,n}$, $\forall n$ and $\sigma^2_{2,k,n}$, $\forall n, k$ accordingly. In simulations, we observe the effect of parameters $\gamma, K, N, L, M, \gamma_{\text{ch}}$. We know that there is always a non-zero probability of having an infeasible solution. To measure the ratio of infeasibility, we define P_{outage} showing the percentage of infeasible designs. We run 100 Monte Carlo trials in each case. To evaluate the P values for a method, we average the results over Monte Carlo trials with feasible solutions.

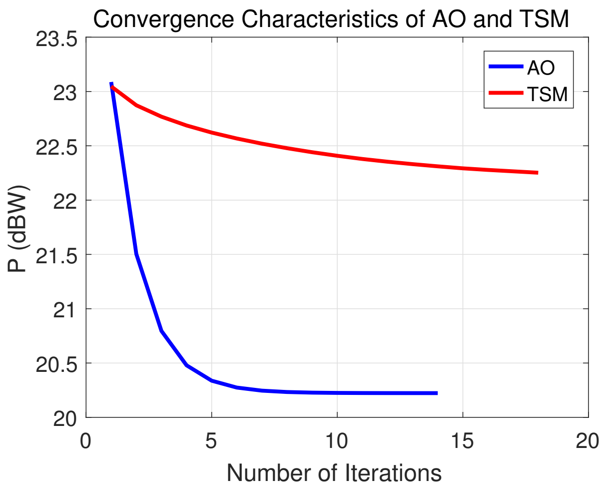

Figure 6.1: Convergence characteristics of AO and TSM.

In Fig. 6.1, we see a typical convergence graph of AO and TSM for $(K, N, L, M) = (4, 4, 4, 8)$, $\gamma = 5$ dB and $\gamma_{\text{ch}} = 0.01$. We observe that P values decrease smoothly and both algorithms obtain a solution after a few iterations.

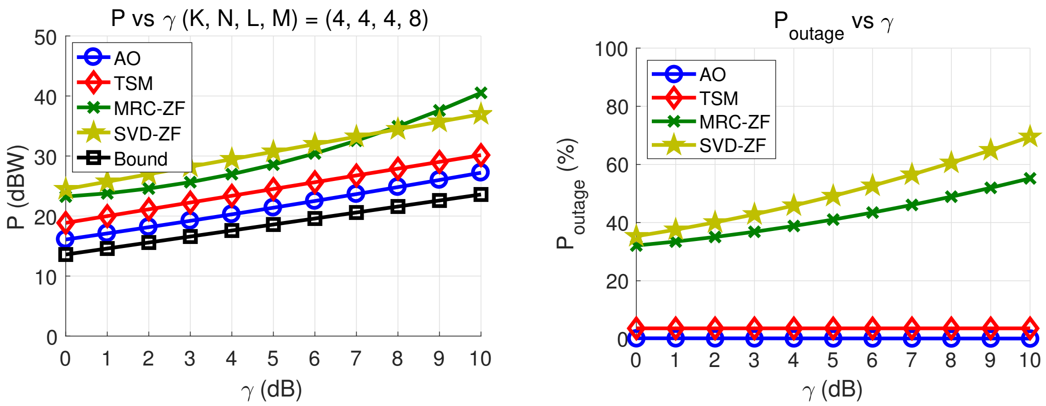

Figure 6.2: P and P_{outage} vs γ. $(K, N, L, M) = (4, 4, 4, 8)$, $\gamma_{\text{ch}} = 0.01$.

In Fig. 6.2, we observe the effect of the SINR threshold γ. For all γ values, the performance loss compared to the bound is roughly 3 and 6 dB for AO and TSM, respectively. MRC-ZF and SVD-ZF have significantly worse performance than those of convex optimization methods. We observe that P_{outage} values of both methods increase with γ. Even when $\gamma = 0$ dB, the infeasibility ratio is about 30 percent for both methods. The results imply that even for a relatively low channel estimation error, the methods MRC-ZF and SVD-ZF may fail to solve the joint beamforming design problem with a large probability. We observe that AO can solve the problem with almost 100 percent whereas the TSM feasibility ratio is slightly smaller than that of AO.

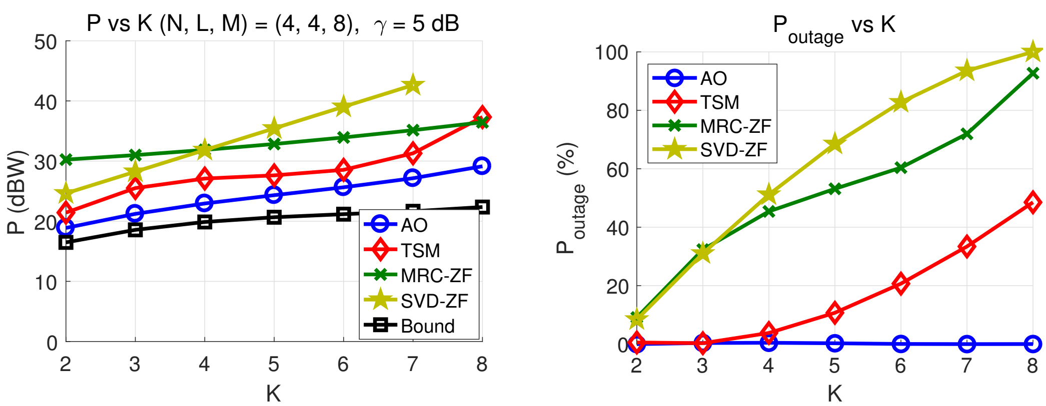

Figure 6.3: P and P_{outage} vs K. $(N, L, M) = (4, 4, 8)$, $\gamma = 5$ dB, $\gamma_{\text{ch}} = 0.01$.

Fig. 6.3 shows the performances as the number of UEs K varies. We observe that the performance loss of all methods compared to the bound increase with K. This is due to the fact that bound can only be achieved when the interference due to undesired users is eliminated which becomes harder as K increases. We see that for large K values, the feasibility ratios of MRC-ZF and SVD-ZF become very small meaning that these methods cannot be used when the number of users is not small enough. Although it outperforms MRC-ZF and SVD-ZF, TSM performance also degrades for a large number of users. On the other hand, AO can successfully design beamformers with 100 percent feasibility and it requires less power for all K values compared to the other three methods.

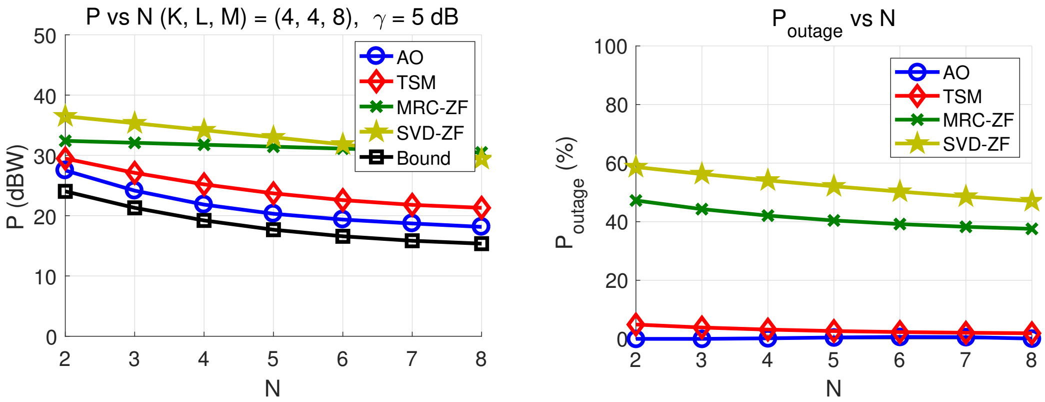

Figure 6.4: P and P_{outage} vs N. $(K, L, M) = (4, 4, 8)$, $\gamma = 5$ dB, $\gamma_{\text{ch}} = 0.01$.

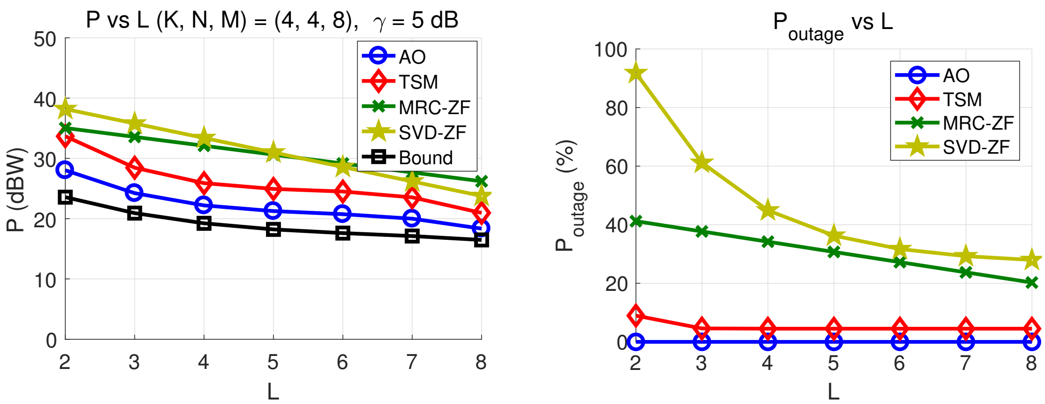

Figure 6.5: P and P_{outage} vs L. $(K, N, M) = (4, 4, 8)$, $\gamma = 5$ dB, $\gamma_{\text{ch}} = 0.01$.

In Fig. 6.4-6.5, we observe the effects of the number of RRHs N and the number of RRH antennas L. The results show that AO has the best performance for all cases. Its outage ratio is always 0 percent and the power difference with the bound is generally less than 5 dB. The difference becomes smaller as N or L increases. As in the previous cases, MRC-ZF performs better than SVD-ZF and worse than TSM. We also observe that there is a significant difference in the bound values between $N = 2$ and $N = 8$ and the same fact is true for $L = 2$ and $L = 8$.

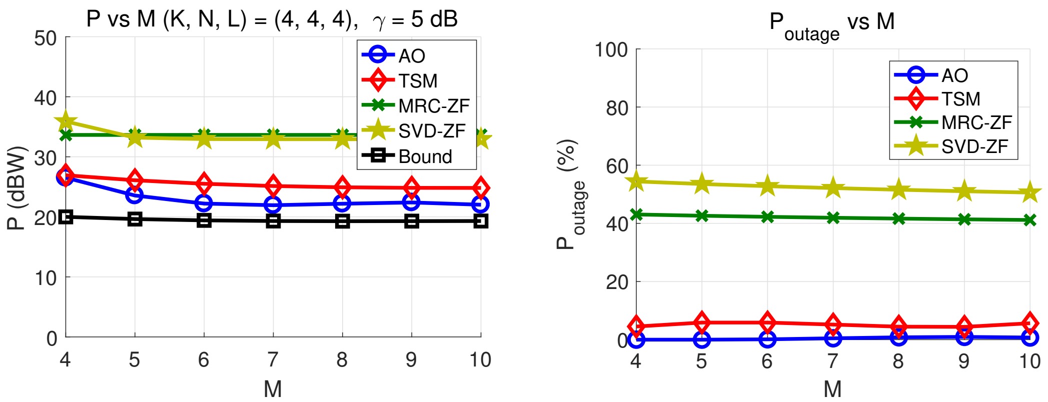

Figure 6.6: P and P_{outage} vs M. $(K, N, L) = (4, 4, 4)$, $\gamma = 5$ dB, $\gamma_{\text{ch}} = 0.01$.

In Fig. 6.6, we see the effect of the number of CP antennas M. The main observation is that the performance enhancement obtained by increasing M is very limited. Adding an extra antenna to CP mainly affects the power spent in fronthaul transmissions. In our channel model, CP-to-RRH channels are better than RRH-to-UE channels as RRHs are stationary and one can place them by optimizing the corresponding fronthaul channel conditions. Therefore, the portion of P_{CP} in the total power P is small in general and hence the effect of M on the performance is small compared to the effects of N and L.

Table 6.2: P values in dBW for various quadruples of (K, N, L, M) for $\gamma = 5$ dB and $\gamma_{\text{ch}} = 0.01$

K	N	L	M	AO	TSM	MRC-ZF	SVD-ZF	Bound	AO − Bound
2	2	4	4	27.52	28.15	33.3	33.61	24.43	3.11
3	2	4	6	27.15	29.42	30.26	31.23	23.82	3.33
4	2	4	8	27.5	29.47	32.41	36.49	24.03	3.47
3	3	4	4	24.07	27.02	30.67	31.32	20.54	3.53
4	4	4	4	25.69	26.23	35.31	36.62	20.48	5.21
3	4	3	4	23.73	25.54	30.44	32.83	19.7	4.03
2	4	2	4	23.59	25.11	31.4	33.33	21.28	2.31

In Table 6.2, we compare the performances when the ratios $\frac{K}{M}, \frac{K}{N}, \frac{K}{L}$ are fixed. The first three rows show the cases where $\frac{K}{M}, N, L$ are fixed; the first, fourth, and fifth rows are related to the case where $\frac{K}{N}, M, L$ are fixed, and finally, the last three rows correspond to the case where $\frac{K}{L}, M, N$ are fixed. We observe that for every three cases, the performance loss of the best method AO compared to the bound is an increasing function of the number of users K. This is due to the fact that achieving bound requires perfect elimination of the interference due to undesired users which becomes harder as the number of users increases.

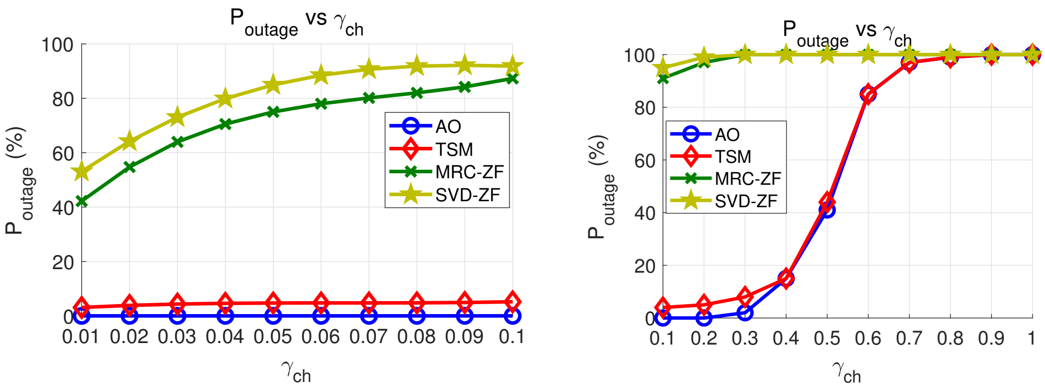

Figure 6.7: P_{outage} vs γ_{ch}. $(K, N, L, M) = (4, 4, 4, 8)$, $\gamma = 5$ dB.

Fig. 6.7 presents the feasibility ratios versus the channel estimation error quality. We observe that if the channel estimation error is large enough, all methods completely fail in the design process. We conclude that convex optimization-based methods are more robust to channel errors compared to methods adapted from known beamforming algorithms.

Fig. 6.8 shows the normalized average run-times for all methods and rank-1 percentages of (P9) and (P10). We observe that complexity is high for convex optimization-based methods. The average run-time of AO is slightly larger than that of TSM. Among all methods we consider, SVD-ZF is the less complex one since it directly finds the solution (if feasible) by solving a linear matrix equation without any solver. On the other hand, its performance is generally not satisfactory in most cases. We observe that the SDR approach optimally solves (P9) and (P10) as the results are always rank-1.

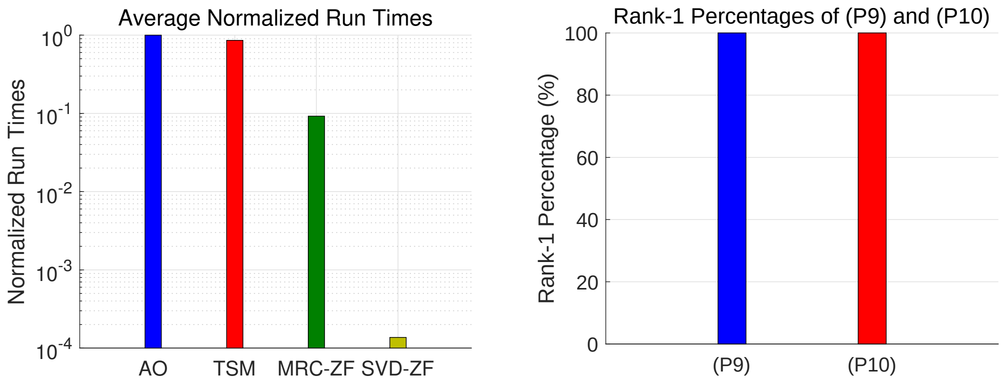

Figure 6.8: Average Complexity Comparison (left) and Rank-1 Percentages of (P9) and (P10) (right).

In the second part of simulations, we observe the power allocation of users, power-sharing between fronthaul and access links, and the effect of different user SINR thresholds. We consider two scenarios where RRH and UE locations are fixed. In both cases, there is a CP with 4 antennas, 2 RRHs each with 4 antennas, and 4 UEs. We only consider the AO method to present the results. The first scenario includes various RRH-to-UE distances and the second one considers a symmetric placement. In Fig. 6.9, we present the RRH and UE placements of the two scenarios.

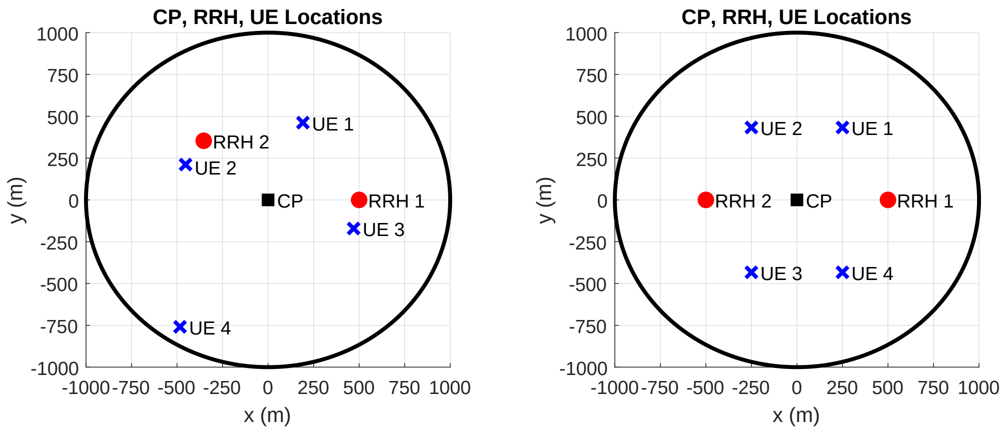

Figure 6.9: Scenario 1 (left) and Scenario 2 (right) RRH and UE placements.

To present the power allocation of users for both fronthaul and access links, we define

$$P_{\text{CP},k} = \mathbf{v}_k^H \mathbf{v}_k, \; P_{\text{RRH},k} = \mathbf{v}_k^H \left(\widehat{\mathbf{G}} \mathbf{W}^H \mathbf{W} \widehat{\mathbf{G}}^H + \text{tr}\left(\mathbf{W}^H \mathbf{W} \mathbf{\Sigma}_1 \right) \mathbf{I}_M \right) \mathbf{v}_k,$$
$$P_{\text{RRH,amp-noise},k} = \frac{1}{K} \sigma_{\text{RRH}}^2 \, \text{tr}(\mathbf{W}^H \mathbf{W}), \; \forall k \tag{6.39}$$

where $P_{\text{CP},k}$, $P_{\text{RRH},k}$, $P_{\text{RRH,amp-noise},k}$ are the fronthaul link power, access link power and RRH amplified noise power for k-th user. Notice that we have

$$P_{\text{CP}} = \sum_{k=1}^{K} P_{\text{CP},k}, \; P_{\text{RRH}} = \sum_{k=1}^{K} \left(P_{\text{RRH},k} + P_{\text{RRH,amp-noise},k}\right). \tag{6.40}$$

We know that RRH receiver noise is amplified and forwarded to users in AF-type relaying. The related term is given in (2.12) as the first part of the noise term. We equally divide RRH amplified noise power between users as shown in (6.39).

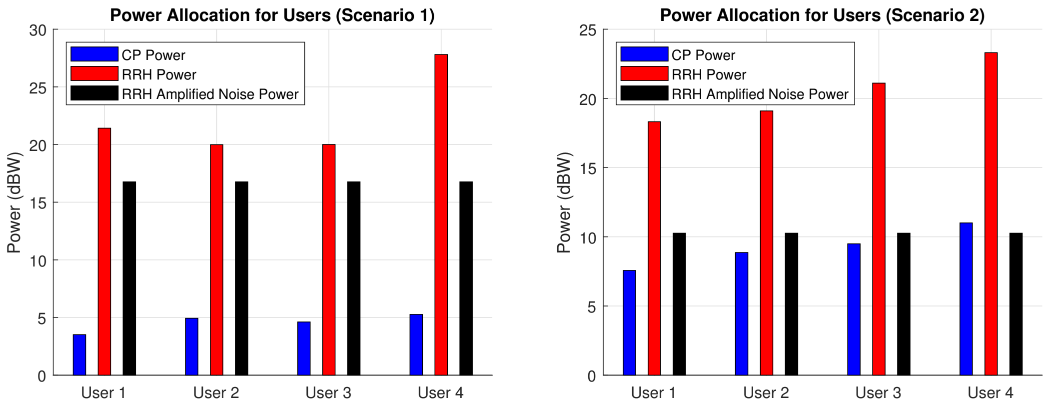

Figure 6.10: Power Allocations for Scenario 1 (left) and Scenario 2 (right).

In the left part of Fig. 6.10, we observe the power allocation of users for Scenario 1. We take equal SINR thresholds $\gamma_k = \gamma = 5$ dB for all users. Notice that fronthaul powers are smaller compared to access link powers. This is due to the path-loss and antenna gain model that we use. As CP and RRHs are stationary, we assume that one can optimize the locations of CP and RRHs so that the corresponding channel conditions are good. We also assume that CP antenna array design is more flexible compared to RRH and user equipment, and hence we use higher gain antennas for CP. We also observe that $P_{\text{RRH},4} > P_{\text{RRH},1} > P_{\text{RRH},2} \approx P_{\text{RRH},3}$. This is expected considering the locations of users. The distance between UE 4 and both two RRHs is large and hence it requires the largest power. On the other hand, since UE 2 and 3 are close to some RRH, they require the smallest power. UE 1 distance to both RRHs is at an intermediate level and hence the corresponding power is in between the other three UEs. As a final remark, we observe that RRH amplified noise powers are significantly large and this shows that a well-optimized network design is needed to obtain sufficiently large user SINRs for AF type relaying.

We present the power allocation of users for Scenario 2 in the right part of Fig. 6.10. In this case, we use a symmetric placement of RRHs and UEs and consider the effect of different user SINR thresholds by taking $\gamma_1 = 4, \gamma_2 = 6, \gamma_3 = 8, \gamma_4 = 10$ dB. We observe that as the SINR threshold increases, the corresponding user power of both fronthaul and access links also increases. The operator can adjust the user SINR thresholds according to the priority of users. The power required to serve a more prior user will be larger as presented in this example scenario.

6.6 Conclusions

In this study, we analyzed the joint beamformer design problem in downlink C-RAN with wireless fronthaul. We considered the case where AF type relaying is used in RRHs without the capability of baseband processing. We assumed that channel coefficients are available with some additive error with known second-order statistics. We derived a novel theoretical lower bound for the total power spent under SINR constraints. We proposed two convex optimization-based methods and two other methods adapted from known beamforming strategies to observe the tightness of the bound. We have shown that the first two methods have better performances but their complexities are also higher. In general, the performance of the best method is close to the bound and the difference is less than 1 dB for some cases. The results show the effectiveness of the bound as well as the performances of various solution techniques. For C-RAN systems, there are other beamforming design techniques that are not analyzed in this study but studied in the literature. We have found at least one method performing close to the bound and this is enough to show the tightness of the bound proposed.

As future work, the approach used in this study to derive a performance bound can be adapted to DF and DCF based relaying and also to full-duplex RRH case. One can also search the necessary conditions required for the equality case of the bound to gain insight into the optimal algorithm.

CHAPTER 7

POWER OPTIMIZATION FOR INTEGRATED ACCESS AND BACKHAUL

7.1 Problem Definition

In this chapter, we describe a study on beamformer design for a downlink full-duplex IAB system.

Throughout the analysis, we use the system model described in Section 2.4.3. The backhaul and access link signals can be written as

$$\begin{aligned} x_{\text{backhaul},n} &= \sum_{k=1}^{K} \mathbf{g}_{n,0}^{H} \mathbf{v}_k s_k^B + \sum_{k=1}^{K} \sum_{m=1}^{N} \mathbf{g}_{m,n}^{H} \mathbf{w}_{k,m} s_k^A + z_{\text{SBS},n}, \\ x_{\text{access},k} &= \sum_{n=1}^{N} \mathbf{h}_{k,n}^{H} \mathbf{w}_{k,n} s_k^A + \sum_{\ell \neq k}^{K} \sum_{n=1}^{N} \mathbf{h}_{k,n}^{H} \mathbf{w}_{\ell,n} s_\ell^A + \sum_{\ell=1}^{K} \mathbf{h}_{k,0}^{H} \mathbf{v}_\ell s_\ell^B + z_{\text{UE},k}. \end{aligned} \tag{7.1}$$

We follow three main assumptions to define and solve the design problem, proposed in [14].

Assumption 1: SBS n can perfectly eliminate the interference signal due to SBS $m \neq n$ in decoding the k-th user backhaul data if $k \in \mathcal{K}_n \cap \mathcal{K}_m$. This can be achieved since SBS-to-SBS channels are slowly changing and can be estimated with negligible error. As the signal s_k^A is known by the n-th SBS, using the effective channel knowledge between m-th SBS and n-th SBS, the interference signal $\mathbf{g}_{m,n}^H \mathbf{w}_{k,m} s_k^A$ can be perfectly eliminated.

Assumption 2: SBSs decode user backhaul data using the successive interference cancellation (SIC) method.

Assumption 3: All MBS-to-SBS, SBS-to-SBS, SBS-to-UE, MBS-to-UE channels are perfectly known.

n-th SBS decodes the k-th UE data if $k \in \mathcal{K}_n$. We assume that SBSs apply SIC method and decoding order of user backhaul data is chosen such that if $i < j$ then s_i^B is decoded before s_j^B.

Considering the assumptions on interference cancellation and SIC, the corresponding backhaul SINR term can be written as

$$\text{SINR}_{k,n}^B = \frac{|\mathbf{g}_{n,0}^H \mathbf{v}_k|^2}{\sum_{\ell=1}^{K} |\mathbf{g}_{n,0}^H \mathbf{v}_\ell|^2 f_{k,n}(\ell) + \sum_{\ell \notin \mathcal{K}_n} \left| \sum_{m \neq n}^{N} \mathbf{g}_{n,m}^H \mathbf{w}_{\ell,m} \right|^2 + \frac{1}{\beta_{\text{SI}}} \sum_{\ell=1}^{K} \|\mathbf{w}_{\ell,n}\|^2 + \sigma_{\text{SBS},n}^2}. \tag{7.2}$$

Here the function $f_{k,n}(\ell)$ is used to determine interference signals left in each stage of SIC process and defined as

$$f_{k,n}(\ell) = \begin{cases} 1, & \text{if} \quad \ell \in \mathcal{K}_n \quad \text{or} \quad \ell > k \\ 0, & \text{else} \end{cases} . \tag{7.3}$$

To simplify the notations, we define augmented channel and beamformer vectors/matrices as given in (7.4).

$$\begin{aligned} \mathbf{h}_k &= [\mathbf{h}_{k,1}^T \; \mathbf{h}_{k,2}^T \; \cdots \; \mathbf{h}_{k,N}^T]^T, \quad \forall k, \\ \mathbf{g}_n &= [\mathbf{g}_{n,1}^T \; \cdots \; \mathbf{g}_{n,n-1}^T \mathbf{0}_{1\times L} \; \mathbf{g}_{n,n+1}^T \; \cdots \; \mathbf{g}_{n,N}^T]^T, \quad \forall n, \\ \mathbf{w}_k &= [\mathbf{w}_{k,1}^T \; \mathbf{w}_{k,2}^T \; \cdots \; \mathbf{w}_{k,N}^T]^T, \quad \forall k. \end{aligned} \tag{7.4}$$

Using the augmented variables and network link matrix $\mathbf{C}$ including the knowledge of $\mathcal{K}_n$'s for all n, and $\mathcal{N}_k$'s for all k, we can rewrite (7.2) as

$$\text{SINR}_{k,n}^B = \frac{|\mathbf{g}_{n,0}^H \mathbf{v}_k|^2}{\sum_{\ell=1}^{K} |\mathbf{g}_{n,0}^H \mathbf{v}_\ell|^2 f_{k,n}(\ell) + \sum_{\ell=1}^{K} |\mathbf{g}_n^H \mathbf{w}_\ell|^2 c_{\ell,n} + \frac{1}{\beta_{\text{SI}}} \sum_{\ell=1}^{K} \mathbf{w}_\ell^H \mathbf{B}_n \mathbf{w}_\ell + \sigma_{\text{SBS},n}^2}. \tag{7.5}$$

In (7.5), the matrix $\mathbf{B}_n = \text{diag}\left(\mathbf{0}_{(n-1)L},\ \mathbf{1}_L,\ \mathbf{0}_{(N-n)L}\right)$ satisfies $\mathbf{B}_n \mathbf{w}_\ell = \mathbf{w}_{\ell,n}$.

For the access link, we can write the corresponding user SINR terms as

$$\text{SINR}_k^A = \frac{\left|\sum_{n=1}^{N} \mathbf{k}_{k,n}^H \mathbf{w}_{k,n}\right|^2}{\sum_{\ell \neq k}^{K} \left|\sum_{n=1}^{N} \mathbf{h}_{k,n}^H \mathbf{w}_{\ell,n}\right|^2 + \sum_{\ell=1}^{K} \left|\mathbf{h}_{k,0}^H \mathbf{v}_\ell\right|^2 + \sigma_{\text{UE},k}^2}. \tag{7.6}$$

Using the augmented variables, we can rewrite (7.6) as

$$\text{SINR}_k^A = \frac{|\mathbf{h}_k^H \mathbf{w}_k|^2}{\sum_{\ell \neq k}^{K} |\mathbf{h}_k \mathbf{w}_\ell|^2 + \sum_{\ell=1}^{K} |\mathbf{h}_{k,0} \mathbf{v}_\ell|^2 + \sigma_{\text{UE},k}^2}. \tag{7.7}$$

We consider a QoS problem where total transmit power is minimized under user data rate (equivalently SINR) constraints. The transmit power is one of the major costs of an operator. By minimizing the power consumption, we also decrease the cost of cooling the equipment. Furthermore, the inter-cell interference will also be minimized when the transmit power is optimized.

To satisfy a certain data rate for a user, we need to guarantee that both backhaul and access link SINRs of that user should be large enough. In other words, if $\text{SINR}_k^A \geq \gamma_k$ and $\text{SINR}_{k,n}^B \geq \gamma_k$, $\forall n \in \mathcal{K}_n$ then the data rate $R_k = \log_2(1+\gamma_k)$ for the k-th user is achievable.

Using the definition of the network link matrix $\mathbf{C}$, we can write a relation between access link beamformers and entries of $\mathbf{C}$. After some mathematical calculations, we obtain

$$c_{k,n}\mathbf{w}_{k,n} = \mathbf{0} \iff c_{k,n}\mathbf{B}_n\mathbf{w}_k = \mathbf{0} \iff \sum_{n=1}^{N} c_{k,n}\mathbf{w}_k^H\mathbf{B}_n\mathbf{w}_k = 0. \tag{7.8}$$

To obtain (7.8), we use the fact that the matrices $\{\mathbf{B}_n\}_{n=1}^{N}$ are Hermitian and PSD.

We also use a transmit power constraint for MBS and SBSs, which is a natural constraint due to hardware limitations. The power transmitted by MBS and SBSs is limited above as given in (7.9).

$$\begin{aligned} P_{\text{MBS}} &= \sum_{k=1}^{K} \mathbf{v}_k^H \mathbf{v}_k \leq P_{t,1}, \\ P_{\text{SBS},n} &= \sum_{k=1}^{K} \mathbf{w}_{k,n}^H \mathbf{w}_{k,n} = \sum_{k=1}^{K} \mathbf{w}_k^H \mathbf{B}_n \mathbf{w}_k \leq P_{t,2}. \end{aligned} \tag{7.9}$$

The total power P can be expressed as

$$P = P_{\text{MBS}} + \sum_{n=1}^{N} P_{\text{SBS},n} = \sum_{k=1}^{K} \left(\mathbf{v}_k^H \mathbf{v}_k + \mathbf{w}_k^H \mathbf{w}_k\right). \tag{7.10}$$

To minimize P under SINR and power constraints, we also optimize the cooperation strategy by optimizing the network link matrix $\mathbf{C}$. The design problem (P_{IAB}) can be expressed as

$$(\text{P}_{\text{IAB}}): \quad \min_{\mathbf{v}_k, \mathbf{w}_k, \mathbf{C}} \sum_{k=1}^{K} \left(\mathbf{v}_k^H \mathbf{v}_k + \mathbf{w}_k^H \mathbf{w}_k\right)$$

$$\text{s.t.} \quad \frac{|\mathbf{h}_k^H \mathbf{w}_k|^2}{\sum_{\ell \neq k}^{K} |\mathbf{h}_k \mathbf{w}_\ell|^2 + \sum_{\ell=1}^{K} |\mathbf{h}_{k,0} \mathbf{v}_\ell|^2 + \sigma_{\text{UE},k}^2} \geq \gamma_k, \quad \forall k \tag{7.11}$$

$$\frac{|\mathbf{g}_{n,0}^H \mathbf{v}_k|^2}{\sum_{\ell=1}^{K} |\mathbf{g}_{n,0}^H \mathbf{v}_\ell|^2 f_{k,n}(\ell) + \sum_{\ell=1}^{K} |\mathbf{g}_n^H \mathbf{w}_\ell|^2 c_{\ell,n} + \frac{1}{\beta_{\text{SI}}} \sum_{\ell=1}^{K} \mathbf{w}_\ell^H \mathbf{B}_n \mathbf{w}_\ell + \sigma_{\text{SBS},n}^2} \geq \gamma_k,$$

$$\forall k, n \tag{7.12}$$

$$\sum_{n=1}^{N} c_{k,n} \mathbf{w}_k^H \mathbf{B}_n \mathbf{w}_k = 0, \quad \forall k \tag{7.13}$$

$$\sum_{k=1}^{K} \mathbf{v}_k^H \mathbf{v}_k \leq P_{t,1} \tag{7.14}$$

$$\sum_{k=1}^{K} \mathbf{w}_k^H \mathbf{B}_n \mathbf{w}_k \leq P_{t,2}, \quad \forall n. \tag{7.15}$$

In (P_{IAB}), (7.11) is the access link SINR constraint, (7.12) is the backhaul link SINR constraint, (7.13) denotes the relation between access link beamformers and network link matrix, (7.14)-(7.15) denote the transmit power constraints for MBS and SBSs.

For a fixed $\mathbf{C}$, we can solve (P_{IAB}) with SDP using standard SDP-solvers. To perform SDP, we first define new variables $\mathbf{V}_k = \mathbf{v}_k \mathbf{v}_k^H$ and $\mathbf{W}_k = \mathbf{w}_k \mathbf{w}_k^H$. The new variables $\mathbf{V}_k$ and $\mathbf{W}_k$ are Hermitian, PSD, and rank-1 for all k. The objective and constraints (except the rank-1 constraint) become linear (and hence convex) in (P_{IAB}) in terms of $\mathbf{V}_k$'s and $\mathbf{W}_k$'s. In the SDP approach, we omit the rank constraint and solve the relaxed problem using an SDP solver tool. As in the solutions of beamformer design problems in C-RAN with wired and wireless fronthaul, it can be shown that the solution of the relaxed problem is always rank-1. This means that the SDP method can optimally solve the original problem $(\mathrm{P}_{\mathrm{IAB}})$ for a fixed $\mathbf{C}$ without any performance loss due to the relaxation of the rank constraint.

Although we can optimally solve $(\mathrm{P}_{\mathrm{IAB}})$ for a fixed $\mathbf{C}$, it is not practical to try all possible $\mathbf{C}$ matrices as their number grows exponentially with the network size. Starting from the full cooperation case, we use the ILR algorithm to find a suitable $\mathbf{C}$ matrix. We use SeDuMi [82] tool at each stage of ILR as the SDP solver. The details are given in the Algorithm below.

Algorithm 7.1: (SDP-ILR):
Step 1: Solve $(\mathrm{P}_{\mathrm{IAB}})$ for full cooperation case ($\mathbf{C} = \mathbf{0}$). Find the access link beamformer norms $\|\mathbf{w}_{k,n}\|$ for all n, k. If the problem is not feasible, then find the channel norms $\|\mathbf{h}_{k,n}\|$ for all n, k.
Step 2: Delete the link with the smallest beamformer (or channel) norm that is not deleted before. This is done by changing the corresponding entry of $\mathbf{C}$ from 0 to 1.
Step 3: Solve $(\mathrm{P}_{\mathrm{IAB}})$ for the current $\mathbf{C}$ and continue until all links are deleted.
Step 4: Find the configuration (the network link matrix and the corresponding beamformers) with the minimum total power.

ILR algorithm iteratively removes links and solves an SDP problem at each stage. The complexity of the algorithm can be expressed as $\mathcal{O}(K^{5.5}N^{7.5}L^4 + K^{5.5}N^{3.5}M^4)$ using the complexity of SeDuMi solver [82].

7.2 Numerical Results

In this section, we observe the performance of the proposed method. In all simulations, unless otherwise stated, we take $\gamma_k = \gamma, \ \forall k, \ \sigma_{\mathrm{SBS},n} = \sigma_{\mathrm{SBS}}, \ \forall n, \ \sigma_{\mathrm{UE},k} = \sigma_{\mathrm{UE}}, \ \forall k$. We consider a circular area with 1 km diameter where MBS is at the center, 4 SBSs are placed on the vertices of a square with 750 m diagonal, and the UEs are uniformly distributed in the area shown in Fig. 7.1. The UEs are placed outside the inner circle with radius 250 m and outside the circles around SBSs with 50 m radius. (We assume that UEs in the inner circle are directly served by MBS.)

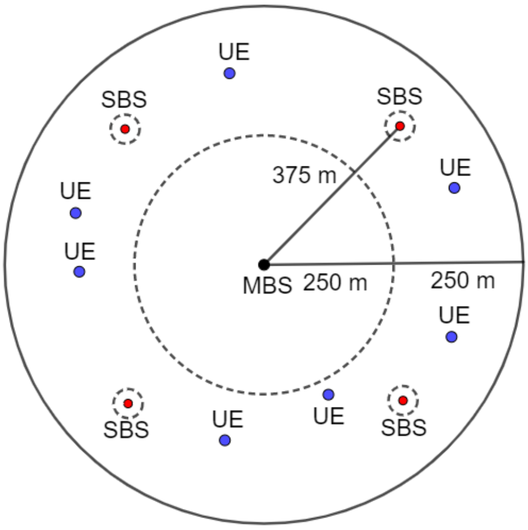

Figure 7.1: Placements of MBS, SBSs and UEs.

The large and small scale path-loss parameters, the noise powers, antenna gains, and other related parameters are listed in Table 7.1. (The table is taken from [14].)

Table 7.1: Simulation Parameters

Parameter	Value
Bandwidth	10 MHz
Macro (small) BS antenna gain	15 dBi (5) dBi
MBS-to-UE path-loss	$128.1 + 37.6 \log_{10}(d_{\text{km}})$
SBS-to-UE path-loss	$140.7 + 36.7 \log_{10}(d_{\text{km}})$
MBS-to-SBS path-loss	$103.4 + 24.2 \log_{10}(d_{\text{km}})$
SBS-to-SBS path-loss	$103.8 + 20.9 \log_{10}(d_{\text{km}})$
Macro (small) cell shadowing std. dev.	8 dB (10 dB)
Small-scale fading	$\mathcal{CN}(\mathbf{0}, \mathbf{I})$
SBS (UE) noise figure	10 dB (10 dB)

In the simulations, we observe the effect of γ, K, L, M on the total power P. We also analyze the MBS and SBS powers, separately. We run 1000 Monte-Carlo trials for each parameter set analyzed, and present the average power values.

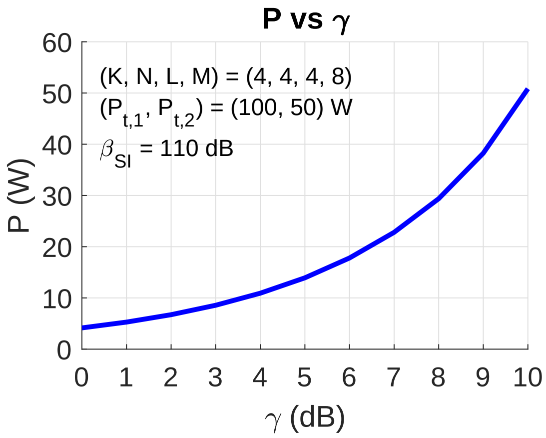

Figure 7.2: P vs γ, $(K, N, L, M) = (4, 4, 4, 8), (P_{t,1}, P_{t,2}) = (100, 50)$ W, $\beta_{\text{SI}} = 110$ dB.

In Fig. 7.2, we see the effect of the SINR threshold γ. We observe that P is an increasing function of γ. It can be claimed that when we further increase γ, the problem becomes infeasible. Even if we use infinite transmit power thresholds ($P_{t,1}, P_{t,2} \to \infty$) there will be a value of γ after which we obtain infeasible results. This is because increasing the transmit power also increases the interference in the system.

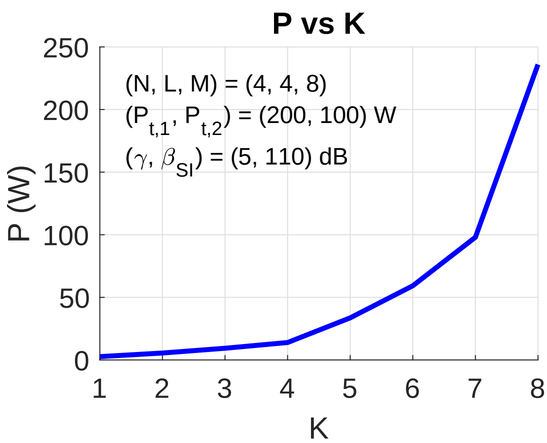

Figure 7.3: P vs K, $(N, L, M) = (4, 4, 8), (P_{t,1}, P_{t,2}) = (200, 100)$ W, $(\gamma, \beta_{\text{SI}}) = (5, 110)$ dB.

Fig. 7.3 shows the effect of the number of users. When the number of users is large, the power required to serve all users becomes also large. This is expected as it will be more challenging to satisfy user SINR constraints when K is larger.

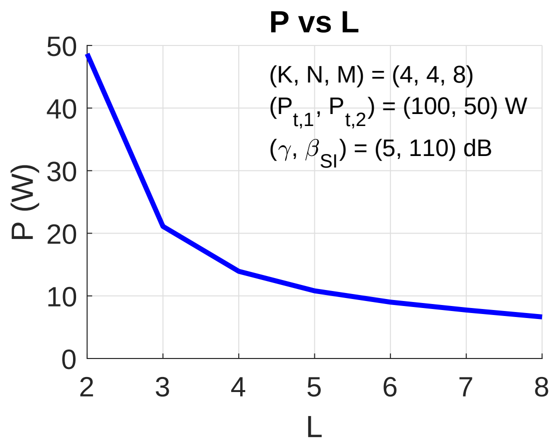

Figure 7.4: P vs L, $(K, N, M) = (4, 4, 8), (P_{t,1}, P_{t,2}) = (100, 50)$ W, $(\gamma, \beta_{\text{SI}}) = (5, 110)$ dB.

The effect of the number of SBS antennas is given in Fig. 7.4. We conclude that the total power consumption can be dramatically decreased using more antennas.

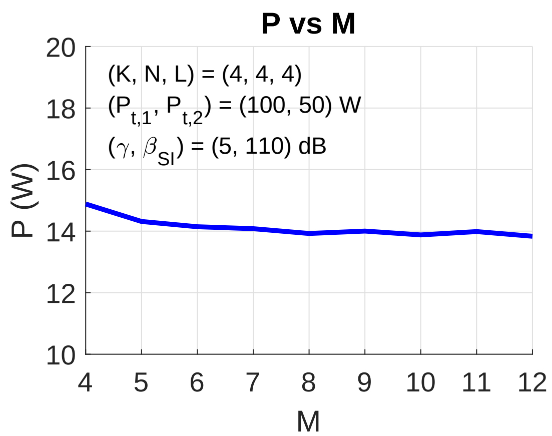

Figure 7.5: P vs M, $(K, N, L) = (4, 4, 4), (P_{t,1}, P_{t,2}) = (100, 50)$ W, $(\gamma, \beta_{\text{SI}}) = (5, 110)$ dB.

We observe in Fig. 7.5 that the impact of M on performances is limited. MBS-to-SBS channels are better than those of SBS-to-UE channels. Therefore, the portion of MBS power is small in total power consumption, making the effect of the number of MBS antennas low. Notice that $M \geq K$ is required to send the user backhaul data properly.

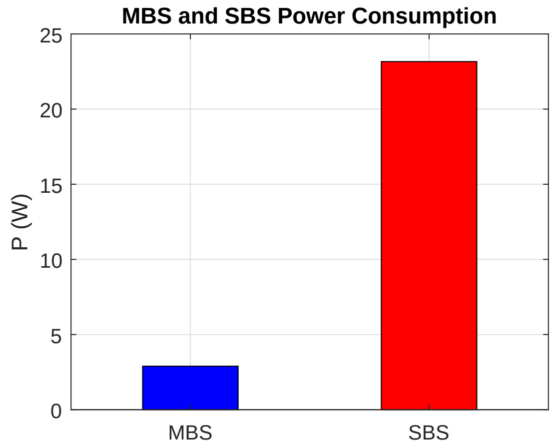

Figure 7.6: P_{MBS} vs P_{SBS}.

In Fig. 7.6, we see the comparison of MBS and total SBS power. The results are obtained by averaging all simulations. We observe that in the simulation setting that we use, total SBS power is roughly ten times higher than those of MBS power.

7.3 Conclusions

In this work, we described an IAB system and compared it with C-RAN. We considered a beamformer design problem in downlink IAB with full-duplex transmission/reception in SBSs. We minimized the total transmit power of MBS and SBSs under user SINR and power transmit constraints. In the design process, we used ILR and SDP methods to jointly optimize the cooperation between SBSs and MBS and SBS beamformer vectors. The results show that the power consumption of IAB can be well optimized by iterative convex optimization algorithms. In this study, we assumed perfect CSI, which may be over-optimistic in a practical scenario. As future work, one can modify the algorithms adopted in this work so that the beamformer designs process is robust to channel errors. We think that the same problem with a statistical channel error model, where second-order statistics of the additive channel errors are known, can be solved after applying a proper modification to algorithms used in this study.

CHAPTER 8

CONCLUSIONS

In this thesis, we have investigated the beamformer design problem for downlink C-RAN and IAB. To minimize the fronthaul data transfer in C-RAN, and optimize the backhaul data sharing in IAB, we have solved combinatorial beamforming design problems where some beamformers of RRHs, CPs, SBSs, and MBSs are set to zero. We aimed to minimize total power consumption by satisfying sufficient SINR for each UE. We have also considered the user selection problem to find the largest UE set to be served. We have derived theoretical performance bounds under imperfect channel knowledge to observe the limits of the algorithms.

We have proposed two heuristic search methods to find proper beamformers for C-RAN with capacity-limited wired fronthaul. Both methods solve a sequence of convex sub-problems to find the cooperation scheme for RRHs. The results show that these methods can be effectively used when full cooperation is not possible due to the limited capacity of fronthaul links.

We have analyzed the power minimization problem under per-RRH power transmit constraints. To minimize the fronthaul and access link powers, we have proposed a smooth approximation method where all discontinuous terms in the objective and constraints are expressed as the limits of some smooth function sequences. To make optimality analysis, we have also derived a novel theoretical performance bound. The detailed simulations show that the proposed method outperforms all baseline methods, and its performance is close to the bound.

We have considered a user admission problem where the SINR constraints are satisfied for the largest possible UE set by minimizing the fronthaul data transfer and total power consumption. All target parameters can be jointly optimized by a novel bound-based link selection method. This method finds a suitable link configuration of RRHs and UEs according to the derivation of a performance bound. The numerical results show the effectiveness of the method proposed.

For C-RAN with wireless fronthaul, we have analyzed a power minimization problem involving multiplicative terms of CP and RRH beamformers. Assuming imperfect channel knowledge, we have derived a novel theoretical performance bound. We have shown the tightness of the bound by considering some convex optimization and hybrid beamforming methods. The comprehensive study on this topic has shown that convex optimization-based methods can perform close to the bound whereas the performance of standard beamforming methods is limited.

We have conducted a study on beamformer design for a downlink full-duplex IAB system. We have proposed a method based on SDP and ILR for perfect channel knowledge. The results show that the proposed method can effectively solve the problem. We aim to generalize the results of this work for imperfect channel cases. We also plan to recommend new techniques and find theoretical performance bounds for IAB systems.

The beamforming design problems in downlink C-RAN and IAB have combinatorial nature and are originally not solvable in polynomial times. Applying relaxations and transformations, we can use various techniques to design proper beamformers. In most cases, it is not practical to run the optimal algorithms. On the other hand, it is possible to derive theoretical performance bounds showing the limits of methods. Considering the performance gaps compared to the theoretical bounds together with the complexities of algorithms, one can select the technique that best fits the application at hand.

There are some possible extensions of this thesis work. One can conduct different studies to enhance the performances of future communication networks further.

- **User-centric beamforming:** In both C-RAN and IAB networks, to obtain the highest coordination gain we have performed beamformer design under a fully centralized approach. The results show that although the performances of the algorithms are satisfactory, some methods may be impractical due to high complexity. As an alternative approach, we can perform user-centric beamforming where coordination of base stations and corresponding beamformers are designed for each user separately. This approach is sub-optimal in terms of performance; however, the algorithm complexities will be low, making this approach attractive.

- **Machine learning and artificial intelligence:** As the network densities increases, it becomes harder to decide cooperation strategies and design beamformers in networks. When multi-hop backhauling is allowed in IAB systems, the problem becomes even harder. Machine learning (ML) and artificial intelligence (AI) can be useful to satisfy quality-of-service requirements for complex scenarios. Through ML/AI, we can enhance the performance of the network when mixed traffic flows coexist. ML/AI-assisted methods can be designed to exploit and forecast changes in the environment and user behavior.

- **Fully digital beamforming with low-resolution ADCs for mmWave band:** Throughout the thesis work, we considered fully digital beamforming. When the number of antennas is high, hybrid beamforming is preferred to decrease the complexity and costs of the design. In general, a small number of RF chains are used for the mmWave band to decrease the complexity due to a massive number of antennas. Furthermore, a fully digital solution will also increase the power consumption due to a large number of analog-to-digital converters (ADCs). To make the design practical and to obtain faster beam tracking and management, one can consider a fully digital massive MIMO solution including low-resolution ADCs in C-RAN and IAB networks.

- **Edge Cloud with C-RAN:** By the evolution of communication systems new use cases become possible to implement. Use cases requiring very low transmission delays can be supported by 5G and beyond. High-frequency trading, electric grid control, autonomous driving are some of the applications requiring latencies less than 10 ms. In C-RAN, due to a large amount of data transmission in fronthaul links, some enhancements might be required to decrease the latency. Multi-access edge computing (MEC) is a potential approach to decrease the latencies in new-generation communication systems. In C-RAN, a cloud-based MEC can be implemented by combining edge and far edge data centers. Baseband processing and edge computing operations of the core network can be performed in the same centralized data centers to obtain low latency and high throughput communications. As future work, the coordination strategies for a C-RAN system with MEC can be analyzed.

- **Functional Splits in C-RAN:** In radio access networks, the centralization of protocols can be implemented in different ways. There are several possible functional splits in new-generation communication systems. One way is to centralize all baseband processing to obtain the maximum coordination gain. This approach will yield strict latency requirements in fronthaul links. To relax the latency requirements, some baseband functions can be performed in RRHs. In this case, the level of coordination becomes limited. Next-generation communication systems should support different function splits where each one can be optimal for a specific scenario. As a different study area, limited coordination cases can be analyzed for C-RAN systems.

- **Reconfigurable Intelligent Surfaces and IAB:** In 6G and beyond, it is expected to use reconfigurable intelligent surfaces (RISs) to change the behavior of the propagation environment. RIS can significantly increase the signal strength without complex signal processing operations. In future IAB networks, RISs can be used together with IAB nodes to increase the coverage of the network. As no backhaul data decoding would be required in relaying, a simple, low-cost, and efficient solution might be obtained by the usage of RISs.

- **Enhancements in Wired Backhaul and Fronthaul Links:** Passive optical networks (PON) and wavelength division multiplexing (WDM) are used to decrease the cost of deployment of wired backhaul/fronthaul links by supporting low latencies and high data rates. The power consumption model of CP in C-RAN with wired fronthaul can be modified considering PON and WDM as future work.

REFERENCES

[1] Cisco. (2020). Cisco Annual Internet Report (2018–2023). Accessed: Aug. 7, 2021. [Online].
Available: https://www.cisco.com/c/en/us/solutions/collateral/executive-perspectives/annual-internet-report/white-paper-c11-741490.html

[2] M. Maternia, and S. E. E. Ayoubi (2016). 5G PPP Use Cases and Performance Evaluation Models. Accessed: Aug. 7, 2021. [Online]. Available: https://5g-ppp.eu/wp-content/uploads/2014/02/5G-PPP-use-cases-and-performance-evaluation-modeling _v1.0.pdf

[3] J. Rodriguez, “Small cells for 5G mobile networks," in *Fundamentals of 5G Mobile Networks*. Hoboken, NJ, USA: Wiley, 2015, pp. 63-104.

[4] Y. Lin, L. Shao., Z. Zhu, Q. Wang, and R. K. Sabhikhi, “Wireless network cloud: architecture and system requirements," IBM J. Res. Dev. 54 (1), 4:1–4:12. 2010.

[5] Q. Wang, D. Jiang, G. Liu and Z. Yan, “Coordinated Multiple Points Transmission for LTE-Advanced Systems," *5th International Conference on Wireless Communications, Networking and Mobile Computing*, 2009, pp. 1-4.

[6] S. Venkatesan, A. Lozano and R. Valenzuela, “Network MIMO: Overcoming Intercell Interference in Indoor Wireless Systems," *41-th Asilomar Conference on Signals, Systems and Computers*, 2007, pp. 83-87.

[7] J. Matias, J. Garay, N. Toledo, J. Unzilla, and E. Jacob, “Toward an SDN-enabled NFV architecture," *IEEE Commun. Mag.*, vol. 53, no. 4, pp. 187-193, Apr. 2015.

[8] M. A. Habibi, M. Nasimi, B. Han and H. D. Schotten, “A Comprehensive Survey of RAN Architectures Toward 5G Mobile Communication System," in *IEEE Access*, vol. 7, pp. 70371-70421, 2019.

[9] M. F. Hossain, A. U. Mahin, T. Debnath, F. B. Mosharrof, and K. Z. Islam, “Recent research in cloud radio access network (C-RAN) for 5G cellular systems - A survey," in *Journal of Network and Computer Applications* vol. 139, pp. 31–48, 2019.

[10] M. Peng, C. Wang, V. Lau and H. V. Poor, “Fronthaul-constrained cloud radio access networks: insights and challenges," in *IEEE Wireless Communications*, vol. 22, no. 2, pp. 152-160, April 2015.

[11] O. Simeone, A. Maeder, M. Peng, O. Sahin, and W. Yu, “Cloud Radio Access Network: Virtualizing Wireless Access for Dense Heterogeneous Systems," *Journal of Communications and Networks*, vol. 18, no. 2, pp. 135-149, April 2016.

[12] Y. Zhang, M. A. Kishk and M. S. Alouini, “A Survey on Integrated Access and Backhaul Systems," arXiv:2101.01286 [cs.NI], Jan. 2021.

[13] “Innovations in 5G Backhaul Technologies: IAB, HFC and Fiber," 5G Americas, White Paper, 2020. [Online]. Available: https://www.5gamericas.org/wp-content/uploads/2020/06/Innovations-in-5G-Backhaul-Technologies-WP-PDF.pdf

[14] E. Chen, M. Tao and N. Zhang, “User-Centric Joint Access-Backhaul Design for Full-Duplex Self-Backhauled Wireless Networks," in *IEEE Trans. on Commun.*, vol. 67, no. 11, pp. 7980-7993, Nov. 2019.

[15] F. E. Kadan and A. Ö. Yılmaz, “Optimized asymmetric cooperation for downlink cloud radio access network under per-base station data transfer constraint," *2017 IEEE Int. Conf. on Commun. (ICC) Workshops*, Paris, 2017, pp. 132-137.

[16] F. E. Kadan and A. Ö. Yilmaz, “Beamformer Design With Smooth Constraint-Free Approximation in Downlink Cloud Radio Access Networks," in *IEEE Access*, vol. 9, pp. 36399-36416, Mar. 2021.

[17] F. E. Kadan, and A. Ö. Yılmaz, “A Bound Based Method for Beamformer Design in Downlink Cloud Radio Access Networks," in *IEEE Commun. Lett.*, doi: 10.1109/LCOMM.2021.3100271.

[18] F. E. Kadan, and A. Ö. Yılmaz, “A Theoretical Performance Bound for Joint Beamformer Design of Wireless Fronthaul and Access Links in Downlink C-RAN," in *IEEE Trans. Wireless Commun.*, doi: 10.1109/TWC.2021.3109837.

[19] C. Wang, X. Dong and Y. Shi, “Robust relay design for two-way multi-antenna relay systems with imperfect CSI," in *J. Commun. Netw.*, vol. 16, no. 1, pp. 45-55, Feb. 2014.

[20] H. Du and P. Chung, “A Probabilistic Approach for Robust Leakage-Based MU-MIMO Downlink Beamforming with Imperfect Channel State Information," in *IEEE Trans. Wireless Commun.*, vol. 11, no. 3, pp. 1239-1247, March 2012.

[21] D. Wang, Y. Wang, R. Sun and X. Zhang, “Robust C-RAN Precoder Design for Wireless Fronthaul with Imperfect Channel State Information," *2017 IEEE Wireless Commun. and Netw. Conf. (WCNC)*, San Francisco, CA, 2017, pp. 1-6.

[22] D. Yan, R. Wang, E. Liu and Q. Hou, “ADMM-Based Robust Beamforming Design for Downlink Cloud Radio Access Networks," in *IEEE Access*, vol. 6, pp. 27912-27922, 2018.

[23] J. Li and M. Haardt, “Robust MIMO Relay Precoder Design for Multiple Operator One-Way Relaying with Imperfect Channel State Information," *Int. Symp. Wireless Commun. Systems*, Ilmenau, Germany, 2013, pp. 1-5.

[24] C. Kuo, S. Wu and C. Tseng, “Robust Linear Beamformer Designs for Coordinated Multi-Point AF Relaying in Downlink Multi-Cell Networks," in *IEEE Trans. Wireless Commun.*, vol. 11, no. 9, pp. 3272-3283, September 2012.

[25] B. K. Chalise and L. Vandendorpe, “Optimization of MIMO Relays for Multipoint-to-Multipoint Comm.: Nonrobust and Robust Designs," in *IEEE Trans. Signal Process.*, vol. 58, no. 12, pp. 6355-6368, Dec. 2010.

[26] B. K. Chalise and L. Vandendorpe, “MIMO Relay Design for Multipoint-to-Multipoint Comm. With Imperfect Channel State Information," in *IEEE Trans. Signal Process.*, vol. 57, no. 7, pp. 2785-2796, July 2009.

[27] P. Ubaidulla and A. Chockalingam, “Relay Precoder Optimization in MIMO-Relay Networks With Imperfect CSI," in *IEEE Trans. Signal Process.*, vol. 59, no. 11, pp. 5473-5484, Nov. 2011.

[28] B. Hu, C. Hua, J. Zhang, C. Chen and X. Guan, “Joint Fronthaul Multicast Beamforming and User-Centric Clustering in Downlink C-RANs," in *IEEE Trans. Wireless Commun.*, vol. 16, no. 8, pp. 5395-5409, Aug. 2017.

[29] B. Hu, C. Hua, C. Chen and X. Guan, “Joint Beamformer Design for Wireless Fronthaul and Access Links in C-RANs," in *IEEE Trans. Wireless Commun.*, vol. 17, no. 5, pp. 2869-2881, May 2018.

[30] S. Park, K. Lee, C. Song and I. Lee, “Joint Design of Fronthaul and Access Links for C-RAN With Wireless Fronthauling," in *IEEE Signal Process. Lett.*, vol. 23, no. 11, pp. 1657-1661, Nov. 2016.

[31] S. Park, C. Song and K. Lee, “Inter-Cluster Design of Wireless Fronthaul and Access Links for the Downlink of C-RAN," in *IEEE Wireless Commun. Lett.*, vol. 6, no. 2, pp. 270-273, April 2017.

[32] J. Zhang, R. Chen, J. G. Andrews, A. Ghosh and R. W. Heath, “Networked MIMO with clustered linear precoding," in *IEEE Trans. Wireless Commun.*, vol. 8, no. 4, pp. 1910-1921, April 2009.

[33] A. Liu and V. K. N. Lau, “Joint Power and Antenna Selection Optimization in Large Cloud Radio Access Networks," in *IEEE Trans. Signal Process.*, vol. 62, no. 5, pp. 1319-1328, March 2014.

[34] B. Dai and W. Yu, “Sparse Beamforming and User-Centric Clustering for Downlink Cloud Radio Access Network," in *IEEE Access*, vol. 2, pp. 1326-1339, 2014.

[35] Y. Huang et al., “Distributed Multicell Beamforming Design Approaching Pareto Boundary with Max-Min Fairness," in *IEEE Trans. Wireless Commun.*, vol. 11, no. 8, pp. 2921-2933, August 2012.

[36] R. Zakhour and D. Gesbert, “Optimized Data Sharing in Multicell MIMO With Finite Backhaul Capacity," in *IEEE Trans. Signal Process.*, vol. 59, no. 12, pp. 6102-6111, Dec. 2011.

[37] F. Zhuang and V. K. N. Lau, “Backhaul Limited Asymmetric Cooperation for MIMO Cellular Networks via Semidefinite Relaxation," in *IEEE Trans. Signal Process.*, vol. 62, no. 3, pp. 684-693, Feb.1, 2014.

[38] H. Wai and W. Ma, “A decentralized method for joint admission control and beamforming in coordinated multicell downlink," *Asilomar Conf. Signals, Systems and Computers*, Pacific Grove, CA, 2012, pp. 559-563.

[39] Y. Shi, J. Zhang and K. B. Letaief, "Group Sparse Beamforming for Green Cloud-RAN," in *IEEE Trans. Wireless Commun.*, vol. 13, no. 5, pp. 2809-2823, May 2014.

[40] A. Chowdhery, W. Yu and J. M. Cioffi, "Cooperative Wireless Multicell OFDMA Network with Backhaul Capacity Constraints," *2011 IEEE Int. Conf. Commun. (ICC)*, Kyoto, 2011, pp. 1-6.

[41] J. Zhao, T. Q. S. Quek and Z. Lei, "Coordinated Multipoint Transmission with Limited Backhaul Data Transfer," in *IEEE Trans. Wireless Commun.*, vol. 12, no. 6, pp. 2762-2775, June 2013.

[42] A. Papadogiannis, D. Gesbert and E. Hardouin, "A Dynamic Clustering Approach in Wireless Networks with Multi-Cell Cooperative Process.," *2008 IEEE Int. Conf. Commun. (ICC)*, Beijing, 2008, pp. 4033-4037.

[43] M. Medard, "The effect upon channel capacity in wireless communications of perfect and imperfect knowledge of the channel," in *IEEE Trans. Inf. Theory*, vol. 46, no. 3, pp. 933-946, May 2000.

[44] Y. Huang, G. Zheng, M. Bengtsson, K.-K. Wong, L. Yang, and B. Ottersten, "Distributed Multicell Beamforming Design Approaching Pareto Boundary with Max-Min Fairness," *IEEE Trans. Wireless Commun.*, vol. 11, no. 8, pp. 2921-2933, 2012.

[45] B. K. Chalise and L. Vandendorpe, "Optimization of MIMO Relays for Multipoint-to-Multipoint Comm.: Nonrobust and Robust Designs," in *IEEE Trans. on Signal Process.*, vol. 58, no. 12, pp. 6355-6368, Dec. 2010.

[46] Z. Wang, D. W. K. Ng, V. W. S. Wong and R. Schober, "Robust Beamforming Design in C-RAN With Sigmoidal Utility and Capacity-Limited Backhaul," in *IEEE Trans. on Wireless Comm.*, vol. 16, no. 9, pp. 5583-5598, Sept. 2017.

[47] Y. Wang, L. Ma, Y. Xu and W. Xiang, "Computationally Efficient Energy Optimization for Cloud Radio Access Networks With CSI Uncertainty," in *IEEE Trans. on Comm.*, vol. 65, no. 12, pp. 5499-5513, Dec. 2017.

[48] D. Yan, R. Wang and E. Liu, "Robust beamforming designs for downlink cloud radio access networks," *2017 9th International Conference on Wireless Communications and Signal Processing (WCSP)*, Nanjing, 2017, pp. 1-6.

[49] Y. Chen, S. He, Y. Huang, J. Ren and L. Yang, "Robust Multigroup Multicast Beamforming Design for Backhaul-Limited Cloud Radio Access Network," in *IEEE Signal Process. Lett.*, vol. 26, no. 1, pp. 189-193, Jan. 2019.

[50] C. Pan, H. Ren, M. Elkashlan, A. Nallanathan and L. Hanzo, "Robust Beamforming Design for Ultra-Dense User-Centric C-RAN in the Face of Realistic Pilot Contamination and Limited Feedback," in *IEEE Trans. on Wireless Comm.*, vol. 18, no. 2, pp. 780-795, Feb. 2019.

[51] J. Tan, Q. Zhang, T. Q. S. Quek and H. Shin, "Robust Energy Efficiency Maximization in Multicast Downlink C-RAN," in *IEEE Trans. on Vehicular Technology*, vol. 68, no. 9, pp. 8951-8965, Sept. 2019.

[52] Y. Shi, J. Zhang and K. B. Letaief, “Robust Group Sparse Beamforming for Multicast Green Cloud-RAN With Imperfect CSI," in *IEEE Trans. Signal Process.*, vol. 63, no. 17, pp. 4647-4659, Sept., 2015.

[53] K. Zhang, W. Tan, G. Xu, C. Yin, W. Liu and C. Li, “Joint RRH Activation and Robust Coordinated Beamforming for Massive MIMO Heterogeneous Cloud Radio Access Networks," in *IEEE Access*, vol. 6, pp. 40506-40518, July 2018.

[54] C. Pan, H. Mehrpouyan, Y. Liu, M. Elkashlan and N. Arumugam, “Joint Pilot Allocation and Robust Transmission Design for Ultra-Dense User-Centric TDD C-RAN With Imperfect CSI," in *IEEE Trans. on Wireless Comm.*, vol. 17, no. 3, pp. 2038-2053, March 2018.

[55] M. Moltafet, S. Parsaeefard, M. R. Javan and N. Mokari, “Robust Radio Resource Allocation in MISO-SCMA Assisted C-RAN in 5G Networks," in *IEEE Trans. on Vehicular Technology*, vol. 68, no. 6, pp. 5758-5768, June 2019.

[56] R. Zakhour and D. Gesbert, “Optimized Data Sharing in Multicell MIMO with Finite Backhaul Capacity," *IEEE Trans. Signal Process.*, vol. 59, no. 12, pp. 6102-6111, Dec. 2011.

[57] D. Yan, R. Wang, E. Liu and Q. Hou, “ADMM-Based Robust Beamforming Design for Downlink Cloud Radio Access Networks," in *IEEE Access*, vol. 6, pp. 27912-27922, 2018.

[58] A. Chowdhery, W. Yu, and J. M. Cioffi, “Cooperative Wireless Multicell OFDMA Network with Backhaul Capacity Constraints", in Proc. *IEEE Int. Conf. Commun. (ICC)*, 2011, pp. 1–6.

[59] Z. Zhao, M. Peng, Z. Ding, C. Wang and H. V. Poor, “Cluster formation in cloud-radio access networks: Performance analysis and algorithms design," *2015 IEEE Int. Conf. Commun. (ICC)*, London, 2015, pp. 3903-3908.

[60] Jian Li, Mugen Peng, Aolin Cheng and Yuling Yu, “Delay-aware cooperative multipoint transmission with backhaul limitation in cloud-RAN," *2014 IEEE Int. Conf. Commun. (ICC) Workshops*, Sydney, NSW, 2014, pp. 665-670.

[61] B. Li, D. Zhu, and P. Liang, “Small cell in-band wireless backhaul in massive MIMO systems: A cooperation of next generation techniques," *IEEE Trans. Wireless Commun.*, vol. 14, no. 12, pp. 7057–7069, Dec. 2015.

[62] I. Ullah, B. B. Haile, E. Mutafungwa, and J. Hamalainen, “Use of beamforming and interference mitigation techniques for relay backhaul enhancement," in *Proc., 39th International Conference on Telecommunications and Signal Processing (TSP). IEEE*, Jun. 2016.

[63] P. Jayasinghe, A. Tölli, J. Kaleva, and M. Latva-aho, “Traffic aware beamformer design for integrated access and backhaul with flexible TDD," in *Proc., IEEE Wireless Communications and Networking Conference (WCNC)*, 2020, pp. 1–6.

[64] A. Prasad, M. A. Uusitalo, and A. Maeder, “Energy efficient coordinated self-backhauling for ultra-dense 5G networks," in *Proc., IEEE 85th Vehicular Technology Conference (VTC Spring)*, Jun. 2017.

[65] D. Meng, X. Li, W. Pu, X. Yang, and D. Li, “An energy-saving scheme with multi-hop transmission for mmWave backhaul networks," in *Proc., IEEE Vehicular Technology Conference (VTC Spring)*, Jun. 2018.

[66] L. Lei, E. Lagunas, S. Chatzinotas, and B. Ottersten, “NOMA aided interference management for full-duplex self-backhauling HetNets," *IEEE Commun. Lett.*, vol. 22, no. 8, pp. 1696–1699, Aug. 2018.

[67] W. Lei, Y. Ye, and M. Xiao, “Deep reinforcement learning-based spectrum allocation in integrated access and backhaul networks," *IEEE Trans. on Cogn. Commun. Netw.*, vol. 6, no. 3, pp. 970–979, Sep. 2020.

[68] Y. Liu, X. Fang, and M. Xiao, “Discrete power control and transmission duration allocation for self-backhauling dense mmWave cellular networks," *IEEE Trans. Commun.*, vol. 66, no. 1, pp. 432–447, Jan. 2018.

[69] S. Ni, J. Zhao, H. H. Yang, and Y. Gong, “Enhancing downlink transmission in MIMO HetNet with wireless backhaul," *IEEE Trans. Veh. Technol.*, vol. 68, no. 7, pp. 6817–6832, Jul. 2019.

[70] T. K. Vu, M. Bennis, M. Debbah, and M. Latva-Aho, “Joint path selection and rate allocation framework for 5G selfbackhauled mm-wave networks," *IEEE Trans. Wireless Commun.*, vol. 18, no. 4, pp. 2431–2445, Apr. 2019.

[71] L. Chen, F. R. Yu, H. Ji, G. Liu, and V. C. M. Leung, “Distributed virtual resource allocation in small-cell networks with full-duplex self-backhauls and virtualization," *IEEE Trans. Veh. Technol.*, vol. 65, no. 7, pp. 5410–5423, Jul. 2016.

[72] L. Tang, X. Yang, X. Wu, T. Cui, and Q. Chen, “Queue stability-based virtual resource allocation for virtualized wireless networks with self-backhauls," *IEEE Access*, vol. 6, pp. 13 604–13 616, 2018.

[73] L. Chen, F. R. Yu, H. Ji, B. Rong, X. Li, and V. C. M. Leung, “Green full-duplex self-backhaul and energy harvesting small cell networks with massive MIMO," *IEEE J. Sel. Areas Commun.*, vol. 34, no. 12, pp. 3709–3724, Dec. 2016.

[74] A. Imran, L. Giupponi, M. A. Imran, and A. Abu-Dayya, “Joint coverage and backhaul self-optimization in emerging relay enhanced heterogeneous networks," in *Proc., IEEE International Conference on Communications (ICC)*, Jun. 2014.

[75] L. Chen, F. R. Yu, H. Ji, V. C. Leung, X. Li, and B. Rong, “A full-duplex self-backhaul scheme for small cell networks with massive MIMO," in *Proc., IEEE International Conference on Communications (ICC)*, May 2016.

[76] Z. Q. Luo, N. D. Sidiropoulos, P. Tseng, and S. Z. Zhang, “Approximation Bounds for Quadratic Optimization with Homogeneous Quadratic Constraints," *SIAM J. Optimiz.*, vol. 18, no. 1, pp. 1-28, 2007.

[77] H. Dahrouj and W. Yu, “Coordinated Beamforming for the Multicell Multi-Antenna Wireless System," *IEEE Trans. Wireless Commun.*, vol. 9, no. 5, pp. 1748-1759, 2010.

[78] Y. Huang and D. P. Palomar, "Rank-Constrained Separable Semidefinite Programming with Applications to Optimal Beamforming," *IEEE Trans. Signal Process.*, vol. 58, no. 2, pp. 664-678, 2010.

[79] L. Comtet, *Advanced Combinatorics: The Art of Finite and Infinite Expansions*. Netherlands: Reidel, pp. 176-177, 1974.

[80] J. Barzilai and J. M. Borwein, "Two Point Step Size Gradient Methods," *IMA J. Numer. Anal.*, pp. 141-148, 1988.

[81] M. Grant and S. Boyd. (Jan. 2020). *CVX: MATLAB Software for Disciplined Convex Programming*, Version 2.2. [Online]. Available: http://cvxr.com/cvx

[82] J. F. Sturm, "Using SeDuMi 1.02, a MATLAB toolbox for optimization over symmetric cones," *Optimization Methods Software*, vol. 11-12, pp. 625–653, 1999.

[83] M.S. Lobo, L. Vandenberghe, S. Boyd and H. Lebret, "Applications of second-order cone programming," *Linear Algebra and its Applications*, vol. 284, no. 1, pp. 193-228, Jan. 1998.

[84] 3GPP, *Radio Frequency (RF) Requirements for LTE Pico Node B (Release 14)*, document 3GPP TR 36.931 V14.0.0, 2017.

[85] J. M. Steele, *The Cauchy-Schwarz Master Class: An Introduction to the Art of Mathematical Inequalities*, Cambridge, Cambridge University Press, 2004.

[86] A. W. Marshall, I. Olkin and B. Arnold, *Inequalities: Theory of Majorization and Its Applications*, 2nd ed. New York: Springer, 2011, pp. 340-341.

[87] R. A. Horn and C. R. Johnson, *Topics in Matrix Analysis*. Cambridge, U.K.: Cambridge Univ. Press, 1991.

[88] MOSEK ApS. (2020). *The MOSEK Optimization Software*. Version 9.2. [Online]. Available: http://www.mosek.com

[89] R. G. Bartle and D. R. Sherbert, *Introduction to Real Analysis*, 4th Edition. Hoboken, NJ: Wiley, 2011, pp. 71–72.

[90] 3GPP, *Further Advancements for E-UTRA Physical Layer Aspects (Release 9)*, document 3GPP TR 36.814 V9.0.0, Mar. 2010.

[91] K. M. Chong, "The Arithmetic Mean-Geometric Mean Inequality: A New Proof," *Mathematics Magazine*, vol. 49, no. 2, pp. 87-88, March 1976.

APPENDIX A

PROOF OF RANK-1 SOLUTION OF (P1-R)

We use the idea in [54] to prove that (P1-r) has always rank-1 solution. Firstly, we define the Lagrangian function of the problem $\mathcal{L}$ as

$$\begin{aligned}\mathcal{L} = &\sum_{k=1}^{K} \operatorname{tr}(\mathbf{W}_k) - \sum_{k=1}^{K} \lambda_k \left(\operatorname{tr}(\mathbf{H}_k \mathbf{W}_k) - \gamma_k \sum_{\ell \neq k} \operatorname{tr}(\mathbf{H}_k \mathbf{W}_\ell) - \gamma_k \sigma^2_{\text{UE},k} \right) \\ &+ \sum_{k=1}^{K} \mu_k \sum_{n=1}^{N} c_{k,n} \operatorname{tr}(\mathbf{B}_n \mathbf{W}_k) - \sum_{k=1}^{K} \operatorname{tr}(\mathbf{W}_k \mathbf{Z}_k)\end{aligned} \tag{A.1}$$

where $\{\lambda_k\}_{k=1}^K, \{\mu_k\}_{k=1}^K$ are non-negative Lagrange multipliers, $\mathbf{Z}_k$ is the dual positive semi-definite matrix associated with the positive semi-definite optimization variable $\mathbf{W}_k$. For the optimal solution of the convex problem (P1-r), the condition $\mathbf{W}_k \mathbf{Z}_k = \mathbf{0}$ should satisfy for all k. Furthermore, by the first order optimality condition, we also have

$$\begin{aligned}\frac{\partial \mathcal{L}}{\partial \mathbf{W}_k} &= \mathbf{I} - \lambda_k \mathbf{H}_k + \sum_{\ell \neq k} \lambda_\ell \gamma_\ell \mathbf{H}_\ell + \sum_{n=1}^{N} \mu_k c_{k,n} \mathbf{B}_n - \mathbf{Z}_k \\ &= \mathbf{0}.\end{aligned} \tag{A.2}$$

It follows that

$$\mathbf{Z}_k = \mathbf{I} + \mathbf{X}_k - \lambda_k \mathbf{h}_k \mathbf{h}_k^H \tag{A.3}$$

where

$$\mathbf{X}_k = \sum_{\ell \neq k} \lambda_\ell \gamma_\ell \mathbf{H}_\ell + \sum_{n=1}^{N} \mu_k c_{k,n} \mathbf{B}_n \tag{A.4}$$

is a positive semi-definite matrix. Therefore, the matrix $\mathbf{I} + \mathbf{X}_k$ is full-rank. The rank of $\lambda_k \mathbf{h}_k \mathbf{h}_k^H$ is at most 1 and hence the rank of $\mathbf{Z}_k$ is at least $NL - 1$ as its dimension is NL. Using the equation $\mathbf{W}_k \mathbf{Z}_k = \mathbf{0}$ and the rank inequality for matrix multiplication, we get

$$\begin{aligned}\text{rank}(\mathbf{W}_k) &\leq NL + \text{rank}(\mathbf{W}_k\mathbf{Z}_k) - \text{rank}(\mathbf{Z}_k) \\ &= NL - \text{rank}(\mathbf{Z}_k) \\ &\leq 1.\end{aligned} \tag{A.5}$$

Assuming positive SINR threshold values, the zero beamformer cannot be a solution and hence we conclude that $\text{rank}(\mathbf{W}_k) = 1,\ \forall k$.

APPENDIX B

ACHIEVABILITY OF RATE

We use the idea given in [43] to show that the rate $\log_2(1 + \text{SINR}_k)$ is achievable for k-th user where SINR_k is defined by (4.5). We find a lower bound to the mutual information $I(r_{\text{wired},k}; s_k)$ between the received signal $r_{\text{wired},k}$ and the information signal s_k. Assuming that s_k is zero-mean and Gaussian distributed, for any given complex constant α we can show that

$$\begin{aligned} I(r_{\text{wired},k}; s_k) &= h(s_k) - h(s_k|r_{\text{wired},k}) \\ &= h(s_k) - h(s_k - \alpha \cdot r_{\text{wired},k}|r_{\text{wired},k}) && \text{(B.1)} \\ &\geq h(s_k) - h(s_k - \alpha \cdot r_{\text{wired},k}) && \text{(B.2)} \\ &\geq \log\left(\pi e \mathbb{E}\left[|s_k|^2\right]\right) - \log\left(\pi e \mathbb{E}\left[|s_k - \alpha \cdot r_{\text{wired},k}|^2\right]\right) && \text{(B.3)} \\ &= \log\left(\frac{\mathbb{E}\left[|s_k|^2\right]}{\mathbb{E}\left[|s_k - \alpha \cdot r_{\text{wired},k}|^2\right]}\right). && \text{(B.4)} \end{aligned}$$

(B.1) is obtained using the fact that the entropy $h(\cdot)$ is invariant under translation. (B.2) can be shown using the fact that conditioning decreases entropy. As s_k is zero-mean and Gaussian, we get $h(s_k) = \log\left(\pi e \mathbb{E}\left[|s_k|^2\right]\right)$. Using the facts that the entropy is maximized for Gaussian distribution when the variance is fixed and $r_{\text{wired},k}$ is also zero-mean, we have $h(s_k - \alpha \cdot r_{\text{wired},k}) \leq \log\left(\pi e \mathbb{E}\left[|s_k - \alpha \cdot r_{\text{wired},k}|^2\right]\right)$. Therefore, we obtain the result in (B.3). Finally, using some simple calculations for log terms, we get the final result in (B.4).

(B.1)-(B.4) are true for any α and specifically we choose

$$\alpha = \mathbb{E}\left[r^*_{\text{wired},k} s_k\right] / \mathbb{E}\left[|r_{\text{wired},k}|^2\right] \tag{B.5}$$

to get

$$I(r_{\text{wired},k}; s_k) \geq \log\left(1 + \frac{|\mathbb{E}\left[r^*_{\text{wired},k} s_k\right]|^2}{\mathbb{E}\left[|r_{\text{wired},k}|^2\right] \cdot \mathbb{E}\left[|s_k|^2\right] - |\mathbb{E}\left[r^*_{\text{wired},k} s_k\right]|^2}\right). \tag{B.6}$$

Using the equation of $r_{\text{wired},k}$ in (2.5) and the fact $\mathbb{E}\left[|s_k|^2\right] = 1$, we obtain that $|\mathbb{E}\left[r^*_{\text{wired},k} s_k\right]|^2 = P_d$ and $\mathbb{E}\left[|r_{\text{wired},k}|^2\right] = P_d + P_m + P_{\text{int}} + P_n$ where $P_d, P_m, P_{\text{int}}, P_n$ are defined in (4.2). Therefore, we conclude that the mutual information between $r_{\text{wired},k}$ and s_k is at least $\log_2(1 + \text{SINR}_k)$ bits where $\text{SINR}_k = \dfrac{P_d}{P_m + P_{\text{int}} + P_n}$.

APPENDIX C

PROOF OF RANK-1 SOLUTION OF (P2-R)

Using the idea in [54], we can prove that (P2-r) has always rank-1 solution. Firstly, we define the Lagrangian function of the problem $\mathcal{L}$ as

$$\begin{aligned}\mathcal{L} = &\sum_{k=1}^{K} \mathrm{tr}(\mathbf{W}_k) - \sum_{k=1}^{K} \lambda_k \rho_k + \sum_{k=1}^{K} \mu_k \sum_{n=1}^{N} c_{k,n}\, \mathrm{tr}(\mathbf{B}_n \mathbf{W}_k) \\ &+ \sum_{n=1}^{N} v_n \left(\sum_{k=1}^{K} \mathrm{tr}(\mathbf{B}_n \mathbf{W}_k) - P_t \right) - \sum_{k=1}^{K} \mathrm{tr}(\mathbf{W}_k \mathbf{Z}_k)\end{aligned} \tag{C.1}$$

where $\{\lambda_k\}_{k=1}^{K}, \{\mu_k\}_{k=1}^{K}, \{v_n\}_{n=1}^{N}$ are non-negative Lagrange multipliers, ρ_k is defined in (4.22), $\mathbf{Z}_k$ is the dual positive semi-definite matrix associated with the positive semi-definite optimization variable $\mathbf{W}_k$. For the optimal solution of the convex problem (P2), the condition $\mathbf{W}_k \mathbf{Z}_k = \mathbf{0}$ should satisfy for all k. Furthermore, by the first order optimality condition, we also have

$$\begin{aligned}\frac{\partial \mathcal{L}}{\partial \mathbf{W}_k} &= \mathbf{I} - \lambda_k (1 + \gamma_k)\, \widehat{\mathbf{H}}_k + \sum_{\ell=1}^{K} \lambda_\ell \gamma_\ell\, \widetilde{\mathbf{H}}_\ell \\ &\quad + \sum_{n=1}^{N} (\mu_k c_{k,n} + v_n) \mathbf{B}_n - \mathbf{Z}_k \\ &= \mathbf{0}.\end{aligned} \tag{C.2}$$

It follows that

$$\mathbf{Z}_k = \mathbf{I} + \mathbf{F}_k - \lambda_k (1 + \gamma_k)\, \widehat{\mathbf{h}}_k\, \widehat{\mathbf{h}}_k^H \tag{C.3}$$

where

$$\mathbf{F}_k = \sum_{\ell=1}^{K} \lambda_\ell \gamma_\ell\, \widetilde{\mathbf{H}}_\ell + \sum_{n=1}^{N} (\mu_k c_{k,n} + v_n) \mathbf{B}_n \tag{C.4}$$

is a positive semi-definite matrix. Therefore, the matrix $\mathbf{I} + \mathbf{F}_k$ is full-rank. The rank of $\lambda_k (1 + \gamma_k)\, \widehat{\mathbf{h}}_k\, \widehat{\mathbf{h}}_k^H$ is at most 1 and hence the rank of $\mathbf{Z}_k$ is at least $NL - 1$ as its dimension is NL. Using the equation $\mathbf{W}_k\mathbf{Z}_k = \mathbf{0}$ and the rank inequality for matrix multiplication, we get

$$\begin{aligned} \text{rank}(\mathbf{W}_k) &\leq NL + \text{rank}(\mathbf{W}_k\mathbf{Z}_k) - \text{rank}(\mathbf{Z}_k) \\ &= NL - \text{rank}(\mathbf{Z}_k) \\ &\leq 1. \end{aligned} \tag{C.5}$$

Assuming positive SINR threshold values, the zero beamformer cannot be a solution and hence we conclude that $\text{rank}(\mathbf{W}_k) = 1, \ \forall k$.

APPENDIX D

PROOF OF THEOREM 4.1

Assume on the contrary that there exists a user k with $\mathrm{SINR}_k > \gamma_k$. Choose a constant $0 < \lambda < 1$ and replace $\mathbf{w}_k$ by $\lambda\mathbf{w}_k$. In that case SINR_ℓ becomes larger for all $\ell \neq k$. If SINR_k becomes also larger then all SINR constraints are satisfied. If SINR_k becomes smaller, we can choose λ small enough to ensure that in the new case $\mathrm{SINR}_k \geq \gamma_k$ holds. This is due to the fact that the expression of SINR_k is continuous with respect to λ. The original SINR value of the k-th user $\mathrm{SINR}_{k,0}$ (corresponding to $\lambda_0 = 1$) is larger than γ_k and if a new value $\mathrm{SINR}_{k,1} < \mathrm{SINR}_{k,0}$ is obtained for some $0 < \lambda_1 < 1$, then by Intermediate Value Theorem, there exists a λ_2 with $0 < \lambda_1 < \lambda_2 < 1$ such that the corresponding SINR value $\mathrm{SINR}_{k,2}$ satisfies $\gamma_k \leq \mathrm{SINR}_{k,2} < \mathrm{SINR}_{k,0}$. In both cases, the term P_{CP} remains the same but P_{tot} becomes smaller making P smaller, which is a contradiction. Therefore, in the optimal case, $\mathrm{SINR}_k = \gamma_k$ must hold for all k.

APPENDIX E

PROOF OF RANK-1 SOLUTION OF (P3) AND (P5))

We use the idea presented in Appendix A and C to show that the solutions of (P3) and (P5) are always rank-1. For (P3), we consider the Lagrangian function

$$\begin{aligned}\mathcal{L}_1 = &\sum_{k=1}^{K}\left(r_k\sum_{n=1}^{N}\frac{\epsilon_1 c_\theta \operatorname{tr}(\mathbf{B}_n\mathbf{W}_k)}{\operatorname{tr}(\mathbf{B}_n\mathbf{W}_k^{(t)})+\theta}+\epsilon_2\operatorname{tr}(\mathbf{W}_k)\right)-\sum_{k=1}^{K}\alpha_{k,1}\rho_k\\ &+\sum_{n=1}^{N}\beta_{n,1}\left(\sum_{k=1}^{K}\operatorname{tr}(\mathbf{B}_n\mathbf{W}_k)-P_t\right)-\sum_{k=1}^{K}\operatorname{tr}(\mathbf{W}_k\mathbf{Z}_{k,1})\end{aligned} \tag{E.1}$$

where $\{\alpha_{k,1}\}_{k=1}^{K}$, $\{\beta_{n,1}\}_{n=1}^{N}$ are non-negative Lagrange multipliers, ρ_k is defined in (4.22), $\mathbf{Z}_{k,1}$ is the dual positive semi-definite matrix associated with the positive semi-definite optimization variable $\mathbf{W}_k$. For the optimal solution of the convex problem (P3), the condition $\mathbf{W}_k\mathbf{Z}_{k,1} = \mathbf{0}$ should be satisfied for all k. By the first order optimality condition, we get

$$\begin{aligned}\frac{\partial\mathcal{L}_1}{\partial\mathbf{W}_k} &= r_k\sum_{n=1}^{N}\left(\frac{\epsilon_1 c_\theta}{\operatorname{tr}(\mathbf{B}_n\mathbf{W}_k^{(t)})+\theta}+\beta_{n,1}\right)\mathbf{B}_n+\epsilon_2\mathbf{I}\\ &+\sum_{\ell=1}^{K}\alpha_{\ell,1}\gamma_\ell\,\widetilde{\mathbf{H}}_\ell-\alpha_{k,1}(1+\gamma_k)\,\widehat{\mathbf{H}}_k-\mathbf{Z}_{k,1}\\ &=\mathbf{0}.\end{aligned} \tag{E.2}$$

It follows that

$$\mathbf{Z}_{k,1} = \epsilon_2\mathbf{I}+\mathbf{F}_{k,1}-\alpha_{k,1}(1+\gamma_k)\,\widehat{\mathbf{h}}_k\,\widehat{\mathbf{h}}_k^H \tag{E.3}$$

where

$$\mathbf{F}_{k,1} = \sum_{n=1}^{N}\left(\frac{r_k\epsilon_1 c_\theta}{\operatorname{tr}(\mathbf{B}_n\mathbf{W}_k^{(t)})+\theta}+\beta_{n,1}\right)\mathbf{B}_n+\sum_{\ell=1}^{K}\alpha_{\ell,1}\gamma_\ell\,\widetilde{\mathbf{H}}_\ell\,. \tag{E.4}$$

$\mathbf{F}_{k,1}$ is a positive semi-definite matrix, and given that $\epsilon_2 > 0$, we have rank$(\epsilon_2\mathbf{I}) = NL$ and rank$(\alpha_{k,1}(1+\gamma_k)\,\widehat{\mathbf{h}}_k\,\widehat{\mathbf{h}}_k^H) \leq 1$. Therefore, we get rank$(\mathbf{Z}_{k,1}) \geq NL-1$. Using the equation $\mathbf{W}_k\mathbf{Z}_{k,1} = \mathbf{0}$ and the rank inequality for matrix multiplication, we obtain the final result as

$$\begin{aligned}\text{rank}(\mathbf{W}_k) &\leq NL + \text{rank}(\mathbf{W}_k\mathbf{Z}_{k,1}) - \text{rank}(\mathbf{Z}_{k,1}) \\ &= NL - \text{rank}(\mathbf{Z}_{k,1}) \\ &\leq 1.\end{aligned} \tag{E.5}$$

The zero beamformer is not a solution for $\gamma_k > 0$, and hence we obtain that $\text{rank}(\mathbf{W}_k) = 1,\ \forall k$.

For (P5), we again consider the Lagrangian $\mathcal{L}_2$, which can be written as

$$\begin{aligned}\mathcal{L}_2 = &\sum_{k=1}^{K}\sum_{n=1}^{N}\left(\frac{\epsilon_1 r_k \operatorname{tr}(\mathbf{B}_n\mathbf{W}_k) + [\operatorname{tr}(\mathbf{B}_n\mathbf{W}_k^{(t)})]^2}{(\operatorname{tr}(\mathbf{B}_n\mathbf{W}_k^{(t)}) + \theta)^2}\right) + \sum_{k=1}^{K}\epsilon_2 \operatorname{tr}(\mathbf{W}_k) \\ &- \sum_{k=1}^{K}\alpha_{k,2}\rho_k + \sum_{n=1}^{N}\beta_{n,2}\left(\sum_{k=1}^{K}\operatorname{tr}(\mathbf{B}_n\mathbf{W}_k) - P_t\right) - \sum_{k=1}^{K}\operatorname{tr}(\mathbf{W}_k\mathbf{Z}_{k,2})\end{aligned} \tag{E.6}$$

where $\{\alpha_{k,2}\}_{k=1}^{K}, \{\beta_{n,2}\}_{n=1}^{N}$ are non-negative Lagrange multipliers, $\mathbf{Z}_{k,2}$ is the dual positive semi-definite matrix associated with the positive semi-definite optimization variable $\mathbf{W}_k$. For the optimal solution of the convex problem (P5), the condition $\mathbf{W}_k\mathbf{Z}_{k,2} = \mathbf{0}$ should be satisfied for all k. By the first order optimality condition, we get

$$\begin{aligned}\frac{\partial \mathcal{L}_2}{\partial \mathbf{W}_k} &= \sum_{n=1}^{N}\left(\frac{\epsilon_1 r_k}{(\operatorname{tr}(\mathbf{B}_n\mathbf{W}_k^{(t)}) + \theta)^2} + \beta_{n,2}\right)\mathbf{B}_n + \epsilon_2\mathbf{I} \\ &\quad + \sum_{\ell=1}^{K}\alpha_{\ell,2}\gamma_\ell\,\widetilde{\mathbf{H}}_\ell - \alpha_{k,2}(1+\gamma_k)\,\widehat{\mathbf{H}}_k - \mathbf{Z}_{k,2} \\ &= \mathbf{0}.\end{aligned} \tag{E.7}$$

Hence, we get

$$\mathbf{Z}_{k,2} = \epsilon_2\mathbf{I} + \mathbf{F}_{k,2} - \alpha_{k,2}(1+\gamma_k)\,\widehat{\mathbf{h}}_k\,\widehat{\mathbf{h}}_k^H \tag{E.8}$$

where

$$\mathbf{F}_{k,2} = \sum_{n=1}^{N}\left(\frac{\epsilon_1 r_k}{(\operatorname{tr}(\mathbf{B}_n\mathbf{W}_k^{(t)}) + \theta)^2} + \beta_{n,2}\right)\mathbf{B}_n + \sum_{\ell=1}^{K}\alpha_{\ell,2}\gamma_\ell\,\widetilde{\mathbf{H}}_\ell \tag{E.9}$$

which is a positive semi-definite matrix. For $\epsilon_2 > 0$, the matrix $\epsilon_2\mathbf{I}$ is full-rank and since the rank of $\alpha_{k,2}(1+\gamma_k)\,\widehat{\mathbf{h}}_k\,\widehat{\mathbf{h}}_k^H$ is at most 1, we conclude that $\text{rank}(\mathbf{Z}_{k,2}) \geq NL - 1$. As in the previous part, we obtain that $\text{rank}(\mathbf{W}_k) = 1,\ \forall k$.

APPENDIX F

PROOF OF THEOREM 4.3

For the upper bound, we use the fact that maximum fronthaul power is reached for full cooperation case and each RRH can transmit at most P_t power. Hence, we obtain the result in (4.67). For the lower bound, using the UE SINR expressions given in (4.5) and the fact

$$\mathrm{tr}(\widetilde{\mathbf{H}}_k \, \mathbf{W}_\ell) \geq 0, \; \forall k, \ell \tag{F.1}$$

we get

$$\mathrm{tr}(\widehat{\mathbf{H}}_k \, \mathbf{W}_k) \geq \gamma_k \, \mathrm{tr}(\mathbf{D}_k \mathbf{W}_k) + \gamma_k \sigma^2_{\text{UE},k}. \tag{F.2}$$

Hence, we have

$$\mathbf{w}_k^H \left(\widehat{\mathbf{h}}_k \, \widehat{\mathbf{h}}_k^H - \gamma_k \mathbf{D}_k \right) \mathbf{w}_k \geq \gamma_k \sigma^2_{\text{UE},k}. \tag{F.3}$$

Since $S_k = \{n_1, n_2, \ldots, n_r\}$ is the index set of RRHs serving the UE k, we have $\mathbf{w}_{k,n} = \mathbf{0}$ for all $n \notin S_k$. Therefore, we can write

$$\mathbf{w}_k^H \left(\widehat{\mathbf{h}}_k \, \widehat{\mathbf{h}}_k^H - \gamma_k \mathbf{D}_k \right) \mathbf{w}_k = (\mathbf{w}'_k)^H \left(\widehat{\mathbf{h}}'_k (\widehat{\mathbf{h}}'_k)^H - \gamma_k \mathbf{D}'_k \right) \mathbf{w}'_k \tag{F.4}$$

where $\mathbf{w}'_k = [\mathbf{w}^T_{k,n_1} \; \mathbf{w}^T_{k,n_2} \; \cdots \; \mathbf{w}^T_{k,n_r}]^T$ and $\widehat{\mathbf{h}}'_k$, $\mathbf{D}'_k$ are defined as in (4.69). Using Cauchy-Schwarz Inequality [85], we can show that

$$\frac{(\mathbf{w}'_k)^H \left(\widehat{\mathbf{h}}'_k (\widehat{\mathbf{h}}'_k)^H - \gamma_k \mathbf{D}'_k \right) \mathbf{w}'_k}{(\mathbf{w}'_k)^H \mathbf{w}'_k} \leq \lambda_{\text{max}} \left(\widehat{\mathbf{h}}'_k (\widehat{\mathbf{h}}'_k)^H - \gamma_k \mathbf{D}'_k \right) \tag{F.5}$$

To satisfy (F.3) we need $\lambda_{\text{max}} \left(\widehat{\mathbf{h}}'_k (\widehat{\mathbf{h}}'_k)^H - \gamma_k \mathbf{D}'_k \right) > 0$. If this condition holds, then we obtain that

$$\mathbf{w}_k^H \mathbf{w}_k = (\mathbf{w}'_k)^H \mathbf{w}'_k \geq \frac{\gamma_k \sigma_k^2}{\lambda_{\text{max}} \left(\widehat{\mathbf{h}}'_k (\widehat{\mathbf{h}}'_k)^H - \gamma_k \mathbf{D}'_k \right)}. \tag{F.6}$$

Given the index set S_k for UE k, the power spent by CP for k-th UE fronthaul data is equal to $\epsilon_1 \log_2(1 + \gamma_k)|S_k|$. The power spent by RRHs for k-th UE is equal to

$\epsilon_2 \mathbf{w}_k^H \mathbf{w}_k$ which is lower bounded as shown in (F.6). Therefore, the minimum value of total power spent for k-th UE $\mathcal{P}_k$ can be found as

$$\mathcal{P}_k = \min_{S_k} \epsilon_1 \log_2(1+\gamma_k)|S_k| + \epsilon_2 \frac{\gamma_k \sigma_k^2}{\lambda_{\max}\left(\widehat{\mathbf{h}}_k'(\widehat{\mathbf{h}}_k')^H - \gamma_k \mathbf{D}_k'\right)} \tag{F.7}$$

We find the value of $\mathcal{P}_k$ by minimizing the right-hand side of (F.7) over all $S_k \subseteq \{1, 2, \ldots, N\}$.

APPENDIX G

PROOF OF (6.3)

Using the fact that $\mathbb{E}[s_k^* s_\ell] = \delta[k-\ell]$, we obtain that $P_d = \left|\widehat{\mathbf{h}}_k^H \mathbf{W}\widehat{\mathbf{G}}^H \mathbf{v}_k\right|^2$. Using the channel error distributions of $\Delta\mathbf{h}_k$ and $\Delta\mathbf{G}$ we get $\mathbb{E}[\Delta\mathbf{h}_k \Delta\mathbf{h}_k^H] = \mathbf{\Sigma}_{2,k}$ and $\mathbb{E}[\Delta\mathbf{G}^H \mathbf{v}_k \mathbf{v}_k^H \Delta\mathbf{G}] = \mathbf{v}_k^H \mathbf{v}_k \mathbf{\Sigma}_1$. Therefore, we conclude that

$$\begin{aligned}
P_{I,1} &= \mathbb{E}[|\mathbf{h}_k^H \mathbf{W}\mathbf{G}^H \mathbf{v}_k|^2] - |\widehat{\mathbf{h}}_k^H \mathbf{W}\widehat{\mathbf{G}}^H \mathbf{v}_k|^2 \\
&= \mathrm{tr}\left(\mathbf{W}^H \mathbb{E}[\mathbf{h}_k \mathbf{h}_k^H]\mathbf{W}\mathbb{E}[\mathbf{G}^H \mathbf{v}_k \mathbf{v}_k^H \mathbf{G}]\right) - \left|\widehat{\mathbf{h}}_k^H \mathbf{W}\widehat{\mathbf{G}}^H \mathbf{v}_k\right|^2 \\
&= \mathrm{tr}\left(\mathbf{W}^H(\widehat{\mathbf{h}}_k \widehat{\mathbf{h}}_k^H + \mathbf{\Sigma}_{2,k})\mathbf{W}(\widehat{\mathbf{G}}^H \mathbf{v}_k \mathbf{v}_k^H \widehat{\mathbf{G}} + \mathbf{v}_k^H \mathbf{v}_k \mathbf{\Sigma}_1)\right) - \left|\widehat{\mathbf{h}}_k^H \mathbf{W}\widehat{\mathbf{G}}^H \mathbf{v}_k\right|^2 \\
&= \mathrm{tr}(\mathbf{W}^H \mathbf{D}_k \mathbf{W}\mathbf{C}_k) - \left|\widehat{\mathbf{h}}_k^H \mathbf{W}\widehat{\mathbf{G}}^H \mathbf{v}_k\right|^2 .
\end{aligned} \tag{G.1}$$

Similarly, we get

$$\mathbb{E}[|\mathbf{h}_k^H \mathbf{W}\mathbf{G}^H \mathbf{v}_\ell|^2] = \mathrm{tr}(\mathbf{W}^H \mathbf{D}_k \mathbf{W}\mathbf{C}_\ell) \tag{G.2}$$

and hence

$$P_{I,2} = \sum_{\ell \neq k} \mathrm{tr}\left(\mathbf{D}_k \mathbf{W}\mathbf{C}_\ell \mathbf{W}^H\right). \tag{G.3}$$

Finally, we use (G.4) to obtain the result in (6.3).

$$\begin{aligned}
P_n &= \mathbb{E}\left[\left|\mathbf{h}_k^H \mathbf{W}\mathbf{z}_{\mathrm{RRH}} + z_{\mathrm{UE},k}\right|^2\right] \\
&= \mathrm{tr}\left(\mathbb{E}[\mathbf{W}^H \mathbf{h}_k \mathbf{h}_k^H \mathbf{W}]\mathbb{E}[\mathbf{z}_{\mathrm{RRH}} \mathbf{z}_{\mathrm{RRH}}^H]\right) + \sigma_{\mathrm{UE}}^2 \\
&= \sigma_{\mathrm{RRH}}^2 \,\mathrm{tr}(\mathbf{D}_k \mathbf{W}\mathbf{W}^H) + \sigma_{\mathrm{UE}}^2.
\end{aligned} \tag{G.4}$$

APPENDIX H

PROOF OF LEMMA 6.8

Using (6.14) and (6.16), we get

$$\begin{aligned} x_1 &\geq c_1 \left[c_2 x_2 + (c_3 x_5 + c_4) \left(x_3 + \frac{c_2}{d_1} x_3 \right) + c_5 \right], \\ y &\geq x_2 + x_5 + (c_3 x_5 + c_6) \frac{x_3}{d_1}. \end{aligned} \tag{H.1}$$

(6.15) and (H.1) yields

$$(d_1 - c_1 c_2) x_2 \geq c_1 \left[(c_3 x_5 + c_4) \left(x_3 + \frac{c_2}{d_1} x_3 \right) + c_5 \right] \tag{H.2}$$

and (6.17) and (H.1) yields

$$\left[\frac{x_5 d_2}{c_1} - (c_3 x_5 + c_4) \left(1 + \frac{c_2}{d_1} \right) \right] x_3 \geq c_2 x_2 + c_5. \tag{H.3}$$

(H.2) implies that $d_1 > c_1 c_2$. By (H.2), (H.3) and some simplifications, we obtain that

$$x_3 \geq \frac{d_1 c_5}{\left(\frac{d_1 d_2}{c_1} - c_2 d_2 - c_3 d_1 - c_2 c_3 \right) x_5 - c_4 (d_1 + c_2)} \tag{H.4}$$

and the denominator in (H.4) should be positive. Using (H.2) and (H.4) we get

$$x_2 \geq \frac{d_2 c_5}{\left(\frac{d_1 d_2}{c_1} - c_2 d_2 - c_3 d_1 - c_2 c_3 \right) x_5 - c_4 (d_1 + c_2)}. \tag{H.5}$$

Using (H.1), (H.4) and (H.5) we find that

$$y \geq x_5 + \frac{d_2 c_5 + c_5 (c_3 x_5 + c_6)}{\left(\frac{d_1 d_2}{c_1} - c_2 d_2 - c_3 d_1 - c_2 c_3 \right) x_5 - c_4 (d_1 + c_2)}. \tag{H.6}$$

Define $x = a x_5 - b$ where $a = \dfrac{d_1 d_2}{c_1} - c_2 d_2 - c_3 d_1 - c_2 c_3,\ b = c_4 (d_1 + c_2)$. Since x is the denominator of (H.4), it is positive. As x_5 and b are positive, we conclude that

a is also positive. We can write (H.6) in terms of x as

$$y \geq \frac{1}{a}\left(b + c_3c_5 + x + \frac{c_3c_5b + c_5(d_2 + c_6)a}{x}\right). \tag{H.7}$$

Finally, using (H.7) and Arithmetic-Geometric Mean Inequality [91], we get the result in (6.18).

APPENDIX I

RANK PROPERTIES OF RELAXED VERSIONS OF (P9) AND (P10)

In proofs, we use some rank properties. For any two square matrices $\mathbf{A}, \mathbf{B}$ with dimension n, we have $\text{rank}(\mathbf{A} \otimes \mathbf{B}) = \text{rank}(\mathbf{A})\text{rank}(\mathbf{B})$, $\text{rank}(\mathbf{A}+\mathbf{B}) \leq \text{rank}(\mathbf{A})+\text{rank}(\mathbf{B}) \leq \text{rank}(\mathbf{AB}) + n$.

For (P9) we will show that $\text{rank}(\boldsymbol{\mathcal{W}}) \leq K$. Firstly, we define the Lagrangian function

$$\mathcal{L}_1 = \text{tr}(\mathbf{B}_1 \boldsymbol{\mathcal{W}}) - \sum_{k=1}^{K} \lambda_{k,1}[\text{tr}(\mathbf{A}_{k,1} \boldsymbol{\mathcal{W}}) - \gamma_k \sigma_{\text{UE}}^2] - \text{tr}(\mathbf{Z} \boldsymbol{\mathcal{W}}) \tag{I.1}$$

where $\{\lambda_{k,1}\}_{k=1}^{K}$ are non-negative Lagrange multipliers and $\mathbf{Z}$ is the dual PSD matrix associated with the PSD optimization variable $\boldsymbol{\mathcal{W}}$. For the optimal solution of (P9), the condition $\mathbf{Z}\boldsymbol{\mathcal{W}} = \mathbf{0}$ should be satisfied. By the first order optimality condition, we have

$$\mathbf{0} = \frac{\partial \mathcal{L}_1}{\partial \boldsymbol{\mathcal{W}}} = \mathbf{B}_1 - \sum_{k=1}^{K} \lambda_{k,1} \mathbf{A}_{k,1} - \mathbf{Z} \quad \text{and hence} \quad \mathbf{Z} = \mathbf{B}_1 - \sum_{k=1}^{K} \lambda_{k,1} \mathbf{A}_{k,1}. \tag{I.2}$$

Using Kronecker product rank properties, we obtain that $\text{rank}(\mathbf{U}^H \mathbf{T}_k \mathbf{U}) \leq 1$. It is easy to show that $\mathbf{B}_1$ is positive definite (PD) (assuming $\sigma_{\text{RRH}} > 0$) and $(1 + \gamma_k)\mathbf{U}^H \mathbf{T}_k \mathbf{U} - \mathbf{A}_{k,1}$ is PSD. Hence, we can write $\mathbf{Z} = \mathbf{Z}_1 - \mathbf{Z}_2$ where $\mathbf{Z}_1$ is PSD with full-rank and $\mathbf{Z}_2 = \sum_{k=1}^{K}(1 + \gamma_k)\mathbf{U}^H \mathbf{T}_k \mathbf{U}$ is PSD with rank at most K. By the rank properties of sum and product of matrices, we obtain that

$$\begin{aligned} \text{rank}(\boldsymbol{\mathcal{W}}) &\leq \dim(\boldsymbol{\mathcal{W}}) + \text{rank}(\mathbf{Z}\boldsymbol{\mathcal{W}}) - \text{rank}(\mathbf{Z}) = \dim(\boldsymbol{\mathcal{W}}) - \text{rank}(\mathbf{Z}) \\ &\leq \dim(\boldsymbol{\mathcal{W}}) - (\text{rank}(\mathbf{Z}_1) - \text{rank}(\mathbf{Z}_2)) = \text{rank}(\mathbf{Z}_2) \leq K \end{aligned} \tag{I.3}$$

where $\dim(\boldsymbol{\mathcal{W}})$ denotes the dimension of $\boldsymbol{\mathcal{W}}$.

For (P10) we will show that $\mathrm{rank}(\mathbf{V}_k) = 1,\ \forall k$. We again define the Lagrangian function

$$\mathcal{L}_2 = \sum_{k=1}^{K} \mathrm{tr}(\boldsymbol{\tau_0}\mathbf{V}_k) - \sum_{k=1}^{K} \lambda_{k,2} \left[(1+\gamma_k)\,\mathrm{tr}(\mathbf{A}_{k,2}\mathbf{V}_k) - \gamma_k \sum_{\ell=1}^{K} \mathrm{tr}(\mathbf{B}_{k,2}\mathbf{V}_\ell) - \gamma_k a_{k,2} \right] \\ - \sum_{k=1}^{K} \mathrm{tr}(\mathbf{Z}_k\mathbf{V}_k) \tag{I.4}$$

where $\{\lambda_{k,2}\}_{k=1}^{K}$ are non-negative Lagrange multipliers and $\mathbf{Z}_k$ is the dual PSD matrix associated with the PSD optimization variable $\mathbf{V}_k$ for all k. For the optimal solution of (P10), the condition $\mathbf{Z}_k\mathbf{V}_k = \mathbf{0}$ should be satisfied for all k. By the first order optimality condition, we have

$$\mathbf{0} = \frac{\partial \mathcal{L}_2}{\partial \mathbf{V}_k} = \boldsymbol{\tau_0} - \lambda_{k,2}(1+\gamma_k)\mathbf{A}_{k,2} + \sum_{\ell=1}^{K} \lambda_{\ell,2}\gamma_\ell \mathbf{B}_{\ell,2} - \mathbf{Z}_k. \tag{I.5}$$

It is easy to show that $\boldsymbol{\tau_0}$ is PD, $\mathbf{A}_{k,2}$ is PSD with rank at most 1, and $\mathbf{B}_{k,2}$ is PSD for all k. Therefore, we can write $\mathbf{Z}_k = \mathbf{Z}_{k,1} - \mathbf{Z}_{k,2}$ where $\mathbf{Z}_{k,1}$ is PSD with full-rank and $\mathbf{Z}_{k,2}$ is PSD with rank at most 1. Applying similar rank inequalities as in the previous part, we get

$$\mathrm{rank}(\mathbf{V}_k) \leq \mathrm{dim}(\mathbf{V}_k) - (\mathrm{rank}(\mathbf{Z}_{k,1}) - \mathrm{rank}(\mathbf{Z}_{k,2})) = \mathrm{rank}(\mathbf{Z}_{k,2}) \leq 1. \tag{I.6}$$

Assuming $\gamma_k > 0$ for all k, the zero beamformer cannot be the solution and hence we get $\mathrm{rank}(\mathbf{V}_k) = 1,\ \forall k$.

CURRICULUM VITAE

PERSONAL INFORMATION

Surname, Name: Kadan, Fehmi Emre
Nationality: Turkish (TC)
Date and Place of Birth: 16 February 1991, İzmir
Marital Status: Married
Phone: +90 538 221 22 88
email: e174115@metu.edu.tr

EDUCATION

Degree	Institution	Year of Graduation
MS	METU Electrical and Electronics Eng.	2015
BS	METU Electrical and Electronics Eng.	2013
High School	İzmir Science High School	2009

WORK EXPERIENCE

Year	Place	Enrollment
2021-Present	Meteksan Defense	Systems Engineer
2013-2021	Aselsan, Inc.	Systems Engineer
2012 July	Aselsan, Inc.	Intern Eng. Student
2011 July	TÜBİTAK SAGE	Intern Eng. Student

FOREIGN LANGUAGES

Advanced English

PUBLICATIONS

1) F. E. Kadan and A. Ö. Yılmaz, “A Theoretical Performance Bound for Joint Beamformer Design of Wireless Fronthaul and Access Links in Downlink C-RAN," in *IEEE Trans. Wireless Commun.*, doi: 10.1109/TWC.2021.3109837.

2) F. E. Kadan and A. Ö. Yılmaz, “A Bound Based Method for Beamformer Design in Downlink Cloud Radio Access Networks," in *IEEE Commun. Lett.*, doi: 10.1109/LCOMM.2021.3100271.

3) F. E. Kadan and A. Ö. Yilmaz, “Beamformer Design With Smooth Constraint-Free Approximation in Downlink Cloud Radio Access Networks," in *IEEE Access*, vol. 9, pp. 36399-36416, 2021, doi: 10.1109/ACCESS.2021.3063668.

4) F. E. Kadan and A. Ö. Yılmaz, “Optimized asymmetric cooperation for downlink cloud radio access network under per-base station data transfer constraint," *2017 IEEE International Conference on Communications Workshops (ICC Workshops)*, 2017, pp. 132-137, doi: 10.1109/ICCW.2017.7962646.